The role of actin-binding proteins in mediating growth cone guidance to neurotrophins

A DISSERTATION

SUBMITTED TO THE FACULTY OF THE GRADUATE SCHOOL OF THE

UNIVERSITY OF MINNESOTA

BY

Bonnie Marie Marsick

IN PARTIAL FULFILLMENT OF THE REQUIREMENTS

FOR THE DEGREE OF

DOCTOR OF PHILOSOPHY

Paul C. Letourneau, Adviser

June, 2010

Acknowledgments

These past few years have been challenging, and at times stressful, but extremely rewarding. I owe a lot of my success to my advisor, Paul Letourneau. His constant support and tutelage have made my graduate experience here fun, exciting, and fruitful. His guidance helped strengthen my passion and excitement for neuroscience and the scientific process.

I also want to thank the members of the Letourneau lab. Murray Blackmore taught me a lot in my first year in the lab, and has since imparted invaluable advice. I also really enjoyed talking with Coco Roche about stimulating scientific questions and techniques, as well as non-scientific conversation.

I want to thank the Graduate Program in Neuroscience at the University of Minnesota. The constant dedication to the success of their students has made navigating graduate school that much easier. And my classmates and friends have provided a strong base of support since our first day at Itasca.

Finally, I want to thank my parents and family. They have always encouraged me to pursue my dreams, and instilled in me the notion that I can accomplish anything with enough effort. Without their support, none of this would have been possible.

Abstract of Thesis

Development of neuronal circuits rely on growth cones, the dynamic tips of growing neurites, to detect and respond to molecular cues expressed in the developing organism. Guidance cues steer growth cones by activating intracellular signaling cascades that culminate in cytoskeletal remodeling. Although many of the guidance cues, receptors and signaling molecules have been identified, the role of actin-binding proteins involved in mediating growth cone guidance are poorly understood. The content of this thesis present evidence for the regulation of two actin-binding proteins crucial in mediating attractive axon guidance to nerve growth factor (NGF) and characterizes the changes in actin filament dynamics that produce attractive growth cone turning.

The first section characterizes a mechanism by which activation of the actin-binding protein ADF/cofilin (AC) mediates attractive guidance of sensory neuronal growth cones to NGF and retinal ganglion cell growth cones to netrin-1 by locally increasing actin filament (F-actin) polymerization. The presented research demonstrates that NGF or netrin-1 induces an increase in F-actin and free F-actin barbed ends in dorsal root ganglion (DRG) or retinal growth cones, respectively, and a gradient of these cues also induce a local F-actin increase toward the cue source. Netrin-1 (retina) and NGF (DRG) also activate AC in both a global and local manner, and directly elevating AC activity mimics the guidance cue-induced F-actin and free F-actin barbed end increase. A cell-permeable gradient of active AC proteins locally elevate growth cone F-actin levels and induce attractive growth cone turning. Disrupting AC function blocks NGF (DRG) and netrin-1 (retina) membrane protrusion and attractive turning.

The next section identifies the membrane-cytoskeletal linker proteins of the ezrin/radixin/moesin (ERM) family as mediators of attractive growth cone guidance to NGF in sensory DRGs. Data are presented that demonstrate a global and local increase in active phospho-ERM proteins at the growth cone leading margin in response to NGF. Disrupting ERM function (with a dominant-negative ERM; DNERM) results in disorganized actin filaments, and DNERM growth cones do not exhibit increased F-actin after addition of NGF or cell-permeable active AC proteins. Moreover, localization of active AC and F-actin barbed ends are displaced from the growth cone periphery in DNERM growth cones. Active phospho-ERM levels increase when AC activity is elevated, and the NGF-induced phospho-ERM increase is blocked in growth cones with reduced AC activity. Attractive growth cone turning to NGF is reduced in growth cones with disrupted ERM function or lowered ERM protein levels.

The final section demonstrates that local protein synthesis is not required for all growth cone guidance. Data is shown to demonstrate that although protein synthesis does occur in response to many guidance cues, attractive growth cone turning to NGF occurs in conditions where local protein synthesis is inhibited.

Table of Contents

Acknowledgments i

Abstract of Thesis ii

Table of Contents iv

List of Tables vii

List of Figures viii

Summary of Publications and Manuscripts xi

Chapter I: Introduction and Rationale 1

1. Nervous system development 2

2. Growth cones 3

3. Guidance and the cytoskeleton 4

4. Actin regulatory proteins 6

5. Signaling 12

6. Adhesions 15

7. Protein synthesis 19

8. Guidance cues 20

9. Summary 24

Chapter II: Activation of ADF/cofilin mediates attractive growth cone turning toward nerve growth factor and netrin-1 26

Introduction 27

Methods 30

Results 37

Figures 53

Discussion 74

Chapter III: Ezrin/radixin/moesin family proteins mediate actin filament dynamics in attractive growth cone guidance to nerve growth factor 81

Introduction 82

Methods 86

Results 92

Figures 101

Discussion 113

Chapter IV: Protein synthesis in distal axons is not required for growth cone responses to guidance cues 117

Introduction 118

Methods 120

Results 129

Figures 141

Discussion 158

Chapter V: Final Discussion 165

Figure 171

References 173

List of Tables

Table 1. Effects of Protein Synthesis Inhibitors on Rate of Axonal Elongation. 142

Table 2. Effects of Protein Synthesis Inhibitors on Growth Cone Collapse. 143

List of Figures

Chapter II

Figure 1. Nerve growth factor and netrin-1 induce leading edge protrusion. 53

Figure 2. Nerve growth factor and netrin-1 increase growth cone F-actin, and NGF increases free F-actin barbed ends. 54

Figure 3. Growth cones exposed to a gradient of NGF or netrin-1 exhibit asymmetrical F-actin free barbed end distribution. 55

Figure 4. ADF/cofilin family proteins are activated by NGF and netrin-1. 57

Figure 5. Increased AC activity results in increased F-actin, decreased G-actin, and increased F-actin barbed ends. 59

Figure 6. Growth cones exposed to a gradient of XACA3 exhibit asymmetrical F-actin distribution. 61

Figure 7. Growth cones exposed to a gradient of cell-permeable AC exhibit attractive turning. 63

Figure 8. Reducing AC activation or protein levels blocks NGF- and netrin-induced membrane protrusion and guidance. 64

Figure 9. Restoring active AC to CA-LIMK- and ADF-RNAi-expressing growth cones rescues membrane protrusion. 66

Figure 10. Chick DRG growth cones contain higher levels of actin compared to Xenopus spinal neuronal growth cones. 67

Figure S1. FITC-conjugated DNase reliably measures G-actin levels. 68

Figure S2. NGF does not significantly alter retrograde actin flow. 70

Figure S3. A micropipette coated with nitrocellulose and protein establishes a diffusible gradient. 71

Figure S4. Expressing constitutively-active LIMK (CA-LIMK) or ADF hRNA results in decreased AC activity. 73

Chapter III

Figure 1. Ezrin, radixin and moesin localization in chick sensory neurons. 101

Figure 2. NGF globally and locally activates ERM proteins. 102

Figure 3. Disrupting ERM function results in smaller and less motile growth cones with disorganized actin filaments. 104

Figure 4. NGF-associated F-actin increase does not occur in DNERM growth cones. 105

Figure 5. Active ADF/cofilin and free F-actin barbed ends are displaced in DNERM growth cones. 107

Figure 6. ADF/cofilin activity influences ERM activity. 109

Figure 7. ERMs are involved in proper attractive growth cone guidance to NGF. 111

Figure S1. Combined siRNA against radixin and moesin reduces ERM levels. 112

Chapter IV

Figure 1. NGF and Sema3A increase phosphorylation of elF-4EBP1. 144

Figure 2. Nascent protein synthesis in E7 DRG neurons. 145

Figure 3. Effects of cycloheximide on axonal growth by E7 DRG neurons. 147

Figure 4. Protein synthesis inhibition does not block responses to repulsive guidance cues. 149

Figure 5. CHI treatment does not affect Sema3A- and ephrin-A2-induced loss of F-actin, and Sema3A does not increase RhoA content of DRG growth cones. 151

Figure 6. Effects of CHI on growth cone spreading and turning in response to NGF and NT-3. 152

Figure 7. CHI treatment does not affect NGF-induced increase in F-actin, and NGF does not increase ß-actin content of DRG growth cones. 154

Figure 8. Growth cone responses to Sema3A and NGF are not

inhibited by 24 hr CHI treatment in axon compartment. 156

Chapter V

Figure 1. Model for attractive growth cone guidance to NGF. 171

Summary of Publications

Bonnie M Marsick, Kevin C Flynn, Miguel Santiago-Medina, James R Bamburg and Paul C Letourneau. (2010). Activation of ADF/cofilin mediates attractive growth cone turning toward nerve growth factor and netrin-1. *Developmental Neurobiology*, in press.

Modified and presented in Chapter II as published

Florence K Roche, Bonnie M Marsick, and Paul C Letourneau. (2009). Protein synthesis in distal axons in not required for growth cone responses to guidance cues. *The Journal of Neuroscience*. 29:638-652.

Modified and presented in Chapter IV as published

CHAPTER I: Introduction and Rationale

Nervous system development

In nervous system development, newly formed neurons extend neurites that will later mature into axons and dendrites. At the growing neurite tip is a dynamic growth cone that comprises actin filaments, microtubules, and plasmalemma receptors. Neurite extension occurs via a three-step process: leading edge growth cone protrusion by actin filament polymerization, engorgement of microtubules into the growth cone from the neurite shaft, and consolidation of actin filaments at the growth cone rear to form the newest segment of neurite shaft (Dent and Gertler, 2003). Growth cone adhesion to proteins in the surrounding extracellular matrix and on neighboring cells provides the necessary traction for forward advancement.

Patterns of transiently expressed attractive, repulsive, and permissive molecules in the developing embryo guide the growth cone along the proper path to reach its target tissue. Throughout its journey, the growth cone, as well as the cues in its surrounding environment, continually change. Periods of axonal extension, where the growth cone may selectively fasciculate along existing fibers, are punctuated by pausing of the growth cone at "choice points," where short-range cues direct crucial guidance decisions. The expression of directional cues at these choice points are crucial for a growth cone's ability to follow the correct trajectory, and are especially important for the first few "pioneer" growth cones of axons that may help guide subsequent related neurites along a similar trajectory (O'Connor and Bentley, 1993). The different types of cues encountered by the growth cone within the extracelluar environment are regulated in a spatio-temporal manner. Thus, in order for neurites to "choose" the correct paths and reach the appropriate target tissues, the receptor

composition and downstream signaling components constantly adapt to permit the growth cone to exhibit proper responses to future guidance cues.

Upon reaching the correct target tissue, growth cones must then navigate to a specific target region and establish synapses. The initial quantity of connections established early in development is relatively high compared with that in adulthood, largely due to competition for target-derived pro-survival neurotrophins and activity-dependent pruning, which culminates in a specific and refined circuitry.

Growth cones

The receptor-mediated response of the growth cone to diffusible and adhesive cues in the extracellular environment is mediated by remodeling of the underlying cytoskeleton (Tessier-Lavigne and Goodman, 1996). Actin is the dominant cytoskeletal component in the growth cone periphery and provides their structure and shape. Actin filaments (F-actin) form when individual monomers (or globular, G-actin) polymerize. Filaments are polarized with a barbed end that favors monomer addition and a pointed end that favors disassembly or slower polymerization. In the growth cone, actin barbed ends face the leading edge, with the pointed ends toward the growth cone center (Lin et al., 1994). Thus, actin polymerization occurs preferentially at the growth cone leading edge.

Individual filaments in growth cones are organized into two primary superstructures: bundles of linear F-actin form finger-like protrusions (filopodia) and a veil-like meshwork of filaments form lamellipodia. Myosin motor proteins continuously induce retrograde movement or flow of F-actin toward the growth cone

center, where filaments are disassembled and monomers can be recycled (Forscher and Smith, 1988). This actin "treadmilling" translates into leading edge protrusion if the rate of barbed-end polymerization exceeds the rate of retrograde flow, or if actin filaments are coupled to a non-compliant substrate to form a "clutch" (Mitchison and Kirschner, 1988; Suter and Forscher, 2000).

Bundled microtubules course along the neurite shaft, splay into the growth cone center, and occasionally probe the actin-rich periphery along filopodia. Microtubules form cylindrical filaments consisting of tubulin dimers, with a fast- and slow-growing end. Like actin filaments, microtubules are highly dynamic with slow and steady growth punctuated by rapid shrinkage events termed "dynamic instability" (Tanaka et al., 1995; Gordon-Weeks, 2004). Individual microtubules may also exhibit antero- and retrograde sliding in the growth cone (Dent et al., 1999). Together, F-actin and microtubule dynamics are central to a growth cone's ability to respond to cues.

Guidance and the cytoskeleton

Microtubules provide both structural support for a growing neurite and a mechanism for organelle transport to and from the soma. Thus, microtubles are necessary for axon extension, as agents that disrupt microtubule dynamics impair neurite length (Letourneau and Ressler, 1984; Letourneau et al., 1987; Zheng et al., 1993). Microtubules may also play an instructional role in axon guidance decisions (Bentley and O'Connor, 1994; Tanaka et al., 1995; Gordon-Weeks, 2004). For example, microtubules re-orient asymmetrically in growth cones during turning

behaviors (Tanaka and Kirschner, 1995; Challacombe et al., 1996, 1997; Mack et al., 2000) and agents that disrupt microtubule dynamics also block appropriate guidance responses (Challacombe et al., 1997). Furthermore, local microtubule destabilization with taxol produces repulsive growth cone turning (Buck and Zheng, 2002), and locally stabilizing microtubules induces F-actin protrusion and attractive turning (Buck and Zheng, 2002).

While microtubules primarily support advance, growth cone steering is achieved through remodeling F-actin (Mitchison and Kirschner, 1988; Letourneau, 1996; Tessier-Lavigne and Goodman, 1996; Pak et al., 2008). Cytochalasin D, an agent that interrupts actin filament polymerization, abolishes directed growth without impeding advance (Marsh and Letourneau, 1984; Bentley and Toroian-Raymond, 1986; Chien et al., 1993). Thus, it is widely accepted that attractive growth cone turning involves the proximal stabilization and/or polymerization of actin filaments, and growth cone repulsion conversely involves proximal F-actin loss (Seeley and Greene, 1983; Lin and Forscher, 1993). In support of this, global application of attractive guidance cues increase F-actin content and repulsive cues induce F-actin loss (Kalil and Dent, 2005). Furthermore, a gradient of cytochalasin induces growth cone repulsion (Yuan et al., 2003).

Finally, F-actin and microtubules do not function independently within growth cones. Actin filament reorganization in response to guidance cues affects microtubule dynamics. Rearward sliding of microtubules mirrors the rate of F-actin retrograde flow, and reductions in F-actin by cytochalasin permit microtubule entry farther into the growth cone periphery (Forscher and Smith, 1988; Zhou et al., 2002). Stabile

actin filaments can also capture and stabilize the fast growing ends of microtubules (Goode et al., 2000). Therefore, it is clear that F-actin and microtubule dynamics influence each other and these interactions likely serve an important role in growth cone guidance (Kalil and Dent, 2005).

Actin-regulatory proteins

Actin-binding proteins tightly regulate the organization of growth cone actin in a variety of ways. Nucleators stimulate the assembly of new actin filaments (Arp2/3, formins, and cofilin), while others facilitate polymerization (cortactin, profilin, ADF/cofilin, Ena/Mena/VASP), limit polymerization (thymosin, calbindin), stimulate filament disassembly (ADF/cofilin), arrange networks of filaments (fascin, Arp2/3), or link actin to other cellular proteins (myosins, ERMs, talin) (Pak et al., 2008; Lowery and Van Vactor, 2009). Although many actin-binding proteins have been identified, along with their respective effects on actin, relatively few have been characterized in the context of specific guidance cues or in relationship (competitive or cooperative) to other actin-binding proteins.

Two candidates implicated in altering growth cone actin in response to guidance cues are ADF/cofilin and the ezrin/radixin/moesin (ERM) family of proteins. Both are present in developing growth cones, regulated through phosphorylation, and play a role in cell chemotaxis.

ADF/cofilin

Actin depolymerizing factor (ADF) and cofilin (from here on referred to as AC) are related proteins and have qualitatively overlapping expression and effects on actin turnover (Bamburg, 1999). Since their initial discovery and characterization as regulators of F-actin length, it is now clear that AC have broad functions in several cellular processes, including cell migration, signaling and apoptosis (Bernstein and Bamburg). AC also serve an important role in nervous system development (Gungabissoon and Bamburg, 2003).

Active AC preferentially bind ADP-actin and can remodel filaments through either inducing depolymerization, enhancing filament length and number through monomer nucleation, or by the creation of new sites for polymerization through filament severing (Carlier et al., 1997; Maciver, 1998; Sarmiere and Bamburg, 2004). The regulation of AC activity has proven complex. The first identified and most studied mechanism is inactivation through phosphorylation at a conserved serine 3 residue. Numerous kinases have been identified that inactivate AC: ubiquitously expressed LIM kinases 1 and 2 (LIMK1/2) and testicular protein kinases 1 and 2, which are largely restricted to testicular tissue (Arber et al., 1998; Yang et al., 1998; Toshima et al., 2001; Huang et al., 2006). LIMK activity is regulated downstream of the Rho GTPases. Specifically, Rho-associated kinase (ROCK), p21-activated kinase (PAK) and myotonic-dystrophy-related Cdc42-binding kinase (MRCK) activate LIMK through phosphorylation (Arber et al., 1998; Yang et al., 1998; Maekawa et al., 1999; Huang et al., 2006).

Activation of AC through dephosphorylation also occurs via multiple phosphatases, including the slingshot phosphatases 1, 2 and 3 (SSH) (Niwa et al., 2002; Endo et al., 2003; Ohta et al., 2003; Nagata-Ohashi et al., 2004) and chronophin phosphatase (CIN) (Gohla et al., 2005). Slingshot itself is also activated by dephosphorylation, and in this, numerous signaling pathways have been implicated, including calcineurin, cAMP, and PI3K (Meberg et al., 1998; Huang et al., 2006). Some studies also found SSH binding to F-actin itself can cause further activation (Nagata-Ohashi et al., 2004; Kurita et al., 2008), and SSH can dephosphorylate and inactivate LIMK (Soosairajah et al., 2005). Thus, the regulation of AC is complex, with numerous positive and negative feedback mechanisms to control its activity.

Studies of actin dynamics in cell migration have found a necessary role for AC (Carlier et al., 1999; Van Troys et al., 2008). Leading edge activation of AC mediates rapid actin polymerization and subsequent migration of carcinoma cells toward an EGF gradient (Zebda et al., 2000; Mouneimne et al., 2004; Mouneimne et al., 2006), and local uncaging of cofilin in carcinoma cells induces local polymerization and directional turning (Ghosh et al, 2004). Moreover, NGF stimulation in PC12 cells induces active AC that localizes to lamellar protrusions (Meberg et al., 1998).

In neurons, AC proteins and their regulators are expressed at high levels and localize to growth cones (Bamburg and Bray, 1987). Increased AC activity via over-expression of SSH or a constitutively active AC causes increased neurite extension, whereas inhibition of AC produces shorter neurites (Meberg et al., 1998; Meberg and

Bamburg, 2000; Birkenfeld et al., 2001; Endo et al., 2003). In retinal neurons, AC activation mediates brain-derived neurotrophic factor-induced increase in filopodia number and length (Gehler et al., 2004; Chen et al., 2006), and inactive pAC mediate growth cone collapse to semaphorin 3A (Aizawa et al., 2001). Moreover, AC activation was found to mediate the response of *Xenopus laevis* spinal neurons to bone morphogenic proteins, where growth cones turned away from the side with higher activity (Wen et al., 2007).

Lastly, much work over the past 2 decades have identified numerous factors beside Ser3 phosphorylation that regulate AC activity and localization, including pH, phosphatidylinositol (4,5) bisphosphate, oxidation, ubiquitination, tyrosine phosphorylation, and interactions with tropomyosins, cortactin, and 14-3-3 proteins (Bernstein and Bamburg). Studies also suggest AC may interact with other actin-binding proteins in the growth cone. For example, AC can cooperate with Arp2/3 by producing newly polymerized filaments which Arp2/3 preferentially binds (Ichetovkin et al., 2002) or by disassembling branched filaments created by Arp2/3 (Blanchoin et al., 2000; Chan et al., 2009). And the relative ratio of AC:actin may also impact its overall effect on actin. Namely, at low ratios, AC primarily severs filaments, whereas higher ratios result in severing followed by filament stabilization (Sarmiere and Bamburg, 2004; Andrianantoandro and Pollard, 2006). Taken together, these studies suggest that AC may play a critical role of maintaining a balance of actin filaments and monomers to allow the continual response of growth cones to guidance cues.

Ezrin/radixin/moesin

The evolutionarily conserved Ezrin/Radixin/Moesin (ERM) proteins are also expressed in developing growth cones, where they link F-actin and the cell membrane (Niggli and Rossy, 2008). Inactive ERMs reside in the cytosol, where interactions between their N- and C-termini result in a closed conformation (Hayashi et al., 1999). , This intermolecular association between the termini is disrupted by phosphorylation at a conserved threonine residue or through interactions with PIP2. In the active state, ERMs can bind F-actin on their C-terminus and interact with the cell membrane on their N-terminus FERM (4.1-ezrin-radixin-moesin) domain (Henry et al, 1995) either directly, through association with membrane lipids, or indirectly through association with specific membrane proteins such as CD44, CD43, ERM binding phosphoprotein 50 (EBP50) and L1CAM (Bretscher et al., 2002). All three ERMs are broadly expressed in vertebrates with largely overlapping functions, as evidenced by genetic manipulations in drosophila and mice (Doi Y, 1999; Polesello and Payre, 2004). Active phospho-ERM (pERM) proteins localize to actin-rich protrusions, such as intestine microvilli, hair cell stereocilia, and regions of cell-cell contact (Amieva MR, 1995; Henry, 1995) and have extensive roles in cell shape and motility (Bretscher et al., 2002; Niggli and Rossy, 2008)

In nervous tissue, all three ERMs are expressed at high levels during development and decrease postnatally (Paglini G, 1998). In growth cones, radixin and moesin colocalize with F-actin at lamellipodia and filopodia, and ERM knockdown produces short axons with small growth cones and reduced actin (Paglini G, 1998; Castelo, 1999). To investigate radixin's function in real time, Castello and Jay (1999)

used micro-CALI to focally disrupt radixin in growth cones. They found that radixin inactivation in the growth cone center caused it to split in two, and when disrupted on one side, the corresponding region of the growth cone collapsed.

Much effort has been dedicated to deciphering the regulation of ERM activity, and numerous players have emerged. Given their role in cytoskeletal remodeling, the Rho GTPases were attractive candidates. Indeed, multiple studies have found ERM phosphorylation downstream of Cdc42 activity *in vitro* (Nakamura et al., 2000) and Rho activity *in vitro* and *in vivo* (Matsui, 1998; Matsui et al., 1999; Yonemura et al., 2002). Others have found that ERM binding to membrane lipids (PI(4,5)P2) disrupts their intermolecular association, thereby increasing their susceptibility to subsequent threonine phosphorylation (Matsui et al., 1999). Additional signaling molecules implicated in ERM phosphorylation include protein kinase C (PKC), Nck-interacting kinase (NIK) and Akt (Simons et al., 1998; Ng et al., 1999; Mason and Erskine, 2000; Shiue et al., 2005; Baumgartner et al., 2006).

In addition to their role as actin-membrane linkers, ERMs may also play a role in cell signaling. When active, their N-terminal can directly interact with Rho GDI, preventing RhoA inhibition, and possibly Rac1 and Cdc42 (Takahashi, 1997; Hamada et al., 2001). In addition, ezrin was shown to bind PI3K and regulate cell survival (Gautreau A, 1999). This ability to both influence signaling and localize to the cell membrane suggests ERMs may serve as scaffolding proteins for signaling or adaptor molecules (Orian-Rousseau et al., 2007).

Several studies have examined ERM activity downstream of guidance cues. In chick sympathetic neurons, NGF withdrawal induces a loss of growth cone ERM

proteins, which subsequently returns after NGF is returned (Gonzales-Agosti and Solomon, 1996). In growth cones turning toward an electrical field, radixin localizes to the leading edge toward the direction of new growth (Gonzalez-Agosti, 1996). Conversely, Semaphorin 3A treatment results in ERM inactivation through PI3K inhibition, suggesting a role for reduced ERM activity downstream of repulsive guidance cues (Gallo, 2008). Thus, ERM proteins are excellent candidates for mediating membrane-cytoskeletal interactions in navigating growth cones.

Signaling

The remodeling of actin filaments downstream of guidance cues is mediated by signaling molecules, which transduce external cues into changes in actin-binding protein activity. Although the particular signaling cascade triggered depends on the receptor-cue combination, some signaling molecules have emerged as common elements involved in growth cone guidance decisions (Guan and Rao, 2003).

One family of molecules known for its key role in remodeling actin in migrating cells and growth cones is the Rho guanosine triphosphatases (GTPases) (Hall and Nobes, 2000). Rho GTPases are activated by guanosine nucleotide exchange factors (GEFs) that facilitate GTP exchange for GDP, and are inactivated by GTPase-activating proteins (GAPs) that stimulate their intrinsic GTPase activity. Additional regulation occurs through guanine nucleotide dissociation inhibitors (GDIs), which sequester Rho GTPases and restrict their spatial distribution and activation.

RhoA, Rac1 and Cdc42 are the most extensively studied Rho GTPases in the context of axon guidance. In general, RhoA activity is linked to growth cone collapse or retraction, and is mediated by activation of Rho-associated kinase (ROCK) and subsequent myosin light chain (MLC) activation, which results in contraction of bundles or arrays of actin filaments. In support of this, a gradient of a myosin ATPase inhibitor (BDM) induces growth cone repulsion away from the source (Yuan et al., 2003), and global myosin inhibition blocks growth cone repulsion (Brown et al., 2009). Furthermore, attractive growth cone turning to neurotrophins may also involve myosin activity on the growth cone side away from the source, where it inhibits protrusion and facilitates distal growth cone consolidation (Loudon et al., 2006). Rac1 and Cdc42 are associated with actin polymerization and protrusion in lamellipodia and filopodia, respectively (Yuan et al., 2003). Both Rac and Cdc42 activate p21-activated kinase (PAK) whose effectors include MLC and LIMK. Attractive cues activate Rac and Cdc42, and disrupting their activity blocks attractive growth cone turning (Yuan et al., 2003). There is some evidence for cross talk between Rho GTPases, though the nature of these interactions remains poorly understood (Mackay et al., 1995; Nobes and Hall, 1995; Giniger, 2002; Li et al., 2002b; Yuan et al., 2003; Sakumura et al., 2005). And although our understanding of the upstream regulators and downstream targets remain incomplete, some links between cue-receptor signaling and GTPase regulation have been made. For example, P-Rex1 and Trio are GEFs that mediate Rac1 activation downstream of NGF and netrin-1, respectively (Yoshizawa et al., 2005; Briancon-Marjollet, et al., 2008).

Additional regulators of growth cone guidance include the cyclic nucleotides. For example, *Xenopus* spinal neuron attraction to netrin-1 can be switched to repulsion by inhibiting cAMP and its downstream target, PKA (or cGMP and its target PKG) (Ming et al., 1997; Song and Poo, 1999). Furthermore, growth cone repulsion can be switched to attraction by elevating cAMP, cGMP, or their targets PKA or PKG. Interestingly, *Xenopus* neurons cultured *in vitro* on laminin have lower cAMP levels compared to neurons grown on L1 or Ncadherin, and respond to netrin accordingly (Hopker et al., 1999; Song and Poo, 1999). However, other studies in mice contradict this role of cAMP and PKA as a "switch", but rather suggest PKA activity regulates a growth cone's sensitivity to netrin-1. That is, increased PKA activity results in attractive guidance when growth cones are further from the netrin source (Moore and Kennedy, 2006; Moore et al., 2008a). These results highlight the notion that growth cone guidance factors may not necessarily generalize to other cell types or organisms. Furthermore, they underscore the fact that growth cones *in vivo* constantly integrate multiple cues at any given space and time throughout their journey.

Finally, changes in intracellular calcium during growth cone guidance are also important, although complex. Local increases in calcium signaling can evoke attraction (as with netrin) or repulsion (as with myelin-associated glycoprotein), and it appears multiple factors impact the outcome of growth cone behavior when confronted with changes in calcium (Gomez and Zheng, 2006). Aspects of calcium distribution include the basal (resting) calcium level, the magnitude and frequency of local calcium changes, and the slope in calcium change across the growth cone width.

Additional factors include the mode of increase, either via channel type (such as L-type, voltage-gated, TRP) or through release from intracellular stores (ryanadine receptors, IP3) (Gomez and Zheng, 2006). Downstream of these fluctuations, changes in calcium-dependent signaling molecules such as calcineurin, calmodulin, PKC, CAMKII and calpain can all influence the activities of actin-binding proteins and growth cone guidance. Furthermore, calcium has been linked to Rho GTPase activity, where increased intracellular calcium activates Rac and Cdc42, while inactivating RhoA (Jin et al., 2005). Despite our growing knowledge about calcium's role in growth cone guidance, we have yet to completely understand which developmental situations rely on calcium changes and how these changes are regulated and translated into specific cytoskeletal modifications.

These common signaling cascades involved in growth cone guidance culminate in altering the activity of cytoskeletal-binding proteins. How this activity is regulated depends on the specific actin-binding protein. Post-translational modifications like phosphorylation, as in the case of ADF/cofilin and ERMs, are common. Other means include spatially restricting proteins to certain growth cone regions, competitive binding, protein degradation, and receptor-ligand endocytosis. Together, signaling enables an external guidance cue to trigger internal actin reorganization, and is a significant component in adhesion and neurite extension.

Adhesions

To accomplish forward extension, growth cones gain traction through receptor-binding to proteins in the extracellular matrix (ECM) or on surrounding

cells. Continual actin-dependent protrusions of the growth cone leading edge provide constant sampling of the surrounding environment. Receptor-ligand binding, if coupled to the cytoskeleton, creates a molecular "clutch" that enables growth cone advancement (Mitchison and Kirschner, 1988). This clutch decelerates retrograde actin flow, allowing leading edge protrusion via actin polymerization. The type, density, and spatial patterning of extracellular molecules and membrane receptors, as well as the state of the growth cone cytoskeleton and signaling milieu, contribute to the extension rate and direction the growth cone takes. In addition to providing physical force, adhesion molecules also trigger signaling cascades that direct growth and guidance. Studies using soluble ECM molecules have demonstrated that adhesion signaling can affect growth and guidance separately from its role in physical traction (Rivas et al., 1992; Kohno et al., 2005).

Numerous adhesion molecules crucial for neuronal differentiation, growth and guidance have been identified and characterized. These neuronal cell adhesion molecules (CAMs) are expressed in space and time coincident with nervous system development and include integrins, N-cadherins, and members of the immunoglobulin (Ig) superfamily, L1CAM and neural cell adhesion molecule (NCAM) (Kiryushko et al., 2004). Components of the extracellular matrix also provide essential adhesion substrates, including fibronectin, collagen and laminin, all of which are recognized by integrin receptors. In particular, laminin is widely-expressed in developing nervous system and stimulates robust neurite initiation and extension both *in vitro* and *in vivo* (McKerracher et al., 1996).

To translate ligand binding into protrusive force, the cytoskeleton must be coupled to CAM receptors. With N-cadherins, this link involves the binding of calcium-sensitive catenins to the cytoplasmic domain of cadherin (Aberle et al., 1996), and with L1, the cytoskeletal link is provided by ankyrins and ERM proteins (Davis and Bennett, 1994; Dickson et al., 2002; Mintz et al., 2003). However, the nature of intracellular events involved in force generation has been most thoroughly studied with integrin receptors. Upon binding to ECMs or IgCAMs, integrins cluster together and their cytoplasmic domain recruits paxillin, an adaptor protein that allows docking of additional molecules, including focal adhesion kinase (FAK). Paxillin activates FAK (Mitra et al., 2005), which can then phosphorylate other signaling molecules including the tyrosine kinase Src. Active FAK remodels actin through Rho GTPases, either directly by associating with Rho GAPs and GEFs (Ren et al., 2000), or through Src activation of p21-activated kinase (PAK), a known regulator of the Rho GTPases. FAK and paxillin can also reciprocally activate each other, creating a positive feedback loop. Other essential components of point contacts include vinculin and talin, which tether the cytoskeleton to integrins (Cypher and Letourneau, 1991; Varnum-Finney and Reichardt, 1994; Sydor et al., 1996). This accumulation of proteins culminates in a point contact, a focal region of signaling molecules and stabilized cytoskeleton-substratum connectivity (Gomez et al., 1996; Woo and Gomez, 2006). Point contact formation is essential for growth cone advancement, but must also be disassembled at the growth cone rear to allow continual forward progress.

Adhesion molecules can also modulate the response of growth cones to other guidance cues. Through regulation of the rate of axonal outgrowth, adhesion molecules may indirectly alter the response to guidance cues in that rapid growth may make the growth cone less sensitive to irrelevant cues and conversely more sensitive at crucial choice points by slowing. In support of this, growth cones *in vivo* pause at decision points, allowing for a thorough assessment of instructional cues (Mason and Erskine, 2000). Adhesion molecules also more directly modify a growth cone's response by affecting signaling. For example, NGF increases sensory neuron growth on laminin, but has no such effect on L1 (Liu et al., 2002). In *Xenopus* neurons, netrin is attractive on fibronectin or poly-D-lysine, but repulses growth cones on laminin (Hopker et al., 1999), an effect mediated by lower cAMP levels on laminin compared with other substrates (Ming et al., 1997; Hopker et al., 1999). Although still not well understood, recent studies are revealing an increasingly important role for point contacts in growth cone turning (Robles and Gomez, 2006). In one such case, FAK expression in retinal ganglion cells mimics that of EphA receptors, with higher expression in the temporal retina, and FAK activity mediates the inhibitory response of temporal RGCs to ephrin and stabilizes point contacts in RGCs with low ephrin levels (Woo et al., 2009).

Taken together, adhesions are essential to a growth cone's advance, and the expression patterns of various adhesion molecules modulate crucial guidance decisions.

Protein synthesis

In addition to altering the activity of existing proteins, regulating protein synthesis could offer an additional means for responding to guidance cues. Until recently, protein synthesis was thought to be restricted to neuronal cell bodies. Despite the long distances separating an extending growth cone from its soma, the mechanisms which transport newly synthesized proteins to the neurite tip were originally considered sufficient (Kelly and Grote, 1993). However, the concept of autonomous protein synthesis in growth cones is practical when considering the diverse environments growth cones must traverse en route to their targets, as well as the necessity of continually maintaining optimal levels of receptors and cytoskeletal components. To this end, local protein synthesis is an attractive model to describe how a growth cone re-sensitizes to a cue as it navigates through a concentration gradient, or how it switches a response from attraction to repulsion as a growth cone moves beyond an intermediary guidepost. There may also be some theoretical advantages to relying on local protein synthesis versus modifying the activities of existing proteins (Lin and Holt, 2008). One obvious use would be a rapid method for changing protein expression without the delay of transport from the cell body.

A host of recent studies have indeed shown that transfer and messenger RNAs are found in distal axonal compartments, along with the ribosomal machinery necessary for local protein synthesis (Bassell et al., 1998; Koenig and Giuditta, 1999; Alvarez et al., 2000; Campbell and Holt, 2001; Lin and Holt, 2007, 2008). Some have indeed found that growth cones may utilize protein synthesis to re-sensitize to a cue while migrating up a gradient (Ming et al., 2002; Piper et al., 2005). Others have

found that repulsive guidance cues induce rapid changes in protein expression (Campbell and Holt, 2001; Wu et al., 2005; Piper et al., 2006). Most recently, the asymmetrical synthesis of beta-actin in *Xenopus* growth cones was found to mediate attractive turning to BDNF and netrin-1 (Leung et al., 2006; Yao et al., 2006).

However the vast majority of these studies were conducted with *Xenopus* neurons, so it is not clear how well these data extrapolate to other organisms and systems. Moreover, the body of literature thus far has shown that changes in protein activity can mediate the guidance of growth cones to their target tissues. Therefore, the extent to which protein synthesis is essential and the circumstances under which it is necessary for growth cone guidance remains unclear.

Guidance cues

Guidance cues are molecules expressed in the developing organism that influence the advancement and trajectory of growth cones. These can take two forms: secreted proteins that can diffuse over distances and immobilized proteins expressed on cell surfaces. However, once diffused, secreted proteins are likely bound to the surrounding extracellular matrix or to the surfaces of cells. The effect a cue has on growth cone behavior is not necessarily intrinsic to the cue, but depends on the type and level of receptor expression, the presence of other cues, and the signaling milieu of the growth cone.

Classic *in vivo* experiments suggested the differential expression of cues in tissues underlie the accurate formation of neuronal connections (Sperry, 1943; 1945), a hypothesis that has since been confirmed. Similar experiments *in vivo* have

informed studies *in vitro*, which have parsed out the effect of specific cues on growth cone behavior. Numerous attractive and repulsive guidance cues have been identified. Among the various attractive cues, nerve growth factor (NGF) and netrin-1 have been shown *in vitro* and *in vivo* to attract sensory (DRG) neuronal growth cones and retinal ganglion cells, respectively. However, little is known regarding how these cues reorganize growth cone actin to produce attractive turning.

NGF

The neurotrophins are known to have diverse effects on neurons, including differentiation, survival, and growth. Access to NGF by distal neurites is required for outgrowth and survival (Campenot, 1977). Studies *in vitro* show that gradients of NGF induce attractive growth cone turning (Letourneau, 1978; Gundersen and Barrett, 1979), and contact with a localized NGF source induces local F-actin accumulation (Gallo and Letourneau, 1998). Because sensory neurons are dependent on NGF for survival, it was originally difficult to separate the potential chemotropic properties of NGF from its chemotrophic properties *in vivo*. However, double knockout mice lacking NGF and BAX solved this by removing dependence on NGF for survival, and subsequently enabled the study of its chemotropic properties *in vivo*. In doing so, NGF was conclusively shown to be necessary for sensory innervation of skin and sympathetic targets (Patel et al., 2000; Glebova and Ginty, 2004).

Nerve growth factor is synthesized in developing epithelium and reaches peak levels of approximately 40-90ng/g coincident with the arrival of sensory fibers (Davies et al., 1987). Two NGF receptors are expressed in developing DRG growth

cones: the pan-neurotrophin receptor (p75NTR) and the tropomyosin-related kinase A (trkA) receptor (Weskamp and Reichardt, 1991). When the p75NTR is present alone, it binds NGF with low affinity and mediates apoptosis. When both receptors are expressed, they interact through transmembrane and cytoplasmic domains, and this interaction increases trkA's affinity for NGF (Chao and Hempstead, 1995). Nerve growth factor binding trkA induces receptor dimerization and autophosphorylation, providing substrates for adaptor molecules. Multiple signaling cascades ensue, including activation of protein kinase A (PKA), Ras/MAPK, phosphatidylinositol-3 kinase (PI3K) and Akt. Neuronal survival is promoted through PI3K/Akt and MAPK pathways downstream of trkA activation, which can also interfere with p75-induced apoptosis (Kaplan and Miller, 2000).

Studies have found both p75NTR and trkA are involved to differing degrees in axon growth and guidance. When unbound, p75NTR inhibits neurite outgrowth through RhoA activity, which is then abolished upon NGF binding (Yamashita et al., 1999). In sensory neurons *in vitro*, attractive growth cone guidance to NGF is mediated through trkA and depends on PLC and PI3K signaling, and possibly a subsequent increase in calcium and cAMP (Gallo et al., 1997; Ming et al., 1999). The role of the p75NTR in guidance appears mainly to enhance trkA's affinity for NGF (Gallo et al., 1997; Esposito et al., 2001).

Hence, ample evidence exists for sensory neuronal attraction to NGF, yet how this occurs at the level of growth cone actin and actin-binding proteins remains unknown.

Netrin-1

Netrins are a family of diffusible guidance cues essential for the accurate targeting of multiple projections in the developing nervous system. Numerous studies have shown that netrins can induce attraction or repulsion depending on the growth cone receptor expression (Moore et al., 2007; Round and Stein, 2007). In the developing nervous system, the attractive guidance of dorsal spinal neurons to the floorplate and temporal retinal ganglion cells to the optic nerve head are dependent on netrin binding to its receptor Deleted in Colorectal Cancer (DCC) (Kennedy et al., 1994; Deiner et al., 1997). Netrin binding to DCC activates numerous adaptor proteins and signaling cascades, including PLC-gamma, MAPK, and PI3K (Round and Stein, 2007). Rho GTPases can also be activated, either directly through cytoplasmic adaptor proteins or through changes in growth cone calcium or cAMP/ cGMP levels (Ming et al., 1997; Hong et al., 2000; Nishiyama et al., 2003; Wen et al., 2004). Studies have shown netrin-binding to DCC induces a signaling complex of Nk1, witch activates Pak1, Rac1, and Cdc42, and N-WASP, increasing growth cone F-actin (Li et al., 2002a; Shekarabi et al., 2005). Additionally, inhibiting Rho activity increases DCC membrane insertion, suggesting the Rho GTPases may influence netrin-mediated guidance in complex ways (Moore et al., 2008b).

Netrins can also induce repulsive growth cone turning through activation of a heterodimer of DCC and Unc5 (Round and Stein, 2007). Repulsion to netrin-1 may involve moderate increases in calcium, which can activate calcineurin and protein phosphatase 1 (PP1) (Wen et al., 2004; Round and Stein, 2007). Studies with *Xenopus* neurons *in vitro* have also shown that inhibition of cAMP or PKA activity

converts netrin-mediated attraction to repulsion (Ming et al., 1997; Hopker et al., 1999), though these results may not translate to other systems (Moore and Kennedy, 2006; Moore et al., 2008a).

Thus, netrin-1 has a well-established role as a guidance cue. Yet, similar to NGF, relatively little is known regarding the role of actin-binding proteins in mediating growth cone responses to netrin.

Summary

Since the first description of the growth cone a wealth of information has accumulated on these curious structures. We now have a better understanding of guidance cues, receptors, actin-binding proteins, and signaling molecules involved in the steps taken by growth cones to reach their target tissue. However, our understanding is far from complete. Particularly lacking is a comprehensive grasp on how specific cues evoke guidance behaviors at the level of actin filaments.

This thesis presents evidence to support the hypothesis that AC and ERM activation mediate growth cone guidance to attractive cues. The first chapter examines the role of ADF/cofilin in growth cone guidance to NGF and netrin-1, and demonstrates a mechanism by which activated AC increases F-actin polymerization and content in growth cones. The second chapter examines the role of activated ERM proteins in guidance to NGF, and characterizes how AC and ERM proteins cooperate to produce attractive growth cone turning. Finally, the third chapter demonstrates that changes in local protein synthesis are not necessary to mediate attractive turning to NGF.

Collectively, this thesis presents a mechanism by which a gradient of NGF stimulates proximal AC activation, which then severs filaments and increases free barbed ends to produce proximal F-actin polymerization. This F-actin increase also relies on NGF-mediated ERM activation, which tether actin filaments to the membrane and prevent F-actin loss to retrograde flow. Finally, activation of AC and ERM proteins mediate attractive turning to NGF, a process that occurs independent of local protein synthesis.

Chapter II: Activation of ADF/cofilin mediates attractive growth cone turning toward nerve growth factor and netrin-1

This chapter was modified from the original work published as:

Bonnie M. Marsick, Kevin C. Flynn, Miguel Santiago-Medina, James R. Bamburg, and Paul C. Letourneau

Activation of ADF/cofilin mediates attractive growth cone turning toward nerve growth factor and netrin-1.

Developmental Neurobiology (2010), 70:565-588

Introduction

Accurate wiring of neural networks requires that axonal growth cones follow paths determined by extrinsic guidance cues (Letourneau and Cypher, 1991; Mitchison and Kirschner, 1988; Song and Poo, 1999; 2001; Tessier-Lavigne and Goodman, 1996). These cues direct growth cones by binding receptors to trigger signaling cascades that produce cytoskeletal modifications (Bentley and O'Connor, 1994; Huber et al., 2003; Kozma et al., 1997; Lin et al., 1994; Lowery and Van Vactor, 2009; Tanaka and Sabry, 1995; Theriot and Mitchison, 1991). Despite the identification of numerous cues and signaling cascades, the roles of downstream actin regulatory proteins are poorly understood (Dent and Gertler, 2003).

Neurotrophins, which affect multiple aspects of neuronal development, are also guidance cues (Casaccia-Bonnefil et al., 1999; Chen et al., 1999; Davies, 2000; Henderson, 1996; Schuman, 1999). Studies *in vitro* (Gunderson, 1985; Gunderson and Barrett, 1979; Letourneau, 1978) and *in vivo* (Glebova and Ginty, 2004; Hassankhani et al., 1995; Menesini Chen et al., 1978; Patel et al., 2000) show that the neurotrophin nerve growth factor (NGF) is an attractive cue for sensory and sympathetic neurons and is necessary for target innervation. Netrins are another well-characterized group of guidance cues that induce attraction or repulsion depending on receptor expression (Kennedy et al., 1994; Moore et al., 2007; Round and Stein, 2007).

It is proposed that attractive cues, such as NGF and netrin-1, favor actin stabilization and polymerization in the growth cone proximal side (Dent et al., 2004; Gallo and Letourneau, 1997, 2000; Lebrand et al., 2004; Lin and Forscher, 1993;

O'Connor and Bentley, 1993; Quinn et al., 2008; Sabry et al., 1991; Seeley and Greene, 1983). However, the actin-binding proteins that mediate this actin reorganization are poorly understood. Actin depolymerizing factor and cofilin (AC) family proteins remodel actin filaments by enhancing assembly/disassembly dynamics (reviewed by Andrianantoandro and Pollard, 2006; Chan et al., 2009; Sarmiere & Bamburg, 2003). AC is inactivated by phosphorylation at a conserved serine3 residue by multiple kinases, including LIM kinases 1 and 2 (Arber et al., 1998; Toshima et al., 2001; Yang et al., 1998), and is activated by dephosphorylation via multiple phosphatases (Endo et al., 2003; Huang et al., 2008; Nagata-Ohashi et al., 2004; Niwa et al., 2002; Ohta et al., 2003). Furthermore, AC proteins are inhibited by phosphatidylinositol phosphates in a pH-dependent manner (Frantz et al., 2008).

Several studies suggest that AC may mediate some axonal guidance. AC proteins have roles in axon extension (Bamburg and Bray, 1987; Birkenfeld et al., 2001; Kuhn et al., 2000; Meberg and Bamburg, 2000; Meberg et al., 1998), and are implicated in regulating filopodial responses to neurotrophins (Chen et al., 2006; Gehler et al., 2004). Moreover, a direct role for AC in growth cone guidance was recently shown with X*enopus laevis* spinal neurons' response to bone morphogenic proteins (Wen et al., 2007). In carcinoma cells, AC activation stimulates local actin polymerization during chemotaxis (Ghosh et al., 2004; Mouneimne et al., 2004; 2006).

Here we report that NGF (sensory neurons), and netrin-1 (retinal ganglion cells) stimulate plasma membrane protrusion and actin polymerization in growth cone leading margins, while increasing active AC. Direct increases in active AC also

increase protrusion and growth cone F-actin levels. Local increases in active AC within the growth cone induce attractive turning, and reducing AC activity blunts turning to NGF or netrin-1. These data suggest that two important attractive cues promote growth cone turning by activating AC and inducing actin polymerization in the growth cone region proximal to the attractive cues.

Methods

Materials F-12 medium, B27 additives, poly-D-lysine (MW >300,000), jasplakinolide, Alexa Fluor 488 DNase1, Alexa Fluor 488- and 568–phalloidin, Alexa Fluor 488 and 568 secondary antibodies were purchased from Invitrogen. NGF, recombinant chick netrin, and L1–Fc were purchased from R & D Systems. Fc Fragment was purchased from Jackson Immuno Research. Chariot was purchased from Active Motif. White leghorn fertilized chicken eggs were purchased from Hy-Line North America, LLC. Cytochalasin D and all other reagents were purchased from Sigma-Aldrich, unless otherwise indicated.

Neuronal culture Glass coverslips were coated with 100ug/ml poly-D-lysine, rinsed with water, coated with 1% nitrocellulose dissolved in 100% amyl acetate (Fischer Scientific), dried, and coated overnight with 4 μg/ml recombinant L1–Fc mixed with 8 μg/ml Fc in phosphate buffered solution (PBS; Roche). Video dishes were made by gluing a coverslip (18 mm x 18 mm; Gold Seal) over a hole (5mm) in the bottom of a culture dish (Falcon 35 mm x 10 mm), allowed to dry, rinsed with water, and coated as described. Embryonic day 7 (E7) dorsal root ganglia (DRG) and temporal retina were removed from chick embryos according to procedures approved by the University of Minnesota Institutional Animal Care and Use Committee. Neural tissues were cultured on experimental substrates in F-12 with B27 additives and buffered to pH 7.4 with 10 mM HEPES. Neural tissues were cultured overnight in a humidified incubator at 37°C.

Xenopus laevis embryos were obtained as described previously (Gomez et al., 2003) and staged according to Nieuwkoop and Faber (1994). For spinal cord cultures, neural tubes were dissected from stage 22 embryos and explants were cultured in a 1x modified Ringer's solution.

Explants were plated on acid-washed glass coverslips coated with 25 μg/ ml laminin (Sigma) as described previously (Gomez et al., 2003). Cultures were fixed 12–16 h after plating with 4% Paraformaldehyde in Krebs+Sucrose Fixative (4% PKS) for 15 minutes and rinsed with PBS.

Preparation of NGF-coated beads NGF and BSA were covalently coupled to 6μm carboxylated beads (Polysciences, Inc) as described previously (Gallo et al., 1997).

Neuronal transfection DRG and retinal tissue was dissociated as described in Roche et al., 2009. Approximately 2 x 10^6 cells were transfected with one of the following: 1 ug of plasmid co-expressing GFP and shRNA against human cofilin (control), 1 μg of a plasmid encoding the fluorescent F-actin probe, green fluorescent protein (GFP)–utrophin calponin homology domain (UtrCH) kindly provided by Dr. W. M. Bement (University of Wisconsin, Madison, WI) (Burkel et al., 2007); 2 ug constitutively-active LIMK with 1 ug GFP; or 1ug ADF shRNA using the G-13 program of the Amaxa Biosystems Nucleofector, and the chicken neuron nucleofector reagents. Cells were cultured 24-48 h, as indicated.

RNA interference (RNAi) was performed using a DNA vector to express small hairpin RNAs (shRNA) from a polymerase III promoter. Chick ADF siRNA

oligonucleotides were designed using established criteria based on a corresponding sequence used successfully in mouse (Garvalov et al., 2007; Hotulainen et al., 2005) and inserted into the pSuper expression vector (Brummelkamp et al., 2002) containing the H1 polymerase III promoter. The sequence used in this study is 5'-GTGGAAGAAGGCAAAGAGATT -3'. The H1 pol III-shRNA cassette was then subcloned into pAdtrack plasmids which co-express GFP from a separate promoter, aiding the identification of transfected cells.

Time-lapse microscopy and quantitative fluorescence determinations

A Spot digital camera mounted on an Olympus XC-70 inverted microscope, and MetaMorph software (Molecular Devices) were used for all image acquisitions. In any one experiment, all images were acquired in one session. For collection of fluorescent images, exposure time and gain settings on the digital camera were kept constant, and image acquisition and analysis was performed as described in Roche et al., (2009). In MetaMorph, a line tool was used to outline the terminal 25 μm of each distal axon and growth cone, and background intensity value was subtracted from the fluorescence intensity value of the accompanying neuronal measurement.

Video and kymograph analysis E7 DRG or retinal explants were cultured 24 h, or transfected cells were cultured 48 h on L1-coated video dishes. A growth cone was selected, and imaged at 10 s intervals. When a cue reagent was added (40ng/ml NGF or Chariot+XACA3 for DRGs, or 500ng/ml netrin for retina), a blank frame was taken to mark the time of addition (as seen as a black line in the kymograph). The

video was then opened in ImageJ and three one pixel-wide lines were drawn perpendicular to the growth cone leading edge: one in line with the neurite axis (labeled 0º), and one on either side of the 0º line, at a 30º angle (labeled -30º and 30º). The angle of the 30º lines was taken at the approximate growth cone center at the video start. Using the "stacks → reslice" function, a kymograph was generated and enlarged for better visualization.

Retrograde flow measurements To determine retrograde actin flow rates, DRGs were transfected with GFP-actin, cultured overnight on L1, and imaged every 3 s for 3 min before and after the addition of 40 ng/ml NGF. Kymographs were generated for the distal 10 μm of growth cones (n=8), and flow rates were measured by tracking bright GFP-actin features, which are formed by unequal incorporation of GFP- and non-GFP actin monomers into polymerized filaments at the leading edge. Measuring retrograde flow using the movement of these features has been described previously, including a demonstrated sensitivity of this retrograde flow to the myosin-II inhibitior blebbistatin (Chan and Odde, 2008).

Immunocytochemistry Neuronal cultures were fixed and blocked as described in Roche et al., 2009. Coverslips were incubated with primary antibodies diluted in PBS containing 10% goat serum overnight at 4º C. Affinity purified antibody 12977 (ADF) was used at 1:200 dilution; 4321 (phospho-ADF/cofilin) and 3981 (XAC1) were used at 1:1000 dilution. Because both 12977 and 4321 are rabbit antibodies, we compared staining between groups of neuronal growth cones for which

immunostaining and image acquisition parameters were kept identical. Coverslips were then rinsed 3 times in PBS and incubated in PBS rinse for 1 h. For labeling F-actin, Alexa Fluor 568–phalloidin was applied at a 1:20 dilution, and mixed with secondary antibodies: Alexa Fluor 568 goat anti-rabbit or anti-mouse antibodies at 1:1000 dilution in PBS with 10% goat serum for 1 h. For labeling G-actin, 25 ng/ml Alexa Fluor 488 DNase1 was applied to coverslips for 1 h. For staining total ADC in growth cones subjected to gradients, a pipette coated with NGF, netrin, or BSA was presented to one side of growth cones for 5 min, pipette was removed and incubated 1 min in permeabilization buffer (described below) with 100nM phalloidin, fixed and stained.

Antibodies against γ-actin (7577) and β-actin pAb 2963 were generated in the lab of James Ervasti (University of Minnesota) and were kind gifts; β-actin antibody A1978 was purchased from Sigma and FITC-conjugated AC15 was purchased from Abcam. Generation of γ-actin Ab 7577 was described previously (Hanft et al, 2006) and was used at 1:100 dilution, and pAb 2963 was raised against the unique N-terminal peptide sequence of beta-actin and affinity purified against platelet actin as described in Prins et al., (2008), and was used at 1:25, For *Xenopus* and chick cultures, coverslips were incubated overnight at 4º C, rinsed in PBS, incubated 1 h in secondary. All staining, rinses, and image acquisitions were done in parallel. After rinsing 3 times in PBS, coverslips were mounted in *SlowFade* reagent (Invitrogen).

Pharmacological Inhibitors Cultures were treated with 20 nM cytochalasin D (Invitrogen), 40 nM jasplakinolide, or 500 nM K252a (Calbiochem) for 3 min prior to

NGF addition. Controls were treated with the same volume DMSO vehicle, which never exceeded 5 μl/ml.

Barbed end labeling This protocol was adapted from Chan et al., (1998). In summary, neurons were cultured overnight and treated as indicated. At room temp, the culture media was gently aspirated and a permeabilization buffer (1% BSA, .025% saponin, 138 mM KCL, 10 mM Pipes, 0.1 mM ATP, 3 mM EGTA, 4 mM MgCl2, pH = 6.9) with 100nM Alexa-fluor 488 phalloidin (Invitrogen) was added for 1 min, after which the buffer was aspirated and buffer containing 0.45 uM Rhodamine non-muscle actin (Cytoskeleton) was added for 4 min, after which the buffer was removed and cells were fixed with 4% paraformaldehyde and .05% glutaraldehyde, rinsed, and imaged.

Recombinant proteins and protein loading Recombinant XAC proteins were generated as described previously (Gehler et al., 2004). Proteins were delivered into cells using Chariot reagent (Active Motif; Morris et al., 2001), according to the manufacture's instructions. Briefly, 6 μl Chariot was complexed with 1 μg BSA, XACWT, or XACA3 for 1 h, then added to the culture medium or immobilized onto a nitrocellulose-coated micropipette.

Growth cone turning assay Turning was assessed as described previously (Roche et al., 2009). Briefly, micropipette tips were dipped in a 1% nitrocellulose solution, dried, then dipped several times in a PBS solution of 1 μg/ml NGF, BSA, XACA3, Chariot+XACA3, Chariot+BSA, or 10ug/ml netrin (retina). A growth cone was

imaged at 30 or 60 s intervals for 15 min. The micropipette tip was then positioned 100 μm from a growth cone at a 45° angle to the direction of axon elongation. Images were acquired 45 min after introducing the micropipette tip. NGF or Chariot+XACA3 was added to the culture medium at the beginning of some of the videos. Growth cone turning angles were determined as the change in direction of growth cone migration between the beginning and end of the image acquisition period (Ming et al., 1997).

Effects of Chariot-A3 gradient on GFP–UtrCH distribution in DRG growth cones

This was performed as described previously (Roche et al., 2009).

Statistical analysis Parameters of population values are reported as mean +/- SEM. All statistical analysis was by unpaired Student's t test, Mann-Whitney U test, or ANOVA for multiple comparisons.

Results

Nerve growth factor and netrin-1 induce growth cone leading edge protrusion

Guidance cues regulate growth cone motility. To assess the effects of attractive cues on protrusive activity, we cultured embryonic day 7 (E7) chick dorsal root ganglion (DRG) or temporal retina explants overnight on L1CAM, then imaged growth cones at 10 sec intervals for 5 min before and 5 min after adding 40ng/ml NGF (for DRGs) or 500ng/ml netrin (for retina) to the medium (Lebrand et al, 2004). We then generated kymographs of motility at 3 locations at the growth cone leading edge, in line with the neurite axis (0°) and at 30 degrees to either side of the axis (-30° and 30°). As seen in the kymographs, membrane protrusion from DRG and retinal growth cones increased within seconds of guidance cue addition (Figure 1A, B).

To better quantify this membrane protrusion we plotted the leading edge position in pixel numbers relative to the time of cue addition. These spatial positions were then averaged across five growth cones for each condition. As shown in Figure 1C and D, membrane protrusion is stimulated at all 3 kymograph locations at the growth cone leading edge following NGF or netrin addition.

Nerve growth factor and netrin-1 increase growth cone F-actin and free barbed ends

Since growth cone membrane dynamics depend on the underlying actin cytoskeleton, we next examined the changes in actin organization that accompany this increased membrane protrusion. We visualized monomeric actin (G-actin), using fluorescein-conjugated DNase I (Barak et al., 1981), and fluorescent phalloidin-stained filamentous actin (F-actin) in growth cones treated with control media, NGF

(DRG), or netrin (retina). This method was validated using cytochalasin D and jasplakinolide, agents that prevent and promote actin polymerization, respectively (Figure S1). Fluorescence intensities were quantified by tracing growth cones, subtracting background, and determining the mean growth cone integrated pixel intensity. Compared to controls, DRG growth cones treated with NGF for 5 min had a relative decrease in G-actin and increase in phalloidin-stained F-actin (Figure 2A, C). Similar changes were seen in temporal retina growth cones treated 5 min with netrin (Figure 2B, D). These data show an increased ratio of phalloidin to DNase I labeling (for DRGs, -NGF=0.85 ±0.07, +NGF=2.38 ±0.37; for retina, -netrin=3.96±0.42, +netrin=8.42±1.70), suggesting a shift from G-actin to F-actin in growth cones responding to NGF or netrin.

An increase in F-actin could result from decreased actin filament depolymerization and/or an increase in actin polymerization. To assess the number of F-actin barbed ends available for polymerization, we adapted a method for the first time to primary neurons in which cells are briefly permeabilized with saponin and then rhodamine-actin is added to polymerize the free F-actin barbed ends (Chan et al., 1998). DRG growth cones treated 15 min with 40ng/ml NGF before permeabilization showed significantly more rhodamine-actin addition to free F-actin barbed ends at the leading edge compared to growth cones of neurons treated with medium alone or grown overnight in 40ng/ml NGF (Figure 2E, F). Both cytochalasin D (20nM), which caps barbed ends, and K252a (500nM), an inhibitor of Trk receptors, blocked the NGF-induced increase in F-actin barbed ends available for rhodamin-actin.

The amount of F-actin at the leading growth cone margin is increased by actin polymerization and decreased by retrograde actin transport. Thus, a decrease in retrograde actin flow might contribute to the net F-actin increase that is induced by NGF. We therefore measured retrograde flow at growth cone leading margins by tracking the movement of bright F-actin features in kymographs of DRG neurons transfected to express GFP-actin (Chan and Odde, 2008). We found that retrograde actin flow was not significantly different after adding 40 ng/ml NGF (10. 5 ± 0.6 μm/min; n=9) than before NGF addition (11.4 ± 0.5 μm/min; n=9) (Figure S2). Together, these data suggest that NGF and netrin increase F-actin levels in DRG and retinal growth cones, respectively by stimulating F-actin polymerization.

Gradients of nerve growth factor and netrin-1 locally increase F-actin and free barbed ends

We next tested whether an increase in F-actin occurs locally in growth cones encountering extracellular gradients of NGF and netrin. Gradients were created by coating a micropipette tip with a protein solution and then placing the pipette tip near a growth cone (Roche et al., 2009). Figure S3A shows that a gradient of rhodamine-BSA was rapidly released from a nitrocellulose-coated micropipette tip, was established at 1 min, was sustained at 5, 15, and 15 min, and extended beyond the 100 μm distance from the pipette tip to a theoretical growth cone. Producing gradients this way, DRG growth cones turn toward an NGF source (Figure 3A, 7B, 8B) and retinal growth cones turn toward a netrin source (Figure 8C; Movie S1).

To assess the effects of guidance cue gradients on growth cone F-actin distribution we fixed growth cones 5 min after the introduction of BSA-, NGF-(DRG), or netrin-(retina) coated micropipettes, then labeled F-actin with fluorescent phalloidin. To quantify asymmetries in F-actin distribution, we measured the integrated phalloidin intensity in 20x20 pixel-wide boxes in three regions across the growth cone width, and calculated the distal (region1/region2) and proximal (region3/region2) intensity ratios relative to the center (Figure 3B). Pseudo-colored images of fluorescent phalloidin staining intensity in growth cones indicated that F-actin content is higher in growth cone sides proximal to an NGF (DRG) or netrin (retina) source, but this asymmetry was not present in growth cones exposed to a BSA gradient (Figure 3C). Quantification of this phalloidin staining further indicated higher F-actin levels in regions proximal to the NGF or netrin source, but not a BSA source (Figure 3D). These data support the hypothesis that netrin and NGF gradients induce increased F-actin in growth cone regions closer to the attractive cue source.

To determine if local increases in free F-actin barbed ends also occur, we performed our barbed end labeling assay on growth cones subjected to a NGF (DRG) or netrin (retina) gradient for 5 minutes. Growth cones from DRGs had increased barbed ends proximal to the NGF source, where no such asymmetry occurred with a BSA gradient (Figure 3E). A similar increase was also found in retinal growth cones subjected to a netrin gradient. Because recent studies in *Xenopus laevis* growth cones have shown local protein synthesis plays a role in growth cone guidance (Leung et al., 2006; Yao et al, 2006), we bath-applied the protein synthesis inhibitor cycloheximide at 20μM (see image in panel E) five minutes prior to introduction of the NGF

gradient, and found this local increase in F-actin barbed ends still occurred. The majority of barbed end labeling was at the leading edge, so to quantify the distribution we traced a 5 pixel-wide line from the distal base of the growth cone along the leading margin to the proximal base, and obtained an intensity profile (Figure 3E). This intensity line was then divided, and the pixel intensities along the line segments proximal and distal to the cue were summed. We found the proximal/distal ratio of barbed end staining intensity was significantly higher in DRG growth cones exposed to an NGF gradient versus a BSA gradient (Figure 3E). Together, these data suggest NGF (DRG) and netrin (retina) locally stimulate actin polymerization proximal to the cue source.

ADF/cofilin family proteins are activated by NGF and netrin

We next investigated the role of AC family proteins in this guidance cue-induced F-actin increase. AC proteins are inactivated by phosphorylation at serine 3. Upon dephosphorylation, AC proteins bind to and modify actin filaments. To determine if acute NGF addition affects the level of active AC, we measured the levels of total chick ADF and inactive phosphorylated ADF/cofilin (pAC) in growth cones via immunocytochemistry, using FITC as a control for total protein. Previous work has shown that expression of ADF in chick brain greatly exceeds (about 10 fold) expression of cofilin (Devineni et al., 1999). Compared to untreated growth cones, 5 min treatment with NGF had no significant effect on the total amount of ADF in growth cones, but did significantly lower the total levels of phospho-AC

(Figure 4A). Similarly, 5 min treatment of retinal neurons with netrin significantly reduced total phospho-AC levels but not total ADF (Figure 4B).

Having found that global addition of NGF reduces the content of inactive phospho-AC in DRG growth cones, we wanted to know if a local NGF source stimulates local AC activation. To do so we examined the levels of phospho-AC in regions of growth cones that touched a bead with surface-bound NGF (Gallo and Letourneau, 1998; 2004). DRG cultures were incubated with 6 μm beads conjugated with BSA or NGF for 60 minutes, then fixed and stained for phospho-AC, FITC (total protein), and fluorescent phalloidin binding (F-actin). Compared to growth cone regions that contacted a BSA bead or growth cone regions that did not contact NGF- or BSA- beads, there was a significantly lower phospho-AC level in growth cone regions that contacted an NGF bead (Fig 4C).

Despite the above demonstrations that phospho-AC levels are reduced by global NGF or netrin and reduced near contact with NGF-coupled beads, we were not able to detect local phospho-AC staining differences in growth cones exposed to gradients of NGF or netrin. Several reasons may account for this. Compared to conditions where small growth cone regions were contacting a local and stable NGF source presented on a bead (Fig 4C), the gradient of NGF across the growth cone width using the micropipette is comparatively shallow. Furthermore, the fixation of a relatively small (20kDa) and soluble protein such as phospho-AC, which does not bind F-actin, may not be rapid enough to preserve its distribution in this shallow gradient, and these small differences may be undetectable using our immunocytochemical methods. Although Wen et al (2007) demonstrated asymmetric

phospho-AC distribution in *Xenopus* growth cones responding to BMPs, these growth cones turned away from regions of higher AC activity, suggesting the gradient of pAC may be steeper in this repulsion behavior compared to a growth cone turning toward higher AC activity. Furthermore, *Xenopus* growth cones have less actin compared to our chick growth cones (Fig 10), which suggests differences in actin regulation exist between the two species.

However, the asymmetric labeling of barbed ends in this gradient (Fig 3E) suggests asymmetric AC activation does occur. Thus, in order to probe localized AC activity in our conditions used for growth cone turning, we exposed growth cones to a NGF or netrin gradient for 5 min, and applied our phalloidin-containing permeabilization buffer for 1 minute prior to fixation. Under these conditions, all phospho-AC staining was lost, presumably because inactive phospho-AC is not bound to F-actin and diffuses from the growth cone upon permeablilization. We then stained for total ADF, assuming that active ADF would be bound to F-actin, and not lost upon permeabilization. Under these conditions, we found significantly higher ADF staining proximal to the NGF (DRG) or netrin (retina) source, with no such asymmetry in growth cones exposed to a gradient of BSA (4D). Together, these data suggest that NGF and netrin activate AC in DRG and retinal growth cones, respectively, in both a global and localized manner.

Increased AC activity results in increased F-actin and barbed ends

Results thus far suggest that increased AC activity contributes to the NGF- and netrin-1 – induced increase in growth cone F-actin. To test this, we used the

Chariot reagent, which forms cell-permeable complexes with proteins, to load purified recombinant *Xenopus* ADF/cofilin into our cultured neurons. Chariot-mediated incorporation of these proteins into growth cones was confirmed immunocytochemically, using an antibody against *Xenopus* AC (XAC1) that has little cross-reactivity with chick AC (Shaw et al, 2004). Compared to chick DRGs incubated 1 hour with Chariot alone or wild-type *Xenopus* AC (XACWT) not complexed with Chariot, growth cones treated with Chariot-XACWT had significantly more XAC1 staining (Fig 5A). Thus, using this method we loaded DRG and retinal neurons with Chariot complexes of XACWT or a "constitutively-active" XAC with a serine3 to alanine mutation that renders it non-phosphorylatable (XACA3; Gehler et al., 2004). We assessed G- and F-actin levels as before, and found in both neuronal types that the Chariot-mediated incorporation of XACWT or XACA3 increased phalloidin-stained F-actin levels and reduced DNase I staining of G-actin (Figure 5B, C). The addition of NGF to XAC-loaded DRG growth cones further increased F-actin levels, presumably through activation of endogenous AC. Netrin addition to XAC-loaded retinal growth cones did not significantly alter F-actin levels, which could be due to actin properties in retinal growth cones that limit the extent of F-actin increase upon XAC-loading and netrin addition. In support of this, the magnitude of XAC-induced F-actin increase in retinal neurons was smaller compared to DRGs. Taken together, these data demonstrate that directly elevating AC activity increases F-actin in DRG and retinal growth cones.

Because the severing activity of AC proteins can increase the number of F-actin barbed ends available for polymerization, we assessed if incorporation of AC

into growth cones increases F-actin barbed ends. We treated DRG growth cones 1 h with Chariot alone or Chariot complexed with XACWT or XACA3 and then assayed for F-actin barbed ends. Compared to controls, XACWT- or XACA3-treated growth cones had significantly higher levels of free barbed ends (Figure 5D). In addition, NGF treatment of XACWT- or XACA3-treated neurons further increased barbed end labeling, likely due to activation of endogenous chick AC. In addition, the morphology of NGF-treated growth cones was larger and more flattened than growth cones incubated with Chariot-XAC alone (Fig 5D), suggesting that NGF induces additional changes that contribute to the change in growth cone shape.

Taken together, these data show that direct elevation of active AC increases F-actin levels in DRG and retinal growth cones, mimicking the effects seen with NGF and netrin. Furthermore, the direct elevation of AC also increases F-actin barbed ends in DRG growth cones.

Gradients of cell-permeable active AC induce local increases in F-actin and attractive growth cone turning

Our data show global and local addition of the guidance cues NGF and netrin increase growth cone F-actin and AC activity, and directly increasing AC activity also increases growth cone F-actin. We next examined growth cone turning behavior, F-actin distribution and AC asymmetry in growth cones responding to gradients of cell-permeable Chariot-XACA3. Figure S3B shows that Chariot-rhodamine-BSA complexes diffused similarly from micropipette tips as rhodamine-BSA (Figure S2A). Gradients of Chariot-XACA3 induced attractive turning of both DRG and retinal

growth cones (Figure 7A, movies S2 and S3), while growth cones did not turn in a Chariot-BSA gradient (Figure 7B). Importantly, growth cones also did not turn in a gradient of extracellular XACA3 that was not complexed with Chariot, indicating that growth cone turning is induced by an intracellular, but not extracellular, asymmetry of AC activity. To show that this method does produce an intracellular asymmetry in XAC, we fixed growth cones 15 min after introduction of a micropipette coated with Chariot-XACWT or XACWT alone, then stained the growth cones with an antibody selective for *Xenopus* AC (XAC1). Quantification of growth cone XAC1 staining distribution showed that growth cones exposed to a gradient of XACWT without Chariot had no asymmetry in XAC1 staining, whereas growth cones subjected to a Chariot-XACWT gradient had higher XAC1 staining proximal to the micropipette (Figure 6A). These results indicate that growth cones turn toward the side with higher intracellular AC activity. To determine if this local increase was associated with locally increased F-actin, DRG growth cones were subjected to pipette tips coated with Chariot-XACA3 or XACA3 alone for 15 min, fixed and then stained with fluorescent phalloidin. Similar to our results with an NGF or a netrin gradient, fluorescent phalloidin staining was more intense in the growth cone regions proximal to a Chariot-XACA3 source but not a source of XACA3 alone (Figure 6B).

F-actin distribution in live cells can be visualized by transfection to express an F-actin binding domain of utrophin conjugated to GFP (GFP-UtrCH; Burkel et al., 2007). To examine F-actin distribution in real time we transfected DRG neurons with GFP-UtrCH, and as reported in Roche et al. (2009), the GFP-UtrCH fluorescence intensity was higher in the proximal side of growth cones at two min after introducing

an NGF gradient (6C; Roche et al, 2009). A BSA gradient produced no asymmetry in the distribution of GFP-UtrCH intensity. We used this approach to confirm results based on phalloidin staining that F-actin is more concentrated in the growth cone region proximal to a chariot-XACA3-releasing pipette tip (Figure 6B). DRG neurons were transfected to express GFP-UtrCH, and we assessed F-actin distribution in live growth cones that were subjected to a gradient of Chariot-XACA3. A fluorescence image was taken before and 5 min after introducing a Chariot-XACA3-coated pipette tip to one side of a growth cone. To analyze the response, a 15 pixel wide line was drawn across a growth cone and the "linescan" function was used to generate fluorescence intensity measurements across the growth cone width (in Metamorph). To quantify GFP-UtrCH distribution, the proximal/distal intensity ratios of growth cones before and after introducing the pipette were computed. For GFP-UtrCH expressing growth cones exposed to a Chariot-BSA gradient, this ratio was 1.12±0.05 SE (n=9), and for growth cones exposed to Chariot-XACA3 the ratio was 1.40±0.09 (n=10), which was significantly different from growth cones exposed to Chariot-BSA ($p<0.05$) (Figure 6C). As a control for volumetric changes after introducing the Chariot-XACA3 gradient, we measured fluorescence intensity across GFP only-transfected growth cones. The proximal/distal GFP ratio of 0.90±0.09 (n=8) was not significantly different from GFP-UtrCH transfected growth cones exposed to a Chariot-BSA gradient, suggesting that the increase in proximal UtrCH intensity induced by the Chariot-XACA3 gradient was not due to a local increase in volume.

Taken together these studies indicate that gradients of NGF, netrin and Chariot-XACA3 induce attractive growth cone turning and increased F-actin

distribution in growth cone regions proximal to the pipette tips. In addition, F-actin is more concentrated in growth cone regions containing higher AC activity. This is consistent with our earlier findings (Figure 4C) that staining for phospho-AC (inactive AC) is lower in growth cone regions contacting NGF-beads than in regions free of NGF-beads or in regions contacting BSA-beads, as well as the increased permeabilization-resistant ADF in growth cone regions proximal to a NGF or netrin gradient (Figure 4D).

Our evidence suggests that NGF induces attractive DRG growth cone turning by locally activating AC, which stimulates local actin polymerization in the growth cone region proximal to NGF. In support of this, we showed that a gradient of cell-permeable AC induces growth cone turning with both increased AC content and increased F-actin in the growth cone side toward the AC source. To further examine the role of asymmetric AC activity in mediating growth cone turning, we introduced an NGF gradient to growth cones in the presence of globally applied Chariot-A3 to raise AC activity throughout the growth cone and diminish NGF-induced asymmetry in AC activity (Figure 7B). We found the average turning angle to NGF was reduced compared to NGF turning in the absence of Chariot-A3, although the difference was not statistically significant ($p=0.099$). In like manner, the mean turning angle to a Chariot-A3 gradient was also reduced by global elevation of NGF, compared to A3 turning in the absence of NGF (but not statistically significant, $p=0.23$). In both cases, NGF gradient with global Chariot-A3 and Chariot-A3 gradient with global NGF, the average turning angle was significantly greater than turning toward a Chariot-BSA gradient ($p<0.05$). These data suggest that a small asymmetry in ADF/cofilin activity

across a growth cone can elicit attractive turning, but the reduced turning angles observed with diminished AC asymmetry provides further support that turning toward positive cues is mediated by intracellular asymmetry of AC activity. Furthermore, activation of additional proteins downstream of NGF signaling, including paxillin (Khan et al, 1995), integrins (Grabham and Goldbert, 1997), and microtubule plus end binding protein APC (Zhou et al, 2004) also likely affect growth cone trajectories in addition to AC activation.

Reducing AC activation or protein levels blocks NGF- and netrin-induced growth cone protrusion and turning

If local AC activation is necessary for attractive turning toward NGF and netrin, we would expect that blocking AC activation will block attractive responses to these cues. To test this we transfected neurons with either a constitutively-active LIMK construct (CA-LIMK) to maintain high levels of phosphorylated inactive AC, with a plasmid expressing GFP and a hairpin RNA that generates a small interfering siRNA against chick ADF, or with a GFP- control RNAi plasmid. As expected, neurons transfected with CA-LIMK and cultured 24hrs had higher levels of phospho-AC compared to GFP-transfected controls (Figure S4A). Neurons transfected with ADF-RNAi for 48hrs showed reduced ADF immunostaining, compared to GFP-control RNAi transfected cells or non-transfected cells (Figure S4C), and Western blot analysis showed ADF protein level was reduced in ADF-RNAi transfected chick embryo fibroblasts (Figure S4B).

We then examined growth cone responses to NGF in transfected DRG growth cones. As expected, in GFP-control RNAi DRG growth cones, leading edge protrusion increased immediately after adding NGF. Remarkably, growth cones expressing CA-LIMK or ADF RNAi had no protrusion increase following NGF addition (Figure 8A). Furthermore, compared to GFP controls, CA-LIMK expressing DRG neurons showed reduced attractive turning to NGF (Figure 8B), and the turning of retinal growth cones toward a netrin-coated micropipette was also reduced in CA-LIMK expressing retinal neurons (Figure 8C). Bath application of K252a, an inhibitor of the NGF receptor TrkA, also abolished turning toward NGF. Although the growth cones of CA-LIMK transfected DRG neurons advanced slower than GFP controls (1.4 +/- 0.04 μm/min for GFP, 1.18 +/- 0.16 μm/min for CA-LIMK), growth cones were observed 60 min, long enough to advance more than 60μm and complete a turning response. These data suggest that AC activation by NGF or netrin is necessary for membrane protrusion and attractive turning to NGF or netrin.

Restoring active AC to CA-LIMK and ADF RNAi growth cones rescues membrane protrusion

To determine if the block of NGF-induced membrane protrusion was specifically caused by the reduced AC activity, we added Chariot+XACA3 protein to GFP-control RNAi, CA-LIMK, or ADF RNAi-expressing growth cones, and examined leading edge dynamics. As seen in Figure 9, the addition of Chariot-XACA3 proteins increased growth cone protrusion in DRG neurons transfected with either of the three plasmids. These data support the notion that the reduction in NGF-

induced protrusion seen in CA-LIMK and ADF RNAi-expressing growth cones is due to reduced AC levels and not to other factors associated with the constructs.

Actin protein levels are higher in chick DRG growth cones compared to Xenopus laevis spinal neuronal growth cones

Our data suggest a local increase in AC activity can induce growth cone turning toward the side with higher activity. This finding is in direct contrast with that of Wen et al. (2007), where *Xenopus* spinal neuronal growth cones responding to bone morphogenic protein 7 (BMP7) turned toward the side with lower AC activity and away from the side with higher AC activity. Recent studies have found differing effects on actin organization at different ratios of AC to actin (Andrianantoandro and Pollard, 2006; Blanchoin and Pollard, 1999; Chan et al., 2009; Chen et al., 2004; Pavlov et al., 2007). We therefore sought to compare actin protein levels in chick and *Xenopus* spinal neuronal growth cones. Using immunocytochemistry, we stained chick DRG and *Xenopus* spinal neuron cultures simultaneously, using multiple antibodies against ß- and γ-actin. The very high sequence conservation for ß- and γ-actin among vertebrates suggests that these antibodies should recognize these actin isoforms similarly in frog and chick neurons. The integrated (sum) intensity was measured and normalized to total protein (FITC), except with FITC-conjugated AC15. Measurements of integrated growth cone intensities indicated lower levels of both γ-actin and β-actin in *Xenopus* growth cones compared to chick (Figure 10). These differences remained consistent with multiple antibodies, and when measured as a ratio to total protein using FITC (Figure 10). Additionally, we found *Xenopus*

growth cones had higher levels of DNase and lower levels of phalloidin staining, suggesting *Xenopus* growth cones have a higher G-actin:F-actin ratio compared to chick DRG growth cones.

We do not know the relative concentrations or basal activity of AC in chick versus *Xenopus*, nor possible differences in additional actin-binding proteins. Although further research is needed to determine if these actin differences are sufficient to account for these disparate results, it is not unreasonable to suggest that basal differences in actin expression could affect the net response of growth cones responding to guidance cues. For example, recent studies have shown local protein synthesis is important in growth cone guidance (Campbell and Holt, 2001; Wu et al., 2005; Piper and Holt, 2004), and specifically, local translation of β-actin mRNA in *Xenopus* growth cones (Leung et al., 2006; Yao et al, 2006). However, we recently reported normal growth cone guidance with chick and mouse neurons in the presence of protein synthesis inhibitors (Roche et al, 2009). These data suggest that in growth cones containing less actin, guidance cue-induced local protein synthesis may be more essential for growth cone turning compared to growth cones with higher actin levels, where reorganization of existing actin is sufficient. In the present study, these relative differences in actin levels and organization could affect how activated AC modifies actin filament dynamics.

Figure 1.

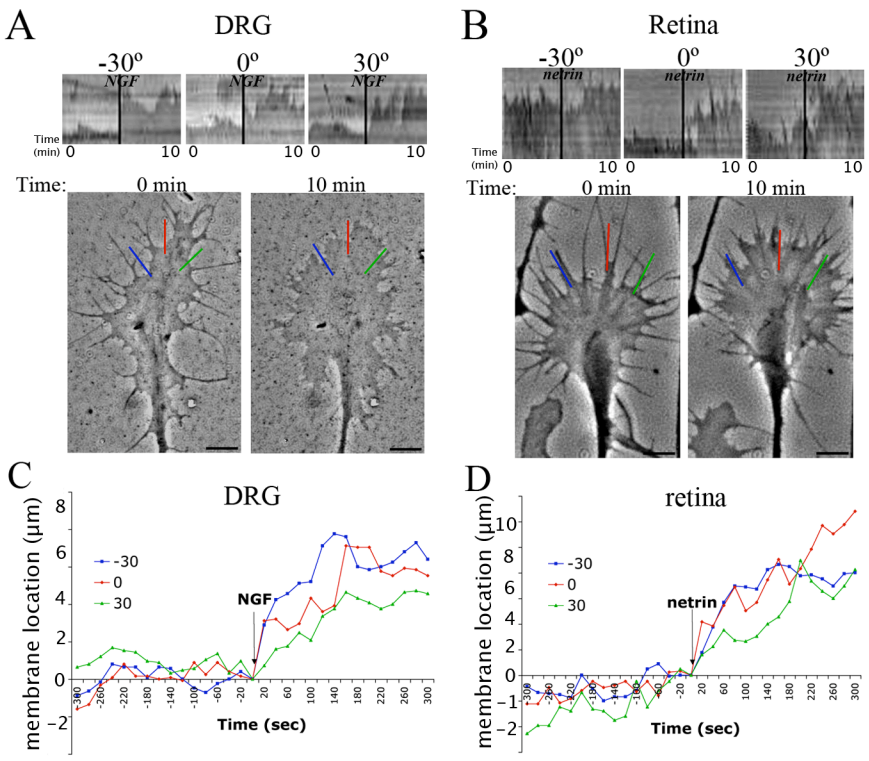

Figure 1. Nerve growth factor and netrin-1 induce leading edge protrusion. Embryonic day 7 (E7) DRG (A, C) or temporal retinal explants (B, D) were cultured overnight on L1CAM. A growth cone was imaged every 10 s for 5 min before and after adding 40ng/ml NGF (A) or 500ng/ml netrin-1 (B). Kymographs at three locations were generated using a line perpendicular to growth cone leading edge: one in line with the neurite axis (0°) and 30° to either side (-30° and 30°). In panels C and D kymographs were quantified to track position of the leading edge before and after addition of NGF (C) or netrin (D), and averaged across 5 growth cones per condition. Scale bars, 10µm.

Figure 2.

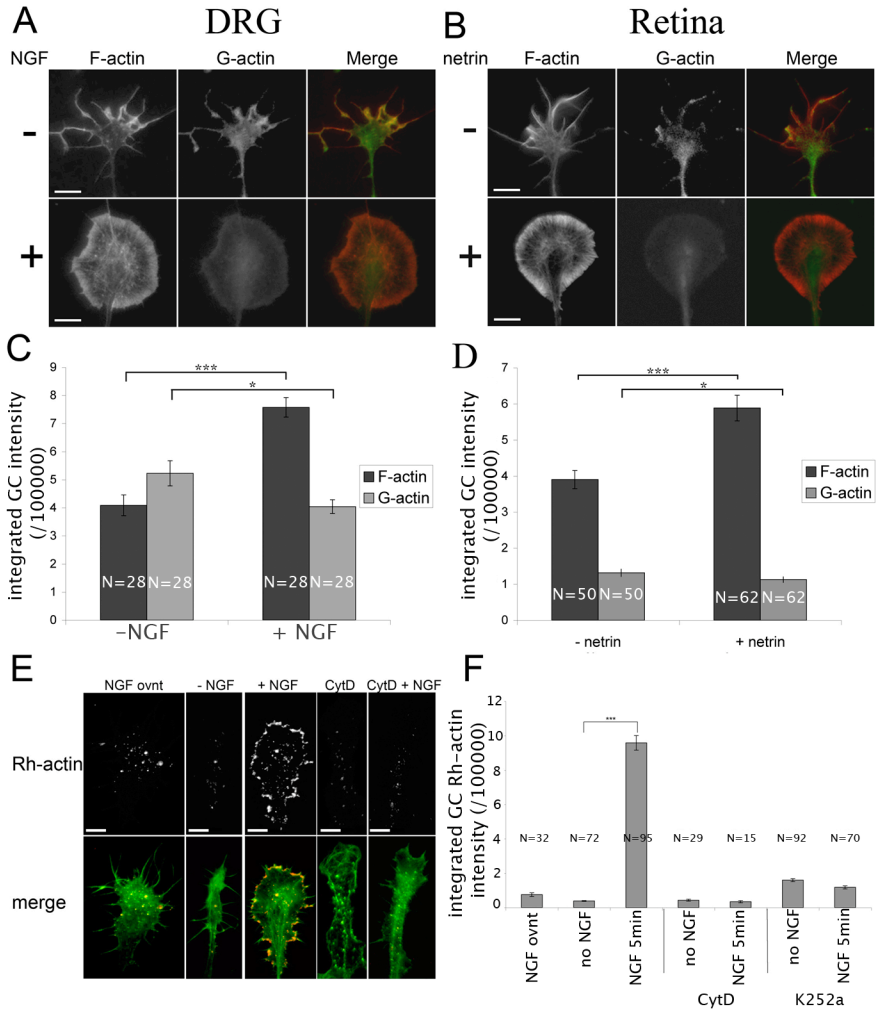

Figure 2. Nerve growth factor and netrin-1 increase growth cone F-actin, and NGF increases free F-actin barbed ends. DRG (A, C) or retinal explants (B, D) were treated 10 min with 40ng/ml NGF (A) or 500ng/ml netrin (B), then fixed. Quantitative fluorescence measurements of growth cone F-actin (Alexa Fluor 568-phalloidin; red) and G-actin (fluorescein-conjugated DNase1; green) were performed. Panels C and D show integrated growth cone fluorescence intensity of F-actin and G-actin in experimental populations. Panel E shows DRG growth cones stained to label F-actin (Alexa Fluor 488-phalloidin, green) or free actin barbed ends (Rh-actin, red). Panel F shows integrated rhodamine-actin growth cone intensity. Statistical significance using Student's *t* test. Data are means ± SEM; *P<0.05; ***P<0.0001. Scale bars, 10μm.

Figure 3.

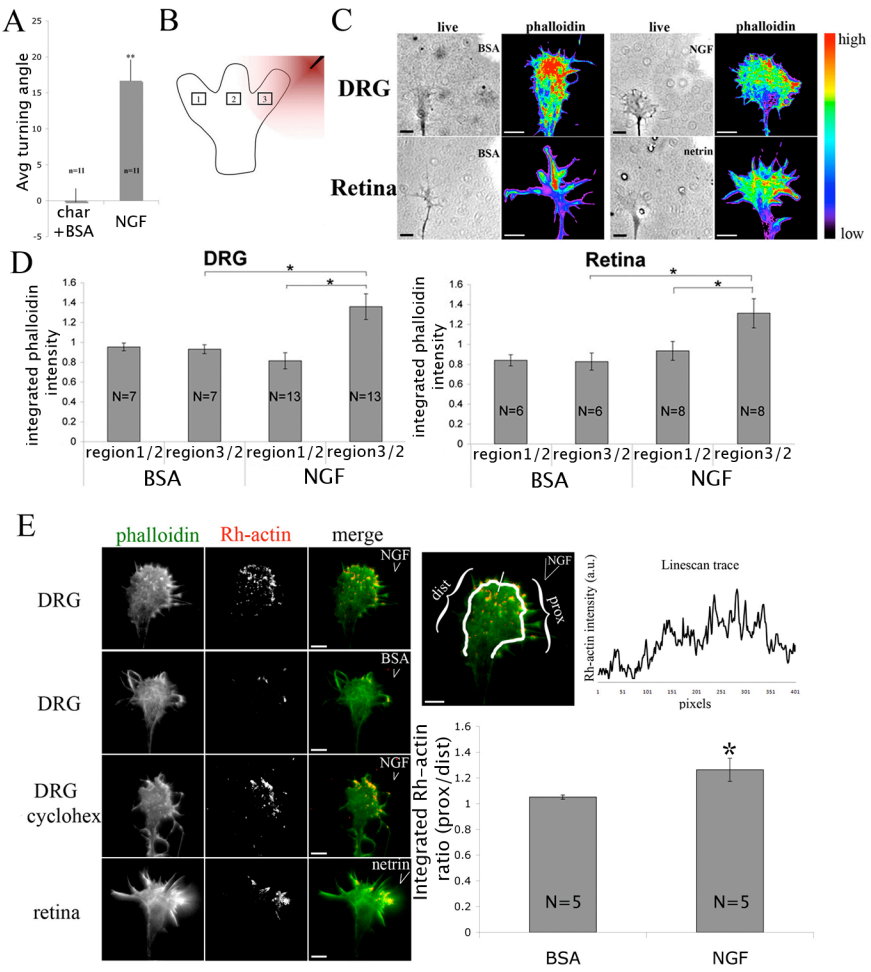

Figure 3. Growth cones exposed to a gradient of NGF or netrin-1 exhibit asymmetrical F-actin free barbed end distribution. DRG growth cones turn toward NGF (A), data is taken from panel 7B of this paper. Panel B depicts method used to quantify F-actin (in 3C, D, 6B) distribution across growth cones by measuring integrated intensities in 20x20 pixel-wide regions. Micropipette releasing protein is located to the right side of growth cones. For panel C, a micropipette releasing BSA, NGF, or netrin is introduced to one side of a DRG or retinal growth cone for 5 min, fixed, stained for F-actin (Alexa-488 phalloidin), and pseudo-colored. Distribution was quantified by taking the integrated intensities proximally (region 3) and distally (region 1), relative to the growth cone center (region 2). Panel E shows phalloidin

(green) and barbed end (red) labeling on growth cones subjected to a gradient of NGF (DRG), netrin (retina) or BSA for 5 min. Barbed end labeling distribution was performed taking the Rh-actin intensity linescan along growth cone membrane border, dividing in half, and computing the integrated ratio of proximal/distal intensity. Statistical significance using Student's *t* test. Data are means ± SEM; *P<0.05; **P<0.001. Scale bars, 10μm.

Figure 4.

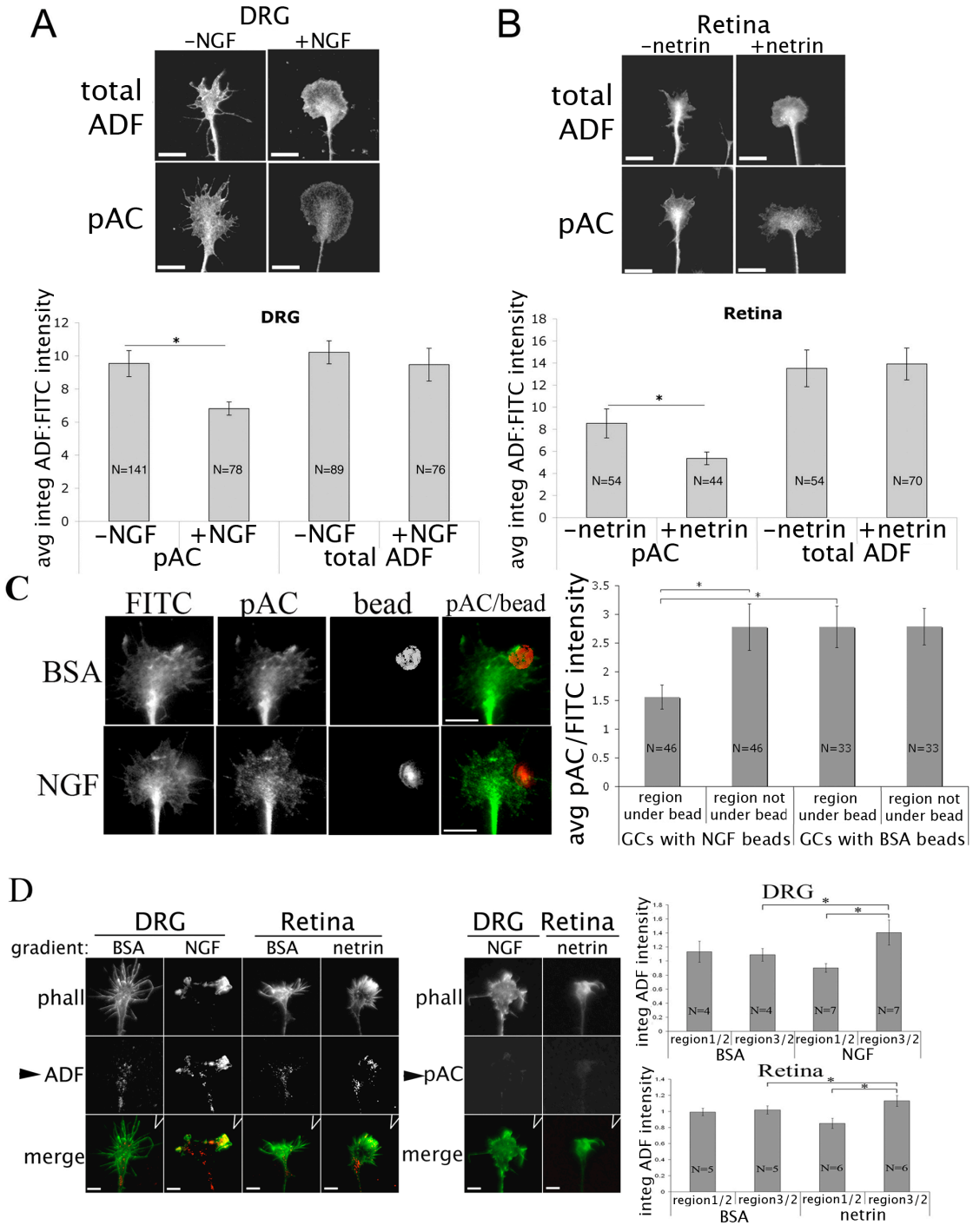

Figure 4. ADF/cofilin family proteins are activated by NGF and netrin-1. DRG (A) or retinal explants (B) were treated with medium or 40ng/ml NGF (A) or 500ng/ml netrin-1 (B) for 5 min, fixed and stained for chick ADF (ab 12977) or phospho-

ADF/cofilin (pAC; ab 4321), and FITC (total protein). Mean growth cone integrated intensity values were normalized to FITC. Panel C shows DRG growth cones incubated with BSA- or NGF-conjugated beads (pseudo-colored red from phase image) for 1 h, fixed, and stained for total protein (FITC), and pAC (green). Average intensities shown for growth cone regions under BSA or NGF beads, as well as regions of the same growth cone not under a bead, and normalized to FITC. Panel D shows pAC and total ADF (ab 12977) staining after growth cones were subjected to a NGF (DRG), netrin (retina) or BSA gradient for 5 min, permeabilized for 1 min with phalloidin, then fixed and stained. Quantifications were performed as in Figure 3B, and experiments were done on three separate days. Statistical significance using ANOVA. Data are means ± SEM; *$P<0.05$. Scale bars, 10 μm.

Figure 5.

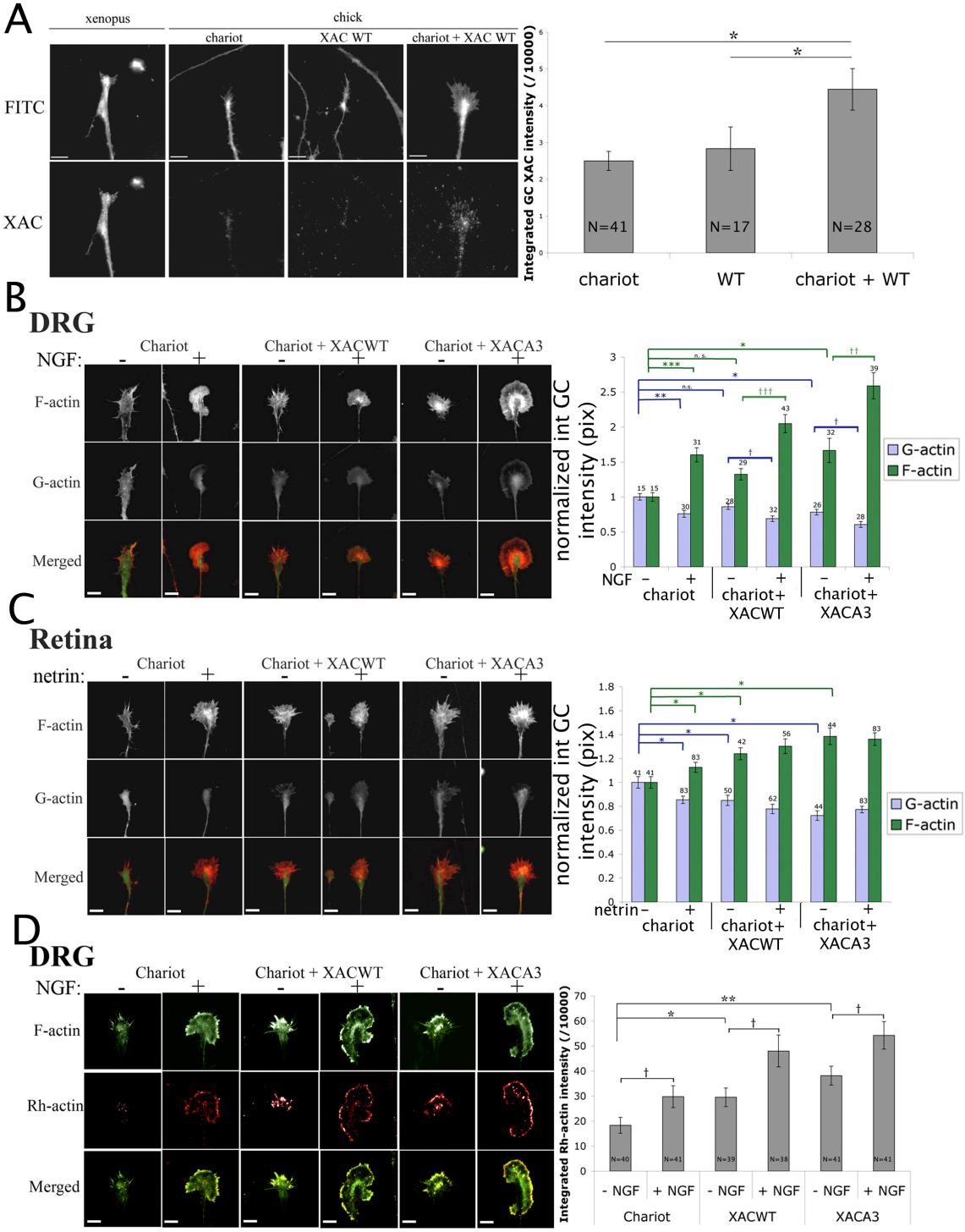
A
xenopus
chick
chariot
XAC WT
chariot + XAC WT
FITC
XAC
Integrated GC XAC intensity (/10000)
N=41
N=17
N=28
chariot
WT
chariot + WT
B
DRG
NGF:
Chariot
Chariot + XACWT
Chariot + XACA3
F-actin
G-actin
Merged
normalized int GC intensity (pix)
G-actin
F-actin
NGF
chariot
chariot+ XACWT
chariot+ XACA3
C
Retina
netrin:
Chariot
Chariot + XACWT
Chariot + XACA3
F-actin
G-actin
Merged
normalized int GC intensity (pix)
G-actin
F-actin
netrin
chariot
chariot+ XACWT
chariot+ XACA3
D
DRG
NGF:
Chariot
Chariot + XACWT
Chariot + XACA3
F-actin
Rh-actin
Merged
Integrated Rh-actin intensity (/10000)
- NGF
+ NGF
Chariot
XACWT
XACA3

Figure 5. Increased AC activity results in increased F-actin, decreased G-actin, and increased F-actin barbed ends. One μg of XACWT or XACA3 in PBS was complexed with Chariot reagent in dH20 for 30 min. Panel A shows chick DRG explants treated 1h with chariot, XACWT alone, or chariot+XACWT, and fixed and stained with the anti-*Xenopus* AC antibody XAC1. The leftmost pair of images show a growth cone of a *Xenopus* spinal neuron stained robustly with XAC1. The histogram shows integrated XAC1 growth cone intensities for chick DRGs shown. For panels B-D, Chariot alone or with recombinant proteins added to DRG (B and D) or temporal retina (C) explants 1 h before addition of control media, 40ng/ml NGF (B, D) or 500ng/ml netrin (C) for 15 min. Panels B and C show growth cones fixed and stained for F-actin (Alexa Fluor 568-phalloidin, red) and G-actin (fluorescein-DNase1, green), and mean growth cone fluorescence intensities are expressed normalized to Chariot, media controls. Panel D shows DRG growth cones that were permeabililzed with Alexa Fluor 488-phalloidin for 1 min (green), then incubated 4 min with 0.45 μM rhodamine-G actin (red) before being fixed and imaged. Mean growth cone fluorescence intensities of phalloidin staining and Rh-actin were determined. Statistical significance using ANOVA are indicated with "*", significance using Student's *t* test are indicated with "†". Data are means +/- SEM; *P<0.05; **P<0.001; ***P<0.0001. Scale bars, 10 μm.

Figure 6.

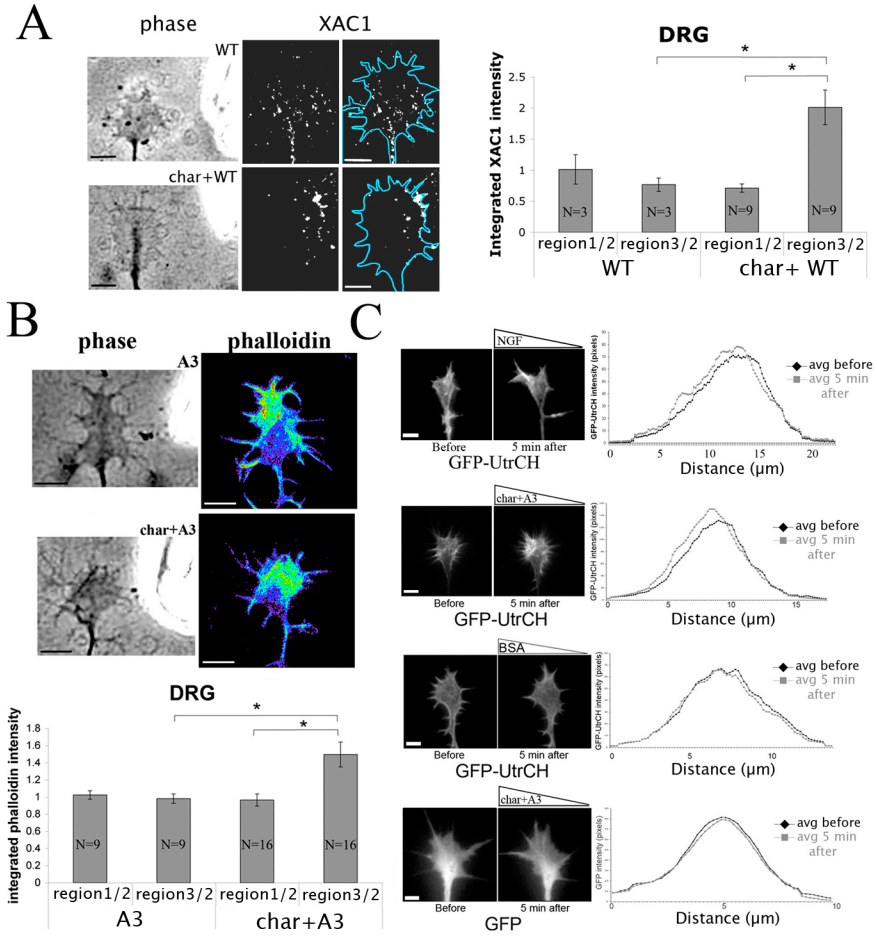

Figure 6. Growth cones exposed to a gradient of XACA3 exhibit asymmetrical F-actin distribution. For panel A, DRG growth cones were subjected to XACWT or chariot complexed with XACWT diffusing from a micropipette for 15min, fixed and stained with XAC1, and quantified as in Fig 3B. Data was taken from three separate days. Panel B shows F-actin (Alexa Fluor 488-phalloidin) distribution (pseudo-colored) in DRG growth cones subjected for 15 min to XACA3 or chariot+XACA3 diffusing from a micropipette, and quantified as in Figure 3B. Panel C shows distribution of GFP-UtrCH or GFP in transfected DRG growth cones that were exposed at one side to a pipette tip releasing NGF (data as reported in Roche et al,

2009), chariot-A3 or chariot-BSA complexes. An image was taken before and 5 min after pipette introduction. The distribution of fluorescence is expressed as the intensity along a 15 pixel-wide line across the growth cone width. Statistical significance using ANOVA. Data are means +/- SEM; *P<0.05. Scale bars, 10

Figure 7.

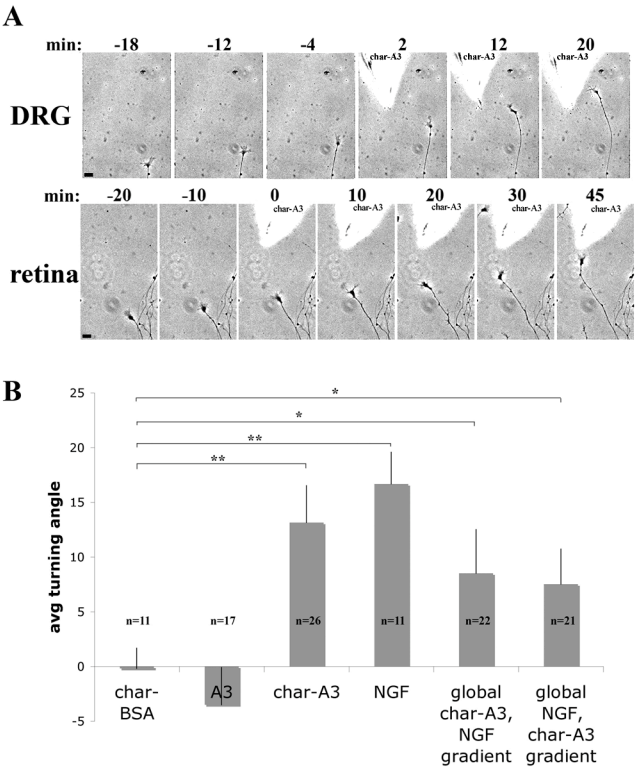

Figure 7. Growth cones exposed to a gradient of cell-permeable AC exhibit attractive turning. Panel A shows time-lapse images of a DRG and a retinal growth cone turning toward a gradient of chariot-A3 diffusing from the micropipette. Time shows minutes relative to addition of the micropipette. Panel B shows average turning angles of DRG growth cones to various gradients. Statistical significance using Student's *t* test. Data are means ± SEM; *P<0.05; **P<0.001. Scale bars, 20 μm

Figure 8.

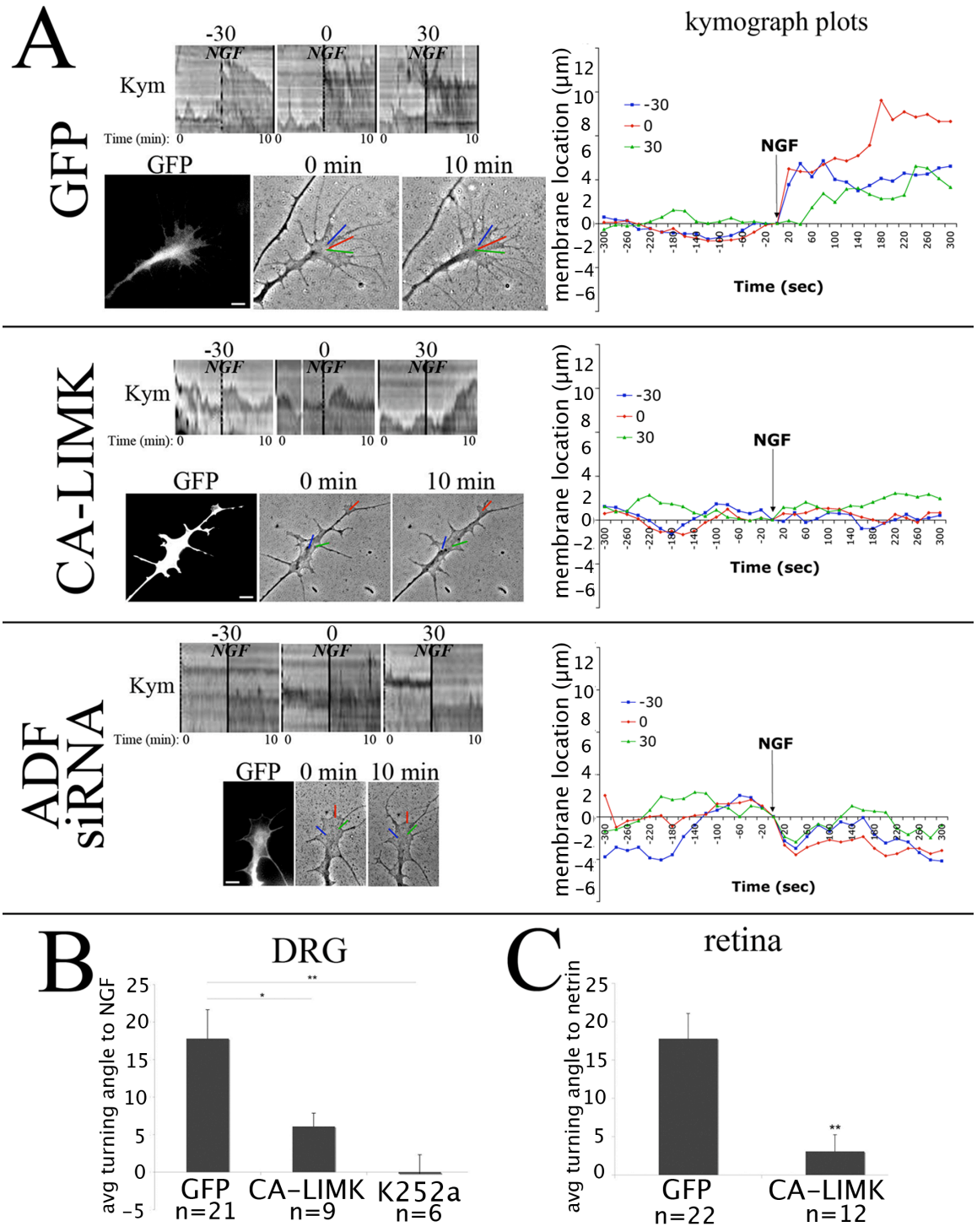
A
GFP
CA-LIMK
ADF siRNA
Kym
Time (min): 0 10 0 10 0 10
-30
0
30
NGF
GFP
0 min
10 min
kymograph plots
membrane location (µm)
Time (sec)
B
DRG
avg turning angle to NGF
GFP n=21
CA-LIMK n=9
K252a n=6
C
retina
avg turning angle to netrin
GFP n=22
CA-LIMK n=12

Figure 8. Reducing AC activation or protein levels blocks NGF- and netrin-induced membrane protrusion and guidance. Panel A shows DRGs that were transfected with GFP-RNAi control, GFP + CA-LIMK, or ADF-RNAi and cultured 48 h on L1. Transfected growth cones were imaged at 10 s intervals for 5 min before and after the addition of 40ng/ml NGF, and kymographs of the leading edge were generated. Quantification of membrane dynamics were performed as in Fig. 1 (n=5). DRG (B) or retinal neurons (C) were transfected with GFP or GFP + CA-LIMK, cultured 48 h, and subjected to a gradient of NGF (B) or netrin-1 (C), and mean turning angles were measured. In B, non-transfected DRG growth cones were treated with 500nM Trk inhibitor K252a 3 min prior to NGF-pipette introduction. Statistical significance using Student's *t* test. Data are means ± SEM; *P<0.05; **P<0.001. Scale bars, 10 μm.

Figure 9.

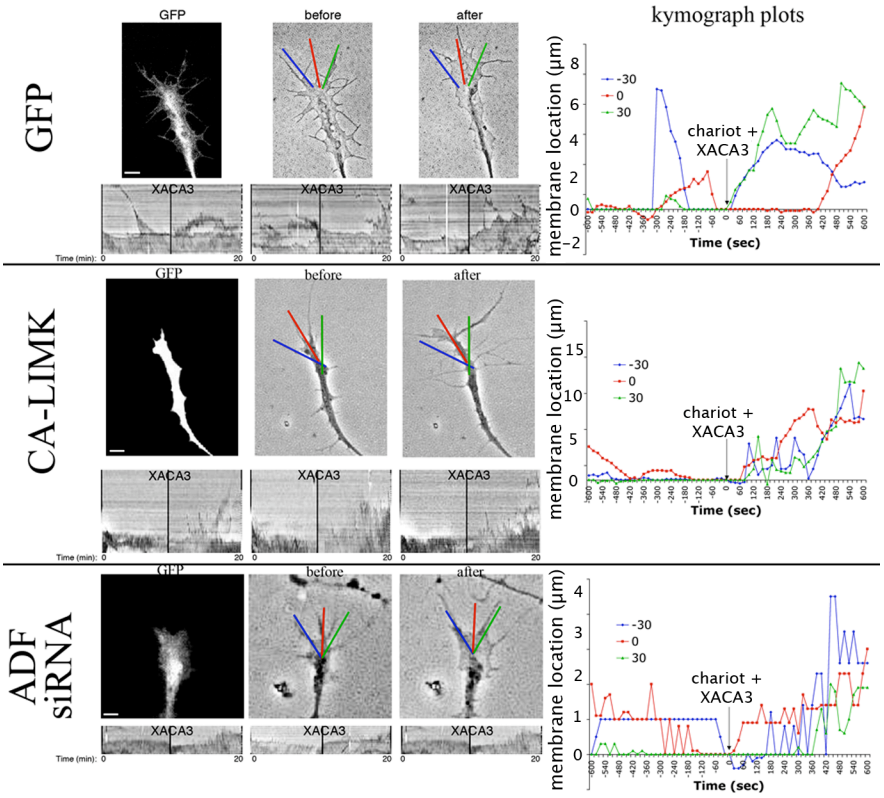

Figure 9. Restoring active AC to CA-LIMK- and ADF-RNAi-expressing growth cones rescues membrane protrusion. DRG neurons were transfected with GFP-RNAi control, GFP + CA-LIMK, or ADF-RNAi, and cultured 48hr on L1. Transfected growth cones were imaged every 10 sec for 10 min before and after the addition of chariot complexed with XACA3. Quantification of membrane dynamics were performed as in Fig. 1. Scale bars, 10 µm.

Figure 10.

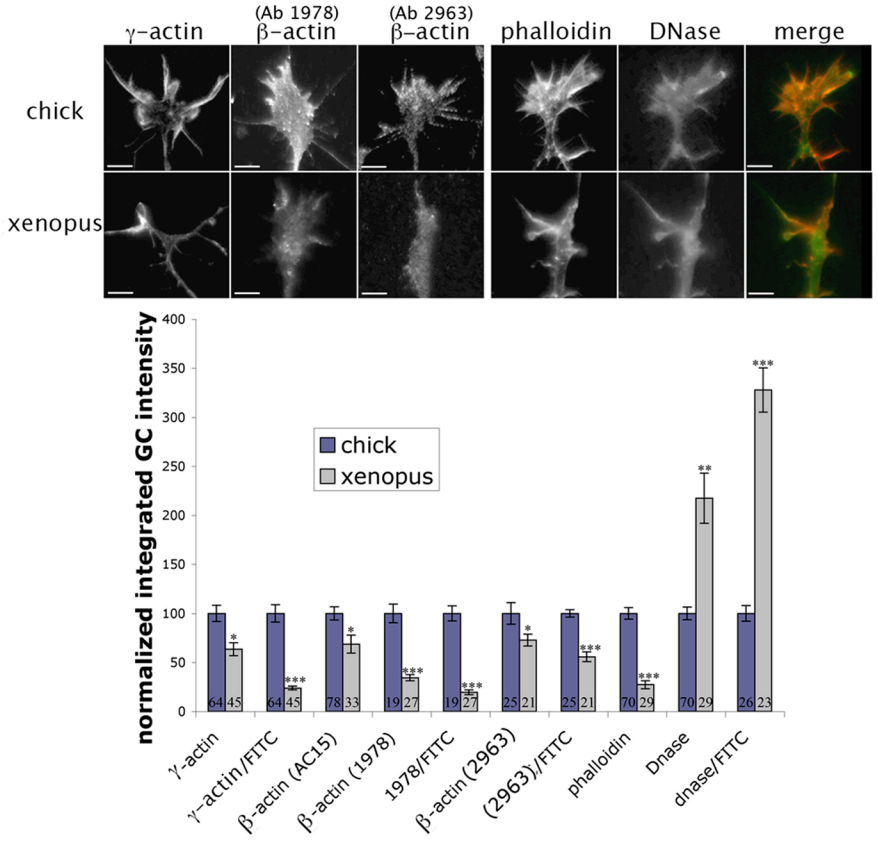

Figure 10. Chick DRG growth cones contain higher levels of actin compared to Xenopus spinal neuronal growth cones. Cultured chick DRG and Xenopus spinal neurons were labeled with antibodies against γ-actin (ab 7577), β-actin (AC15, Abcam; A1978 Sigma), actin (2963, James Ervasti), Alexa-Fluor 488 DNase (green), or Alexa-fluor 568 phalloidin (red). Where primary antibodies were not conjugated to FITC (γ-actin, A1978, 2963), FITC was used as a control for total protein. Integrated growth cone intensities were measured and normalized to chick. Statistical significance using Student's *t* test. Data are means ± SEM; *P<0.05; **P<0.001; ***P<0.0001. Scale bars, 10 μm.

SUPPLEMENTARY FIGURES

Figure S1

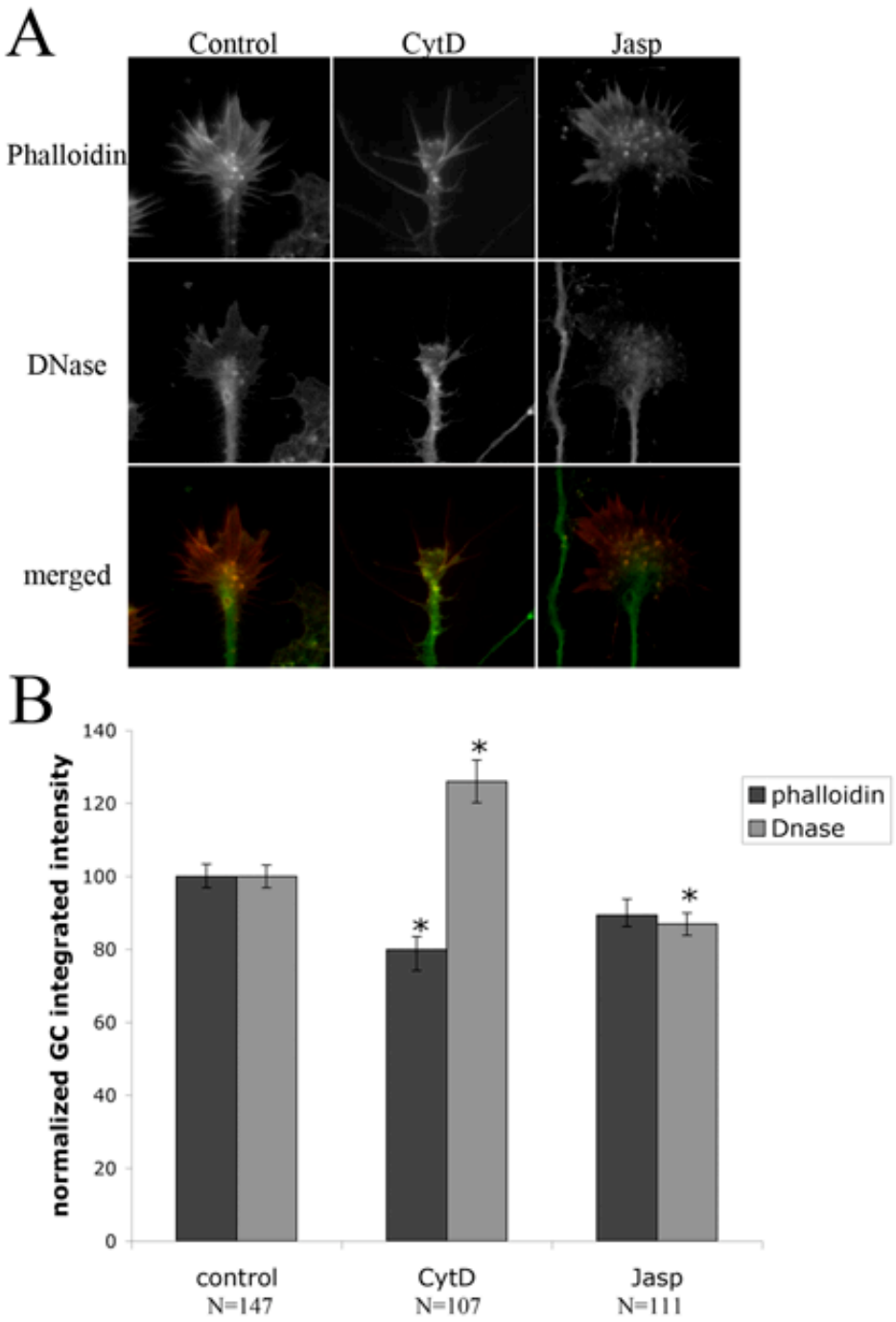

Figure S1. FITC-conjugated DNase reliably measures G-actin levels. DRG explants were cultured overnight on L1 and treated 10 min with control media, 20nM cytochalasin D (CytD), or 40nM Jasplakinolide (jasp) and fixed. Immunochemistry

against F-actin (Alexa Fluor 568-phalloidin; red) and G-actin (fluorescein-conjugated DNase1; green) was performed. DNase 1 intensity increases and decreases with CytD and jasp, respectively. Phalloidin intensity does not increase with jasp, possibly because phalloidin and jasp compete for the same F-actin binding site. Statistical significance using Student's *t* test. Data are means ± SEM; *P<0.05.

Figure S2.

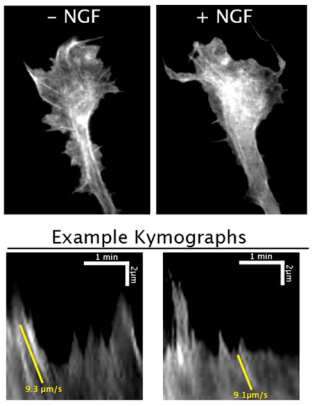

Figure S2. NGF does not significantly alter retrograde actin flow. DRGs were transfected with GFP-actin and growth cones were imaged every 3 s for 3 min before and after 40n/ml NGF addition. Flow rates before and after NGF were calculated by tracking bright actin features, as shown in sample kymographs.

Figure S3.

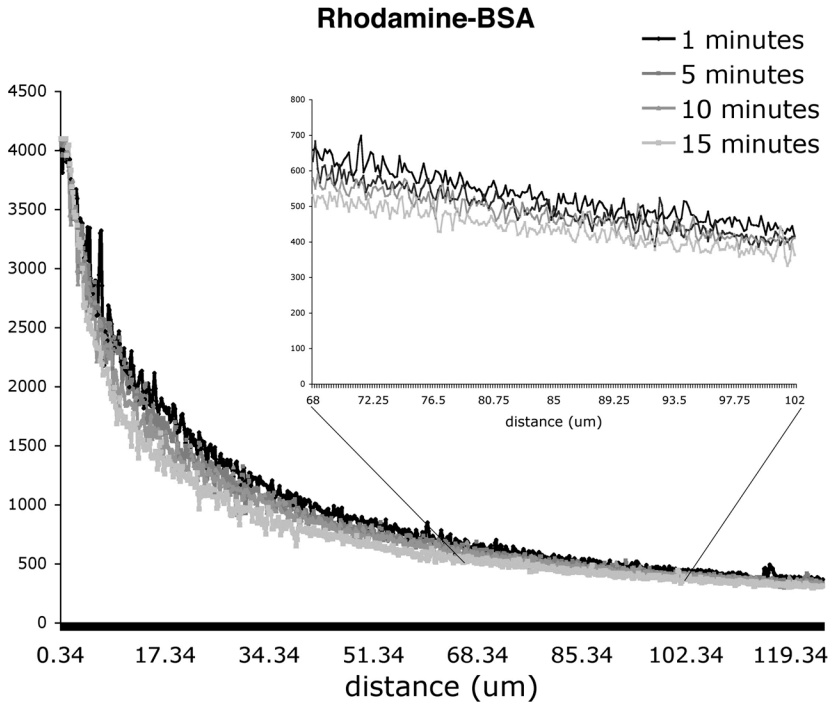
Rhodamine-BSA
1 minutes
5 minutes
10 minutes
15 minutes
4500
4000
3500
3000
2500
2000
1500
1000
500
0
0.34
17.34
34.34
51.34
68.34
85.34
102.34
119.34
distance (um)
800
700
600
500
400
300
200
100
0
68
72.25
76.5
80.75
85
89.25
93.5
97.75
102
distance (um)

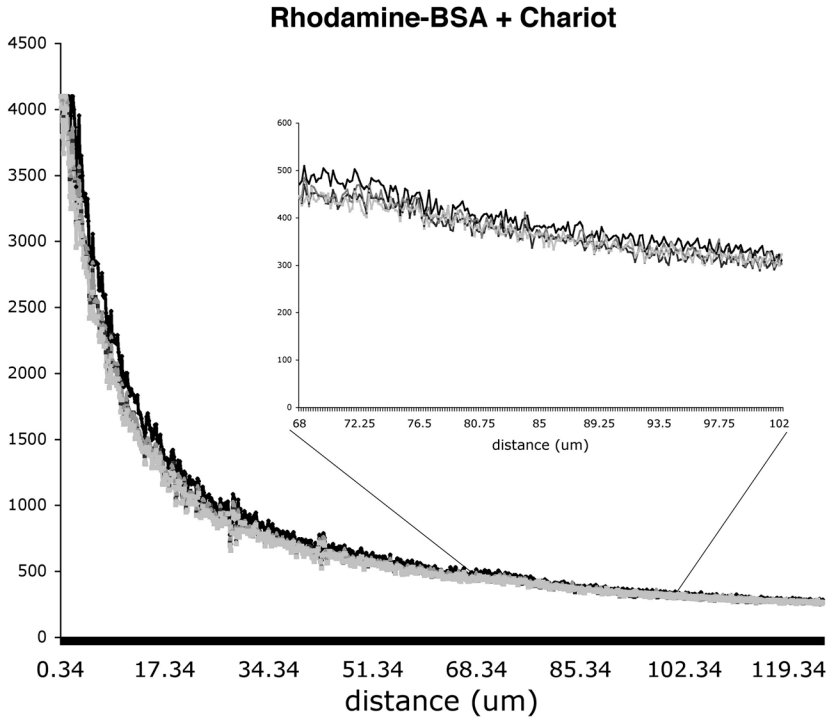
Rhodamine-BSA + Chariot
4500
4000
3500
3000
2500
2000
1500
1000
500
0
0.34
17.34
34.34
51.34
68.34
85.34
102.34
119.34
distance (um)
600
500
400
300
200
100
0
68
72.25
76.5
80.75
85
89.25
93.5
97.75
102
distance (um)

Figure S3. A micropipette coated with nitrocellulose and protein establishes a diffusible gradient. A micropipette was coated with nitrocellulose and 1 μg/ml rhodamine-BSA (A) or rhodamine-BSA complexed with Chariot reagent (B) and lowered into a dish with medium. Fluorescent images were taken after 1, 5, 10, and 15 min. The concentric gradients were measured using the "linescan" function in Metamorph. Insets show the gradients between 68-102μm from the micropipette tip.

Figure S4.

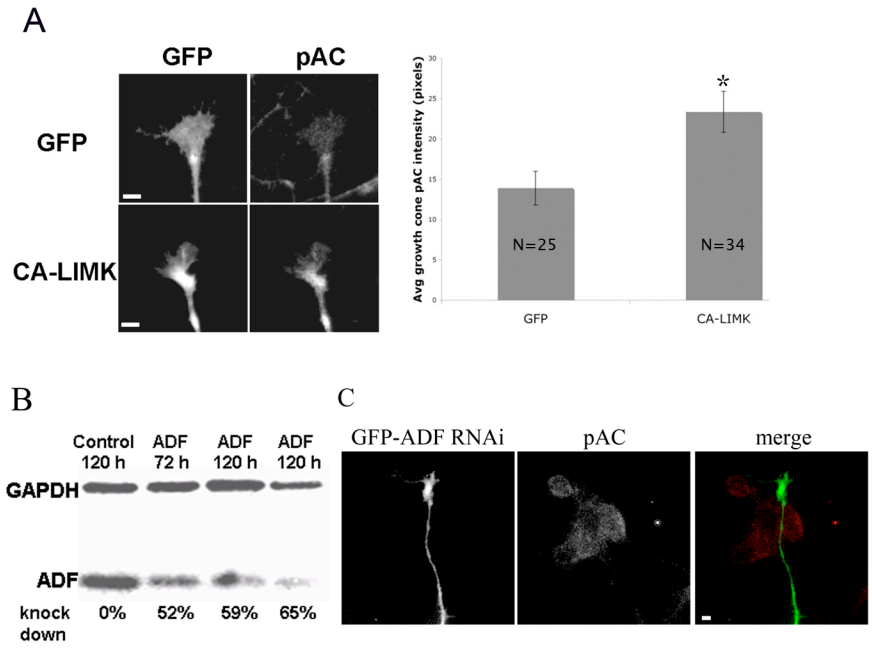

Figure S4. Expressing constitutively-active LIMK (CA-LIMK) or ADF hRNA results in decreased AC activity. A) Dissociated DRGs were transfected with GFP or GFP + CA-LIMK, cultured 24 hr, fixed and stained with pAC. Bar graph shows mean growth cone pAC intensities in GFP- and CA-LIMK-transfected growth cones. B) Western blot of extracts from chick embryo fibroblasts infected with hRNA-expressing adenoviral vectors for the time indicated before preparing cell extracts. Control vector expresses a rat hRNA that does not silence the chick protein. Two different loading volumes of the 120 hr extracts are shown for the chick ADF silencing vector. Infection efficiency for these chick fibroblasts is about 80% (based on GFP co-expression from the virus) suggesting silencing at 72 hr is about 65% and at 120 hr is about 80%. C) DRGs transfected with ADF hRNA, cultured 48hr, then fixed and stained with pAC (red). Note the level of anti-pAC staining of the adjacent non-transfected cell. Scale bars, 10 μm. Statistical significance using Student's *t* test. Data are means ± SEM; *P<0.05.

Discussion

Here we have shown that two attractive cues, NGF and netrin, increase leading edge protrusion in DRG and retinal growth cones, respectively, through increases in F-actin and actin polymerization. These guidance cues decrease inactive (phosphorylated) AC levels in growth cones. Direct elevation of AC activity in DRGs also increases free actin barbed ends and F-actin levels. A diffusible gradient of NGF, netrin or cell-permeable AC stimulates proximal F-actin assembly in growth cones, and elicits attractive turning. Reducing AC activity or protein level blocks guidance cue-induced membrane protrusion and blunts guidance cue-induced attractive turning for DRG and retinal growth cones. These data support a model in which NGF and netrin stimulate attractive turning through local activation of AC, which promotes actin polymerization in the growth cone side toward the guidance cue.

The regulation of actin organization and dynamics by guidance cue signaling has been a focus of growth cone research (for review, see Lowery and Van Vactor, 2009; Pak et al., 2008). Applied globally, repulsive cues reduce growth cone F-actin and protrusion, while attractive cues promote protrusion and increased F-actin (Brown and Bridgman, 2009; Fan et al., 1993; Gallo and Letourneau, 2000; Kalil and Dent, 2005; Roche et al, 2009; Zhou and Cohen, 2003). Specifically, global application of NGF and netrin-1 have been linked to increases in F-actin (Seeley and Greene, 1983; Shekarabi and Kennedy, 2002; Goldberg et al., 2000; Lebrand et al., 2004). More akin to guidance situations, local application of NGF and netrin, were shown to locally promote protrusive activity and increased F-actin (Dent et al., 2004;

Gallo et al., 1997; Gallo and Letourneau, 1998; 2000; Chang et al., 2006), and recent studies have shown gradients of netrin-1 and brain-drived neurotrophic factor induce proximal increases in ß-actin synthesis in *Xenopus* growth cones (Leung et al., 2006; Yao et al., 2006). However, in the nearly two decades of work linking F-actin increases to attractive cues, we understand relatively little about the mechanisms underlying these changes. And despite the identification of numerous actin-binding proteins with diverse effects on actin organization, links between specific proteins downstream of specific guidance cues are not well characterized (Dent and Gertler, 2003; Huber et al., 2003; Lowery and Van Vactor, 2009; Pak et al., 2008; Suter and Forscher, 1998).

In this paper we looked more closely at the role of actin polymerization in growth cone responses to attractive guidance cues. We quantified the increased F-actin in growth cones exposed to globally applied NGF and netrin and the distribution of increased F-actin in growth cones exposed to gradients of these cues. To probe the specific changes in actin organization responsible for these increases, we measured, for the first time, the effects of guidance cues on F-actin barbed ends, which are the sites of actin polymerization. We found that barbed ends are increased throughout growth cones by global NGF exposure and locally in growth cone margins that are proximal to gradients of NGF (DRG) or netrin (retina). We also measured retrograde actin flow, which if reduced, could contribute to increased F-actin in the growth cone leading margin. We found that NGF exposure did not change the retrograde actin flow rate, suggesting increased actin polymerization is the primary mechanism for the increased F-actin induced in the growth cone leading margin by attractive cues. In

migratory cells, similar local stimulation of leading edge actin polymerization is critical for cell polarity and directed migration to chemoattractants (Charest and Firtel, 2007; Pollard and Borisy, 2003; Weiner et al., 1999).

Our results indicate that local activation of the actin regulatory protein ADF/cofilin (AC) is a necessary component of attractive growth cone guidance. Previous work showed that NGF and the related neurotrophin BDNF activate AC in conjunction with neurotrophin-induced increases in motility and filopodial dynamics (Chen et al., 2006; Gehler et al., 2004; Meberg et al., 1998). Similarly, we found that global addition of NGF or netrin reduced total growth cone levels of inactive phospho-AC, and regions of DRG growth cones contacting NGF-coupled beads also had reduced phospho-AC. When growth cones were exposed to NGF (DRG) or netrin (retina) gradients and permeabilized before fixation to release inactive phospho-AC, subsequent immunostaining for remaining ADF bound to the actin cytoskeleton was concentrated in the growth cone region toward the attractive cue, further indicating that AC activity was higher proximal to an attractant. When we reduced AC activity by RNAi or by expressing constitutively active LIMK to inactivate AC by phosphorylation, growth cones failed to respond to attractive guidance cues, indicating the necessity of AC activity for attractive turning to NGF or netrin.

Similar to the effects of NGF and netrin exposure, we found the content of F-actin barbed ends in DRG and retinal growth cones was increased by incorporation of cell-permeable AC, and when DRG or retinal growth cones were subjected to a gradient of cell-permeable AC, the asymmetric incorporation of AC resulted in both increased F-actin and attractive growth cone turning toward the source of cell-

permeable AC. This demonstrates the sufficiency of elevated AC activity for barbed end creation, actin polymerization, and attractive growth cone turning, and is similar to the role of AC in promoting actin polymerization at the front of chemotaxing carcinoma cells (Ghosh et al., 2004; Mouneimne et al., 2004; 2006; Zebda et al., 2000).

Biochemical studies have revealed the complexity of AC in regulating actin filament turnover (for review, see Carlier et al., 1997, Van Troys et al., 2008). Some studies suggest AC activity enhances monomer loss from F-actin pointed ends, thereby replenishing the actin monomer pool (Carlier et al. 1997; Cramer, 1999; Maciver et al., 1998), while other studies attribute increased actin polymerization to AC-mediated severing of F-actin that increases barbed ends for monomer addition (Du and Frieden, 1998; McGough et al. 1997). The ratio of AC:actin is another factor in actin dynamics. At low AC levels relative to actin, cofilin binds actin independently, promoting filament turnover and polymerization at new barbed ends. (Andrianantoandro and Pollard, 2006). At intermediate concentrations, cofilin binds actin cooperatively and rapidly severs actin filaments (Andrianantoandro and Pollard, 2006; Blanchoin and Pollard, 1999; Chan et al., 2009; Pavlov et al., 2007). At high relative concentration cofilin can both nucleate and rapidly sever actin but then stabilizes filaments as they become saturated with cofilin (Andrianantoandro and Pollard, 2006; Chen et al., 2004; Pavlov et al, 2007). Beyond these studies with purified components, the net roles of AC become more complex and varied within cells, where multiple factors, including the G-actin pool size, components that regulate AC activity, and the actions of additional actin regulatory proteins are

integrated in determining actin filament organization and dynamics in migrating cells (Bernstein and Bamburg, 2010; Ressad et al., 1999; Sarmiere and Bamburg, 2003).

Such complexity in regulating actin filaments may indicate why our result concerning AC activity and growth cone turning differs from that of Wen et al. (2007), where *Xenopus* growth cones responded to BMPs by turning toward the side with lower AC activity. We probed other differences between *Xenopus* and chick growth cones and found *Xenopus* growth cones have lower levels of actin and lower F-actin/G-actin ratios compared to chick growth cones, which may impact how actin is re-organized when AC activity increases. An additional consideration is that BMP-receptor signaling may involve different pathways and activities than what is activated downstream of netrin-1 and NGF. For example, netrin-mediated actin polymerization requires the anti-capping activity of Ena/VASP (Gitai et al., 2003; Gomez and Robles, 2004; Lebrand et al., 2004). The GTPase Rac, which is activated by both NGF and netrin (Gitai et al., 2003; Ridley et al., 1992), activates SCAR to enhance the actin nucleating activity of the Arp2/3 complex (Machesky et al., 1999). The actin nucleating and F-actin branching actions of the Arp2/3 complex may interact with the filament severing and debranching actions of AC in a variety of ways to regulate actin organization during lamellipodial and filopodial protrusion (Chan et al., 2009; Blanchoin et al., 2000; Ichetovkin et al., 2002; Ressad et al., 1999; Svitkina and Borisy, 1999). Further, the relative activities of F-actin capping and actin-sequestering proteins directly control the fundamental elements of actin polymerization, free barbed ends and G-actin monomer. Thus, the integration of all actin regulatory activities may dictate that different levels of AC activity should exist

in different growth cones to mediate attractive growth cone turning. In *Xenopus* growth cones increased filopodial protrusion and F-actin accumulation may require low AC activity, while in chick growth cones, increased AC activity promotes actin polymerization to drive protrusion and attractive turning to NGF and netrin.

This paper does not address the mechanisms by which NGF and netrin regulate AC activity, which is becoming a more complex topic (Bernstein and Bamburg, 2010). NGF- and netrin-induced dephosphorylation of AC could occur through activation of a phosphatase or a decrease in kinase activity. Several phosphatases activate AC, including chronophin (Gohla et al., 2005), and isoforms of slingshot, which was recently implicated in carcinoma cell chemotaxis (Eiseler et al, 2009; Niwa et al., 2002). Inactivation of AC is mediated by LIM and TES kinases (Toshima et al., 2001; Yang et al., 1998). LIMK is active when phosphorylated by PAK1, PAK4, or Rho-kinase (ROCK), and is inhibited by dephosphorylation by SSH phosphatase or ubiquitination by Rnf6 (for review, see Bernard, 2007). In addition, several feedback loops may play important roles, such as SSH activation by F-actin, or LIMK inactivation by SHH. Additional regulators of AC include 14-3-3 proteins, which promote inactive phospho-AC by directly binding to phospho-AC and LIMK (Gohla and Bokoch, 2002), and incorporation of 14-3-3 into retinal growth cones blocks BDNF-mediated activation of AC (Gehler et al., 2004). AC activity is also regulated by pH, phosphoinositides, and other proteins such as tropomyosin or Aip1 (for review, see Sarmiere and Bamburg, 2003). In summary, multiple regulators affect AC activity.

In summary, our data support a model in which two important cues, NGF and netrin, induce attractive growth cone turning by locally activating AC and stimulating actin polymerization in growth cone regions proximal to the guidance cue source. Further studies are needed to clarify how the activities of multiple actin-binding proteins and associated regulatory factors are integrated to mediate the effects of guidance cues on growth cone trajectories.

Chapter III: Ezrin/radixin/moesin family proteins mediate actin filament dynamics in attractive growth cone guidance to nerve growth factor

Introduction

Proper establishment of neural networks requires growth cones to correctly navigate to target tissues (Mitchison and Kirschner, 1988; Letourneau and Cypher, 1991; Tessier-Lavigne and Goodman, 1996). Molecular cues in the developing organism bind membrane receptors on the growth cone and initiate intracellular signaling cascades (Bentley and O'Connor, 1994; Huber et al., 2003; Lowery and Van Vactor, 2009). These signaling cascades alter the activities of actin-binding proteins, which reorganize actin filaments to steer the direction of neurite growth. Though substantial progress has been made in identifying the guidance cues and receptors involved in this process, our understanding of the role and regulation of actin-binding proteins associated with specific guidance cues is far from complete (Dent and Gertler, 2003). In particular, little is known about the role of membrane-cytoskeletal linkers, or how multiple actin-regulatory proteins act in concert to mediate axon guidance.

In addition to its role in cell survival and differentiation, nerve growth factor (NGF) attracts sensory and sympathetic neuronal growth cones *in vitro* and *in vivo* (Letourneau, 1978; Menesini Chen et al., 1978; Gundersen and Barrett, 1979; Patel et al., 2000; Glebova and Ginty, 2004), and stimulates growth cone actin polymerization (Gallo et al., 1997; Gallo and Letourneau, 1998, 2000; Goldberg et al., 2000). In a recent study, we found NGF stimulates polymerization by activation of actin depolymerizing factor and cofilin family proteins (ADF/cofilin; AC), which sever actin filaments and increase sites for polymerization (barbed ends) (Marsick, et al., 2010). Attractive growth cone guidance to NGF is blocked when AC activity or

proteins levels are disrupted. We also found a cell-permeable gradient of constitutively-active ADF/cofilin was sufficient to evoke a proximal increase in F-actin and subsequent attractive growth cone turning. Yet how these newly formed actin filaments interact with the growth cone membrane is currently unknown.

Multiple membrane-cytoskeletal linker proteins have been identified in neurons. Ankyrin and spectrin cooperate to link actin filaments to L1CAM at the cell membrane, are expressed in neuronal growth cones, and may mediate growth cone guidance (Ooashi and Kamiguchi, 2009). Talin and vinculin link actin filaments to integrins, are involved in cell migration and are also present in growth cone. Talin appears to affect filopodial motility and vinculin inactivation results in filopodial bending (Sydor et al., 1996), however a role for these proteins in growth cones responding to guidance cues has not been established.

The evolutionarily conserved ezrin/radixin/moesin (ERM) proteins also provide a physical link between actin filaments and the membrane (Bretscher et al., 2002). Inactive ERMs reside in the cytosol, where interactions between their N- and C-termini result in a closed conformation (Hayashi et al., 1999). When this interaction is disrupted by phosphorylation at a conserved threonine residue or through interactions with PIP2, ERMs can simultaneously bind F-actin on the C-terminus and membrane proteins at the N-terminus (Henry et al., 1995). Active ERMs are concentrated in actin-rich protrusions and have well-established roles in cell shape and motility (Amieva and Furthmayr, 1995; Henry et al., 1995; Bretscher et al., 2002). They are also highly expressed in developing nervous system, and in growth cones, radixin co-localizes with F-actin in peripheral lamellipodia and filopodia

(Paglini et al., 1998; Castelo and Jay, 1999). Knockdown of radixin and moesin impairs growth cone morphology and motility, and focal ablation of radixin using microscale chromophore-assisted laser inactivation (Micro-CALI) produces local lamellipodial collapse or growth cone splitting (Paglini et al., 1998; Castelo and Jay, 1999). Moreover, radixin localizes toward the new direction of advance in growth cones responding to an electric field, and the repulsive guidance cue Semaphorin 3A induces ERM inactivation, suggesting ERMs may mediate cytoskeletal stability in growth cone guidance (Gonzalez-Agosti and Solomon, 1996; Gallo, 2008). Previous studies found increased ERM activation downstream of NGF in sensory neurons and PC12 cells, making these linker proteins attractive candidates for mediating growth cone guidance to NGF (Jeon et al., ; Amieva and Furthmayr, 1995; Gonzalez-Agosti and Solomon, 1996).

Despite numerous studies characterizing ERM protein localization and activation, their function in navigating growth cones remains unclear. Studies in non-neuronal cells, along with the changes in growth cone morphology when ERMs are disrupted, suggest they stabilize actin filaments at the cell periphery. However, ERM proteins may also regulate the distribution and activity of membrane receptors (McClatchey and Fehon, 2009). In neurons, ERM proteins interact with numerous membrane proteins, including L1CAM (Dickson et al., 2002; Mintz et al., 2003; Haas et al., 2004; Cheng et al., 2005) and the extracellular matrix receptor CD44 (Ikeda et al., 1996). Because ERM activity can be regulated by extracellular cues, this receptor-actin linkage could provide a rapid and dynamic mode for modulating growth cone motility. In addition, ERMs could physically tether receptors to specific locations in

the growth cone membrane, or impinge lateral movement to influence distribution and clustering. Finally, ERM proteins have also been shown to prevent the inhibition of Rho GTPases by binding to Rho GDI, suggesting ERMs may influence signaling, as well as the localization of signaling molecules at the plasma membrane and lipid raft microdomains (Takahashi et al., 1997; Hamada et al., 2001). Thus, ERM proteins may locally stabilize actin filaments at the membrane and provide scaffolding for localizing molecules to the growth cone leading margin.

Here, we report that an NGF gradient asymmetrically activates ERM proteins at filopodial tips and the lamellipodial leading edge in chick DRG growth cones. Expression of a dominant-negative ERM (DNERM) construct disrupts growth cone morphology actin organization. The increase in growth cone F-actin normally seen after NGF addition is blocked in DNERM growth cones, and free F-actin barbed ends are displaced from the growth cone periphery. ADF/cofilin activation by NGF remains in DNERM growth cones, but active AC proteins are mislocalized to the growth cone center. Interestingly, we found increasing AC activity directly increases phospho-ERM levels, and disrupting AC activity with a constitutively-active LIMK blocks NGF-induced ERM activation. Moreover, NGF stimulation results in active AC, free F-actin barbed ends, and phospho-ERM proteins localized to the growth cone leading edge, and attractive turning to NGF is blocked when ERM function or protein levels are disrupted. Together, these data suggest a model in which NGF locally activates ADF/cofilin and ERM proteins, which both stimulate an increase in stable growth cone F-actin levels toward the cue source to mediate attractive growth cone turning.

Methods

Materials F-12 medium, B27 additives, poly-D-lysine (MW >300,000), jasplakinolide, Alexa Fluor 488 DNase1, Alexa Fluor 488- and 568–phalloidin, Alexa Fluor 488 and 568 secondary antibodies were purchased from Invitrogen. NGF, and L1–Fc were purchased from R & D Systems. Fc Fragment was purchased from Jackson Immuno Research. Chariot was purchased from Active Motif. White leghorn fertilized chicken eggs were purchased from Hy-Line North America, LLC. Cytochalasin D and all other reagents were purchased from Sigma-Aldrich, unless otherwise indicated.

Neuronal culture Glass coverslips were coated with 100ug/ml poly-D-lysine, rinsed with water, coated with 1% nitrocellulose dissolved in 100% amyl acetate (Fischer Scientific), dried, and coated overnight with 20µg/ml laminin or 4 µg/ml recombinant L1–Fc mixed with 8 µg/ml Fc in phosphate buffered solution (PBS; Roche). Video dishes were made by gluing a coverslip (18 mm x 18 mm; Gold Seal) over a hole (5mm) in the bottom of a culture dish (Falcon 35 mm x 10 mm), allowed to dry, rinsed with water, and coated as described. Embryonic day 7 (E7) dorsal root ganglia (DRG) were removed from chick embryos according to procedures approved by the University of Minnesota Institutional Animal Care and Use Committee. Neural tissues were cultured on experimental substrates in F-12 with B27 additives and buffered to pH 7.4 with 10 mM HEPES. Neural tissues were cultured overnight in a humidified incubator at 37°C.

Preparation of NGF-coated beads NGF and BSA were covalently coupled to 6μm carboxylated beads (Polysciences, Inc) as described previously (Gallo et al., 1997).

Neuronal transfection DRGs were dissociated as described in Roche et al., 2009. Approximately 2 x 10^6 cells were transfected with one of the following: 1 ug of plasmid expressing GFP, 1 μg of a plasmid encoding the N-terminus of ezrin (DNERM; a generous gift from Dr. Janis Burkhardt), 1 ug of GFP combined with siRNA against chick radixin (10nM) and moesin (10nM), or 1 ug constitutively-active LIMK with 1 ug GFP using the G-13 program of the Amaxa Biosystems Nucleofector, and the chicken neuron nucleofector reagents. To assess retrograde actin flow, or for barbed end labeling studies, 2 μg GFP or DNERM were combined with .5 μg RFP- or GFP-actin. Cells were cultured 24-48 h, as indicated.

Time-lapse microscopy and quantitative fluorescence determinations

A Spot digital camera mounted on an Olympus XC-70 inverted microscope, and MetaMorph software (Molecular Devices) were used for all image acquisitions. In any one experiment, all images were acquired in one session. For collection of fluorescent images, exposure time and gain settings on the digital camera were kept constant, and image acquisition and analysis was performed as described in Roche et al., (2009). For experiments measuring growth cone fluorescence intensity values, a line tool was used to outline the terminal 25 μm of each distal axon and growth cone in MetaMorph, and background intensity value was subtracted from the fluorescence intensity value of the accompanying neuronal measurement. For phospho-ERM

filopodial intensity measurements, growth cones were selected at random from phalloidin images, and a line was drawn on each filopodium using the line tool; lines were then transferred to the corresponding phospho-ERM image and background-subtracted phospho-ERM intensity values were recorded.

Retrograde flow measurements To determine retrograde actin flow rates, DRGs were co-transfected with RFP-actin and GFP or DNERM, cultured overnight with NGF, and imaged every 3 s for 6 min. Kymographs were generated for the distal 10 μm of growth cones, and flow rates were measured by tracking bright GFP-actin features, which are formed by unequal incorporation of GFP- and non-GFP actin monomers into polymerized filaments at the leading edge. Measuring retrograde flow using the movement of these features has been described previously, including a demonstrated sensitivity of this retrograde flow to the myosin-II inhibitior blebbistatin (Chan and Odde, 2008).

Immunocytochemistry Neuronal cultures were fixed and blocked as described (Roche et al., 2009). Coverslips were incubated with primary antibodies diluted in PBS containing 10% goat serum overnight at 4º C. Affinity purified antibody 12977 (ADF) was used at 1:200 dilution; 4321 (phospho-ADF/cofilin) was used at 1:1000 dilution, ERM antibodies against ezrin, moesin, and phospho-ERM were purchased from Cell Signaling Technology and used at 1:100 dilution, 13H9 was a generous gift from Lorene Lanier and was used at 1:1000, R3653 specific for radixin was purchased from Sigma Aldrich and used at 1:100, and polyclonal antibody 457-3

specific for radixin was used at 1:100. Coverslips were then rinsed 3 times in PBS and incubated in PBS rinse for 1 h. For labeling F-actin, Alexa Fluor 568–phalloidin was applied at a 1:20 dilution, and mixed with secondary antibodies: Alexa Fluor 568 goat anti-rabbit or anti-mouse antibodies at 1:1000 dilution in PBS with 10% goat serum for 1 h. For labeling G-actin, 25 ng/ml Alexa Fluor 488 DNase1 was applied to coverslips for 1 h. For staining total active ADF, NGF or BSA was added for 5 min, media was removed and cultures were incubated 1 min in permeabilization buffer (described below) with 100nM phalloidin, then fixed and stained. After rinsing 3 times in PBS, coverslips were mounted in *SlowFade* reagent (Invitrogen).

Pharmacological Inhibitors Cultures were treated with 20 nM cytochalasin D (Invitrogen) or 20 nM jasplakinolide for 3 min. Controls were treated with the same volume DMSO vehicle, which never exceeded 5 µl/ml.

Barbed end labeling This protocol was adapted from Chan et al., (1998). In summary, neurons were cultured overnight and treated as indicated. At room temp, the culture media was gently aspirated and a permeabilization buffer (1% BSA, .025% saponin, 138 mM KCL, 10 mM Pipes, 0.1 mM ATP, 3 mM EGTA, 4 mM MgCl2, pH = 6.9) with 100nM Alexa-fluor 488 phalloidin (Invitrogen) was added for 1 min, after which the buffer was removed and buffer containing 0.45 uM Rhodamine non-muscle actin (Cytoskeleton) was added for 4 min, after which the buffer was removed and cells were fixed with 4% paraformaldehyde and .05% glutaraldehyde, rinsed, and imaged.

GFP and DNERM were co-transfected with GFP-actin, which remained after permeabilization and allowed for identification of transfected growth cones.

Central and peripheral barbed end quantifications Quantification of barbed labeling were performed by hand-tracing GFP-actin images in metamorph. A straight line was then drawn across the growth cone width in at least 3 locations and the distance 25% from either side of the growth cone edge was noted and used to trace the central growth cone region. Regions were then transferred to the rhodamine-actin image, where total and central growth cone intensities were measured. Peripheral growth cone intensities were later calculated by subtracting the central intensity from the total for each growth cone.

Recombinant proteins and protein loading Recombinant XAC proteins were generated as described previously (Gehler et al., 2004). Proteins were delivered into cells using Chariot reagent (Active Motif; Morris et al., 2001), according to the manufacture's instructions. Briefly, 6 µl Chariot was complexed with 1 µg BSA or XACA3 for 1 h, then added to the culture medium or immobilized onto a nitrocellulose-coated micropipette.

Growth cone turning assay Turning was assessed as described previously (Roche et al., 2009). Briefly, micropipette tips were dipped in a 1% nitrocellulose solution, dried, then dipped several times in a PBS solution of 1 µg/ml NGF. A growth cone was imaged at 30 or 60 s intervals for 15 min. The micropipette tip was then

positioned 100 μm from a growth cone at a 45° angle to the direction of axon elongation. Images were acquired 45 min after introducing the micropipette tip. Growth cone turning angles were determined as the change in direction of growth cone migration between the beginning and end of the image acquisition period (Ming et al., 1997).

Statistical analysis Parameters of population values are reported as mean +/- SEM. All statistical analysis was by unpaired Student's t test.

Results

Radixin is the predominant ERM protein in chick DRG growth cones

Previous studies have found that radixin and moesin, but not ezrin is expressed in developing DRGs (Castelo and Jay, 1999), and radixin is the most abundant ERM in embryonic chick sympathetic growth cones (Gonzalez-Agosti and Solomon, 1996). To characterize ERM protein expression in our embryonic day 7 (E7) chick DRGs, we performed immunocytochemistry on explants cultured overnight on laminin. Antibodies that recognize all three ERMs (ERM, cell signaling; 13H9) show high expression in growth cones and co-localize with phalloidin-stained F-actin (Fig 1A, B). Although antibodies specific to ezrin and moesin stained neurites, very little were present in growth cones and did not co-localize with F-actin (Fig 1C, D). Two separate antibodies against radixin (R3653; 457-3) demonstrate its presence in peripheral growth cone regions, which resembles the pan-ERM staining pattern (Fig 1E, F). Taken together, we conclude radixin is the predominant ERM protein in E7 chick DRG growth cones.

NGF increases active phospho-ERM levels at filopodial tips

Others have reported that NGF stimulation increases phospho-ERM levels in sympathetic growth cones and PC12 cells (Jeon et al., 2010; Amieva and Furthmayr, 1995; Gonzalez-Agosti and Solomon, 1996). To assess the effect of NGF on active ERM levels in chick DRG growth cones, we cultured explants overnight in the absence of NGF and performed immunochemistry with an antibody specific to the active threonine phosphorylated ERM protein (phospho-ERM) at various time points

after bath application of 40ng/ml NGF. Growth cones cultured without NGF or 40ng/ml NGF overnight had low phospho-ERM levels, which increased in lamellipodia and filopodia after addition of NGF (Fig 2A). The average filopodial phospho-ERM intensity increased after 5 min NGF treatment, peaked after 30 min, then declined after 1-2 hr. This increase was reversed when NGF was added for 15 min and washed out for 1 or 2 hr, where phospho-ERM levels approached pre-NGF levels, and then increased again upon the return of NGF (Fig 2A). These data suggest global NGF rapidly increases active phospho-ERM proteins in peripheral growth cone regions.

To determine if a local NGF source can elicit local changes in ERM phosphorylation, beads with covalently-bound NGF were added to cultures for 15 min and fixed, or a nitrocellulose micropipette coated with NGF was rinsed and brought in contact with a filopodium for 1 min before being fixed. In both cases, filopodia that had contacted NGF showed increased phospho-ERM levels compared to neighboring filopodia that had not contacted NGF (Fig 2B). These data suggest that a local NGF source can produce a local increase in active phospho-ERM. Lastly, because diffusible gradients of NGF are used in vitro to induce attractive growth cone turning, we asked if growth cones subjected to a gradient of NGF would also exhibit asymmetric localization of phospho-ERM. An NGF gradient is created as described in Roche et al. (2009), where a nitrocellulose-coated micropipette is incubated in NGF and not rinsed, which produces a diffusible gradient of NGF when lowered into culture medium. Micropipettes coated with NGF or BSA were brought within 100um to one side of growth cones for 1 min before being fixed. Phospho-ERM distribution

was quantified by dividing the growth cone in half based on its neurite axis, and the proximal/distal ratio of filopodial phospho-ERM intensities was then calculated (Fig 2C). Growth cones subjected to a gradient of NGF had higher phospho-ERM levels proximal to the NGF source compared to the distal side, and no such asymmetry was observed in growth cones subjected to a gradient of BSA (Fig 2C). Together, these data suggest global or local NGF application increases active phospho-ERM levels in DRG growth cones.

Disrupting ERM protein function results in abnormal growth cone morphology and short axons

To asses ERM function in chick sensory neurons, we transfected chick DRGs with a dominant-negative ERM construct (DNERM) consisting of the membrane-binding N-terminus, which competes for active ERM proteins and inhibits their ability to link actin filaments to the membrane (a generous gift from Dr. Janis Burkhardt). We also reduced radixin and moesin protein levels using a mixture of small interfering RNA (siRNA). Knockdown of radixin and moesin protein levels were confirmed with western blot and immunocytochemistry (supplementary figure S1). To examine the effect of ERMs on F-actin organization, we transfected DRGs with GFP or DNERM, cultured them overnight with NGF, fixed and stained with fluorescent phalloidin and then examined growth cone F-actin organization using confocal microscopy. GFP controls showed normal morphology, with actin-rich filopodia and lamellipodia in peripheral regions (Fig 3A arrowheads) and a central domain containing little F-actin (Fig 3A arrows). In contrast, DNERM growth cones

were morphologically simpler with fewer filopodia (Fig 3A arrowheads; 3C), and a dense, disorganized F-actin network in central growth cone regions (Fig 3A arrows). Filopodia also appeared wavy in DNERM growth cones compared to the taut filopodia in GFP controls (Fig 3A arrowheads). Quantification of growth cone phenotypes revealed DNERM growth cones have less actin and fewer filopodia compared to GFP controls (Fig 3B and C) and advanced slower, resulting in shorter axons (Fig 3D and E). These data suggest ERM proteins are involved in establishing or maintaining growth cone F-actin organization, as well as growth cone motility.

Disrupting ERM function blocks NGF-induced F-actin increase

In a previous study, we found acute NGF application increases active ADF/cofilin levels (AC), F-actin content and free F-actin barbed ends. Moreover, increasing ADF/cofilin activity by loading neurons with a constitutively-active AC (A3) protein also increases growth cone actin filament levels and free F-actin barbed ends (Marsick et al., 2010). To assess the role of ERM proteins in this response, we measured F-actin (phalloidin) and G-actin (DNase1) levels in DRG growth cones expressing control GFP or DNERM. Similar to our previous result, GFP growth cones treated 15 min with 40ng/ml NGF had increased F-actin and decreased G-actin levels, but these changes were absent in DNERM growth cones (Fig 4A). Because AC activation is involved in this response, we next asked if NGF-induced activation of AC is affected in DNERM-expressing growth cones. We previously found NGF decreases inactive phospho-AC levels (Marsick et al., 2010), and this decrease was also present in both GFP controls and DNERM-expressing growth cones, suggesting

ERM function does not affect the NGF-induced activation of AC (Fig 4B). To further confirm that increasing AC activity does not increase growth cone F-actin when ERM function is impaired, we used Chariot reagent to load GFP control and DNERM-expressing growth cones with constitutively-active AC (A3), then measured F-actin levels using phalloidin. As previously reported (Marsick et al., 2010), A3 increased integrated growth cone phalloidin intensity in GFP controls, but no significant change was measured in DNERM growth cones (Fig 4C). Together, these data suggest that ERM proteins are needed for active AC to increase growth cone F-actin levels.

Actin filaments at the growth cone leading edge are continuously removed by retrograde actin transport, and in Marsick et al (2010) we found NGF did not alter retrograde flow rates. However, we hypothesized retrograde flow may be affected in DNERM growth cones, where filaments are unable to interact with the membrane. We therefore co-transfected RFP-actin with GFP control or DNERM and tracked the movements of bright actin features to measure the rate of retrograde flow (Chan and Odde, 2008). We found that DNERM growth cones indeed had higher rates of retrograde actin flow compared to GFP controls (Fig 4D). This may partially account for the absence of increased F-actin after NGF in DNERM growth cones, where filaments are more rapidly transported from the leading edge to the growth cone center, thus counteracting the filament-generating effects of polymerization.

Disrupting ERM function results in displaced active AC and free F-actin barbed ends

Thus far, we have found NGF activates ADF/cofilin in DNERM-expressing growth cones, yet no increase in F-actin occurs. We next we wanted to further

characterize the spatial localization of active AC in growth cones with disrupted ERM function. To do so, we employed a technique described previously (Marsick et al., 2010), in which growth cones are permeabilized for 1 min in the presence of phalloidin, fixed, and stained for total ADF. This method permits the diffusion of inactive pAC not bound to F-actin, leaving only active actin-bound ADF. In GFP controls, NGF addition results in active ADF localized to the growth cone leading margin (Fig 5A). However, this peripheral localization does not occur in growth cones expressing DNERM, where the majority of ADF remains in the growth cone center. These data suggest that although the level of AC activation by NGF is not affected in growth cones with impaired ERM function, the spatial location of active AC in the growth cone is. Because activation of AC increases free F-actin barbed ends, we next asked if the localization of free F-actin barbed ends are also affected in DNERM growth cones. As described in Marsick et al (2010), barbed end labeling is performed as follows: cultures are briefly permeabilized with a buffer containing saponin and phalloidin for 1 min, then incubated 4 min in buffer containing saponin, phalloidin and fluorescently-labeled rhodamine-actin (Rh-actin), then fixed and imaged. This method allows visualization of free F-actin barbed ends by the incorporation of Rh-actin. In GFP controls, NGF stimulation increases total integrated barbed end levels in growth cones, particularly at the peripheral leading margin (Fig 5B). However, growth cones expressing DNERM do not exhibit increased Rh-actin labeling at the leading margin. To further quantify barbed end levels and localization, growth cones were traced and the integrated Rh-actin intensity values were measured. Central and peripheral regions were delineated as described in methods, and the Rh-

actin intensities were measured and normalized. In GFP controls, NGF addition increased integrated Rh-actin intensity overall, particularly in the growth cone periphery, where barbed end levels increased 100% (Fig 5C). In contrast, barbed end levels in the peripheral region of growth cones expressing DNERM increased only 45% with the addition of NGF. Collectively, these data suggest ERM proteins play a role in the localization of AC and F-actin barbed ends at the growth cone leading edge in response to NGF.

ADF/cofilin activity increases active phospho-ERM levels

We have shown that NGF increases active phospho-ERM and AC levels, and ERM protein function affects AC and barbed end localization in the growth cone. We next asked if AC activity affects active phospho-ERM levels. We used Chariot to load DRGs with the constitutively-active AC peptide (A3) for 1 hr, then fixed and stained for phospho-ERM. Compared to Chariot alone, Chariot with A3 increased average phospho-ERM levels in growth cone filopodia (Fig 6A). In a previous study, we showed that creating a cell-permeable gradient of active AC (Chariot + A3) diffusing from a micropipette induces a proximal increase in F-actin and attractive growth cone turning (Marsick et al., 2010). To assess if a local elevation of AC activity also locally increases active ERMs, we introduced a Chariot + A3 coated micropipette to one side of a growth cone for 1 min, then fixed. This growth cone showed higher phospho-ERM staining proximal to the pipette (Fig 6A), suggesting increasing AC activity can increase phospho-ERM levels in both a global and local manner.

We next asked if decreasing AC activity also affects active ERM levels. To do so, we measured phospho-ERM levels in DRGs transfected to express constitutively-active LIMK, which phosphorylates and inactivates ADF/cofilin. Compared to GFP controls, LIMK-expressing growth cones cultured overnight in NGF had lower filopodial phospho-ERM levels. Moreover, the phospho-ERM increase with NGF addition in GFP growth cones was blocked in growth cones expressing LIMK (Fig 6B).

Our data thus far suggest AC activity increases active phospho-ERM levels. An early study characterizing radixin in vitro suggested it binds to F-actin barbed ends (Tsukita et al., 1989), and because AC creates barbed ends through filament severing, we hypothesized that active AC is increasing sites for preferential phospho-ERM binding. To evaluate this, we examined the spatial relationship between active AC, F-actin barbed ends, and phospho-ERM in growth cones. DRG cultures were treated with NGF for 5 min, then permeabilized using Alexa Fluor 350–phalloidin (blue), labeled free barbed ends with Rh-actin buffer, then fixed and stained for ADF (presumably showing active AC due to permeabilization) or phospho-ERM. Because phospho-ERM staining was compromised when growth cones were permeabilized prior to fixation, glutaraldehyde and paraformaldehyde were added (each to 0.1%) to the permeabilization buffer to preserve phospho-ERM staining, which did not affect barbed end labeling. As shown previously, NGF increases free barbed ends at the growth cone periphery (Fig 6C). Moreover, both active ADF and phospho-ERM also localized to the periphery, and largely overlap with Rh-actin incorporation. Taken

together, these data suggest the AC-induced increase in free barbed ends may provide preferential binding sites for phospho-ERMs.

Reducing ERM function or protein levels blocks turning to NGF

To assess if ERM activity is necessary for growth cone turning toward NGF, we transfected DRGs to express GFP, DNERM, or GFP with siRNA against radixin and moesin. A transfected growth cone was imaged for 15 min to establish its direction of growth, after which a nitrocellulose-coated micropipette incubated with NGF (as described in Roche et al., 2009) was lowered within 100um to one side of the growth cone, creating a diffusible gradient of NGF. Growth cones were then imaged an additional 45 min, and the turning angles were calculated by comparing the axis of growth before and after the addition of NGF. GFP control growth cones turned toward the NGF source with an average angle of 19.2± 4, but growth cones with DNERM or siRNA had significantly lower turning angles (Fig 7). Together, these data suggest ERM protein function is necessary for attractive growth cone guidance to NGF.

Figure 1.

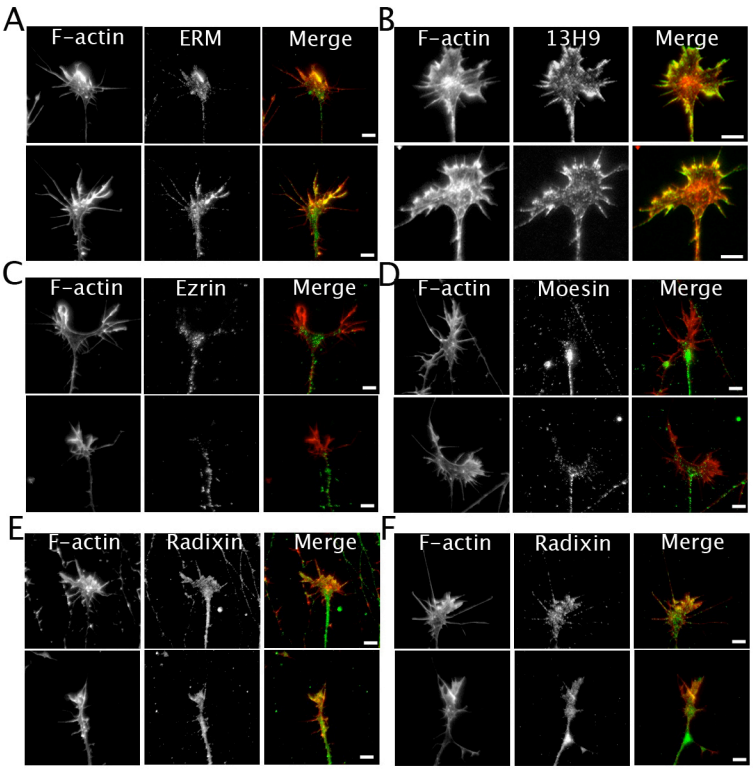

Figure 1. Ezrin, radixin and moesin localization in chick sensory neurons. Embryonic day 7 (E7) DRG explants were cultured overnight on laminin with 40ng/ml nerve growth factor (NGF), fixed and stained with Alexa Fluor 568-phalloidin (red) and antibodies against ERM (A, B) ezrin (C), moesin (D), or radixin (E, 457-3; F, R3653). Scale bars, 10 microns.

Figure 2.

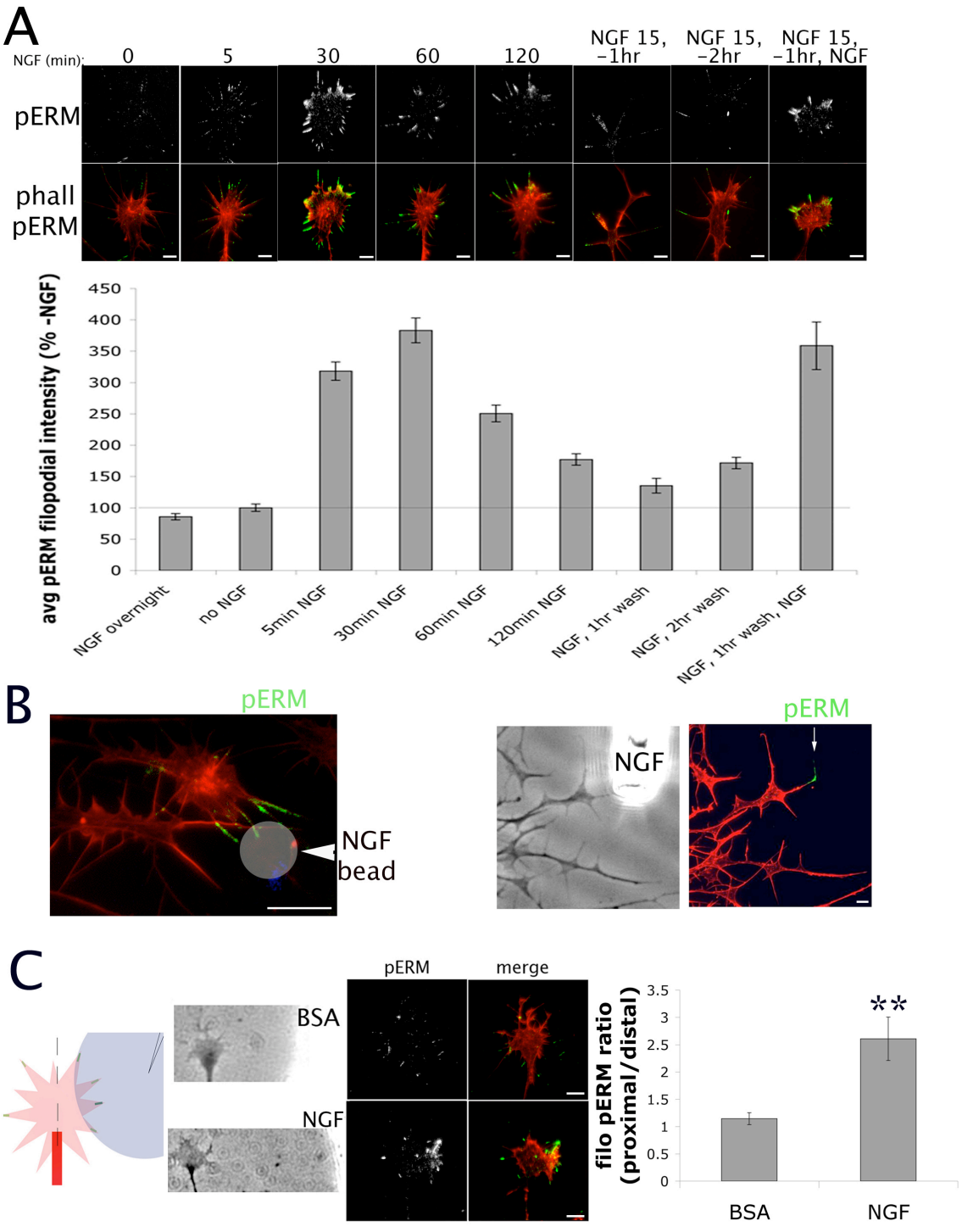
A
NGF (min):
0
5
30
60
120
NGF 15, -1hr
NGF 15, -2hr
NGF 15, -1hr, NGF
pERM
phall pERM
avg pERM filopodial intensity (% -NGF)
450
400
350
300
250
200
150
100
50
0
NGF overnight
no NGF
5min NGF
30min NGF
60min NGF
120min NGF
NGF, 1hr wash
NGF, 2hr wash
NGF, 1hr wash, NGF
B
pERM
NGF bead
NGF
pERM
C
pERM
merge
BSA
NGF
filo pERM ratio (proximal/distal)
3.5
3
2.5
2
1.5
1
0.5
0
**
BSA
NGF

Figure 2. NGF globally and locally activates ERM proteins. (A) DRG explants were cultured overnight on laminin without NGF (except in first bar, 40ng/ml NGF overnight), and NGF was bath-applied for times indicated, fixed, stained with Alexa Fluor 568-phalloidin (red) and phospho-ERM (green), and filopodial phospho-ERM intensities were measured. In B, an NGF-coated bead or micropipette (vigorously rinsed in PBS) was applied for 15 min or 1 min, respectively, cultures were fixed and stained with Alexa Fluor 568-phalloidin (red) and phospho-ERM (green). In C, an NGF-coated micropipette (not rinsed) was lowered to one side of a growth cone on laminin for 1 min, fixed and stained for phalloidin (red) and phospho-ERM (green). The ratio of filopodial phospho-ERM distribution was measured as proximal/distal intensity. Statistical significance using Student's *t* test. Data are means ± SEM; **P<0.001. Scale bars, 10 microns.

Figure 3.

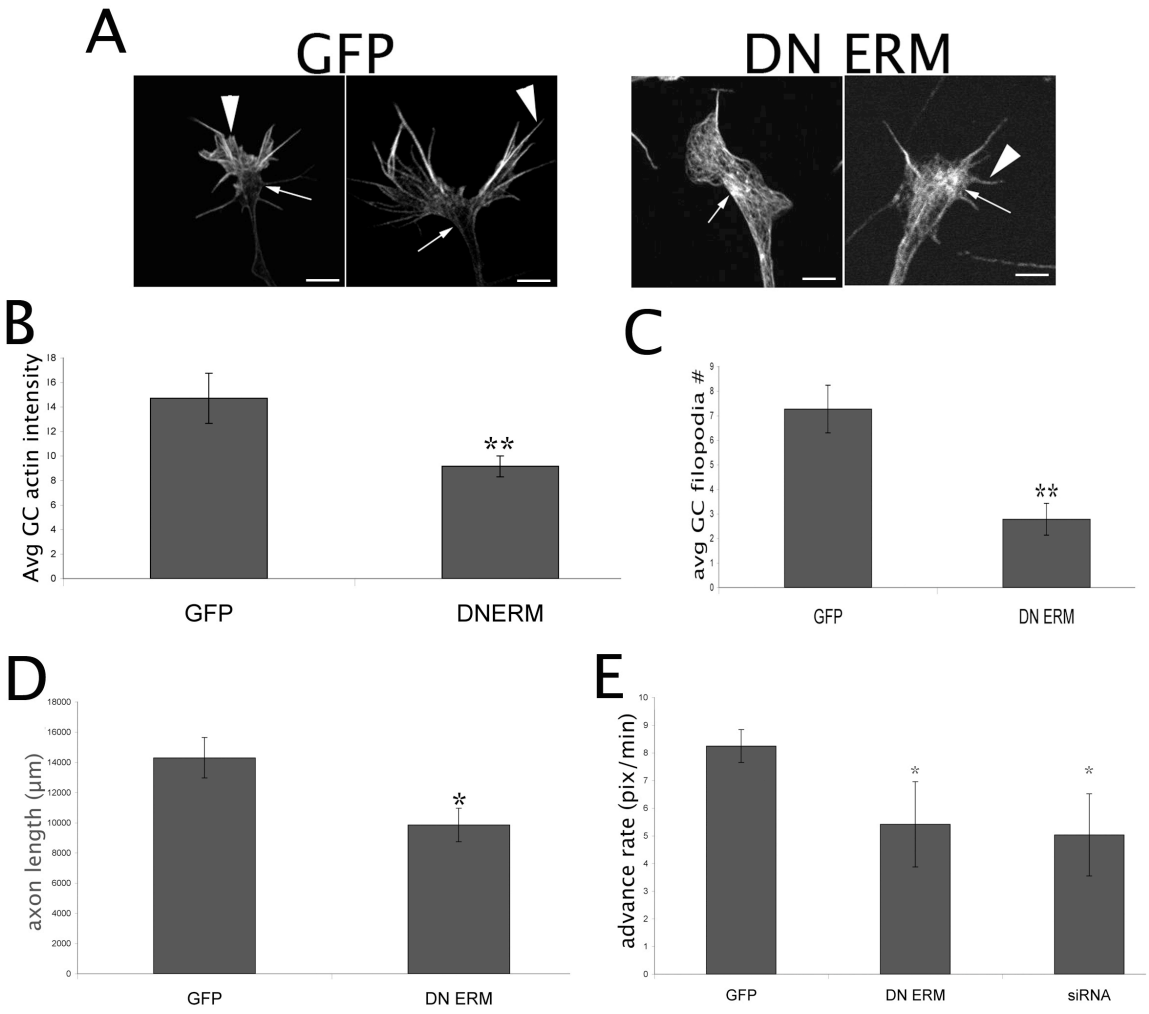

Figure 3. Disrupting ERM function results in smaller and less motile growth cones with disorganized actin filaments. DRGs were transfected with GFP or DNERM and cultured overnight on L1, fixed, F-actin was stained with Alexa Fluor 568-phalloidin (red), and growth cones were imaged using confocal microscopy. Note filopodial morphology (arrowheads) and central domain F-actin content (arrows). In B-E, GFP and DNERM neurons were cultured with 40ng/ml NGF on laminin and analyzed for growth cone actin intensity (B), filopodial number (C), axon length (D), and rate of advance (E). Statistical significance using Student's *t* test. Data are means ± SEM; **P<0.01, *P<.05. Scale bars, 10 microns.

Figure 4.

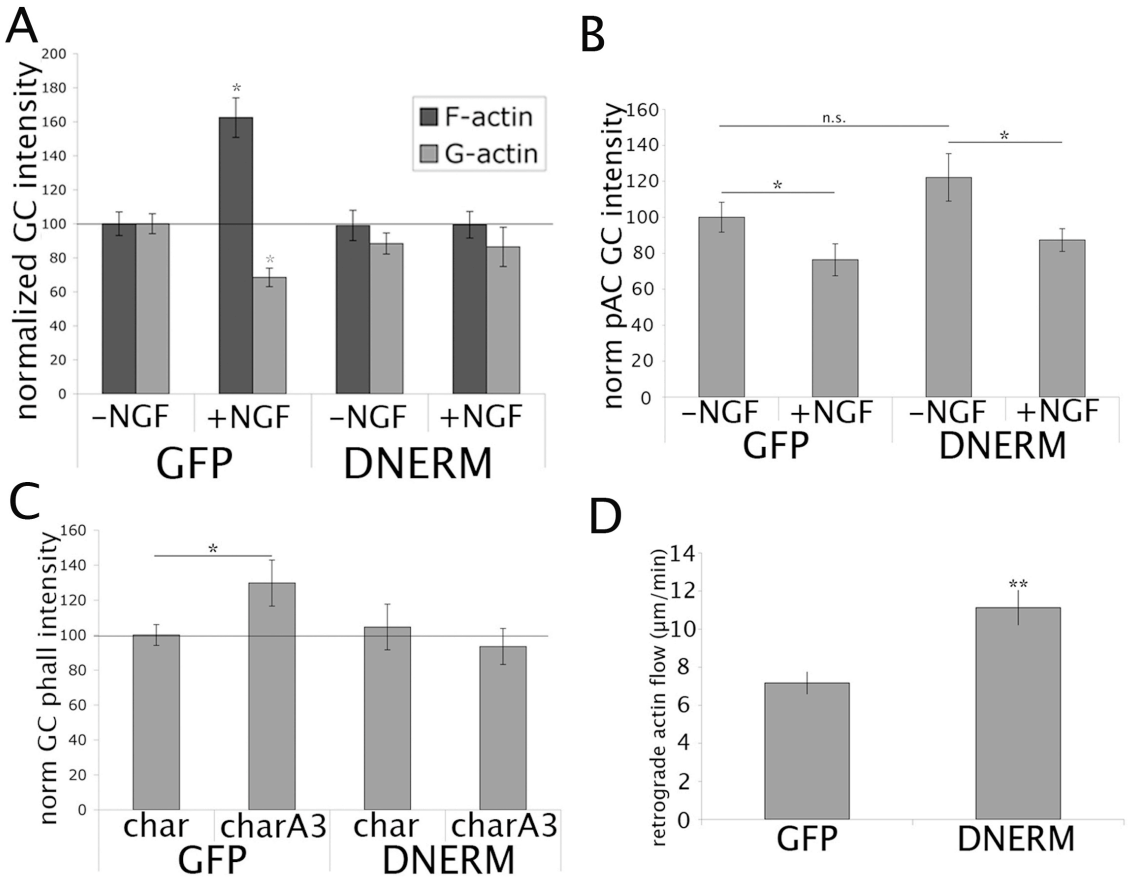

Figure 4. NGF-associated F-actin increase does not occur in DNERM growth cones. DRGs were transfected with GFP or DNERM (A-C) and cultured overnight. (A) Media or NGF was bath-applied for 15 min, cells were fixed and stained with Alexa Fluor 568-phalloidin (F-actin) and FITC-conjugated DNase1 (G-actin), imaged, and GC intensity values were measured. (B) Cultures were treated 15 min with media or 40ng/ml NGF, fixed, and stained with phospho-AC antibody and GC intensities were measured. (C) Cultures were treated with chariot alone or chariot + A3 (active ADF/cofilin) for 1 hr, fixed, stained with Alexa Fluor 568-phalloidin, and growth cone phalloidin intensities were measured. (D) DRGs were co-transfected with RFP-actin and GFP or DNERM and cultured overnight. Growth cones were imaged for 6 min at 3 sec intervals. Bright RFP-actin features were tracked to calculate retrograde

flow rates. Statistical significance using Student's *t* test. Data are means ± SEM; *P<.05, **P<0.001.

Figure 5.

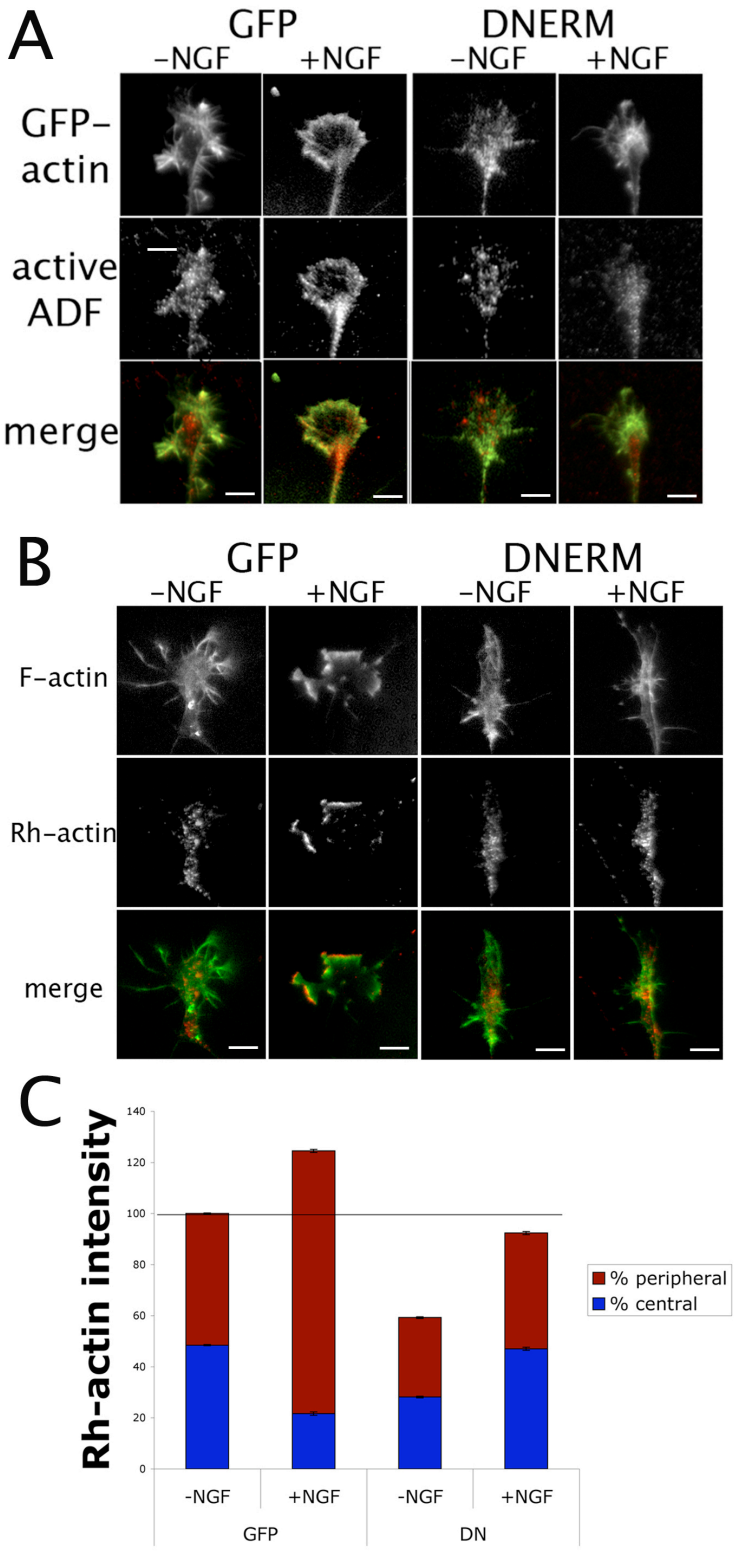
A
GFP
DNERM
-NGF
+NGF
-NGF
+NGF
GFP-actin
active ADF
merge
B
GFP
DNERM
-NGF
+NGF
-NGF
+NGF
F-actin
Rh-actin
merge
C
Rh-actin intensity
140
120
100
80
60
40
20
0
% peripheral
% central
-NGF
+NGF
-NGF
+NGF
GFP
DN

Figure 5. Active ADF/cofilin and free F-actin barbed ends are displaced in DNERM growth cones. DRGs were co-transfected with GFP-actin and GFP or DNERM and cultured overnight. (A) Cells were treated 15 min with media or NGF, permeabilized for 1 min, fixed, and stained with an antibody against total ADF (12977). (B-C) Cells were treated 15 min with media or 40ng/ml NGF, permeabilized 1 min, and barbed end labeling was performed 4min. Cells were then fixed, transfected growth cones were imaged and Rh-actin intensities were measured. Data are means ± SEM; scale bars 10 microns.

Figure 6.

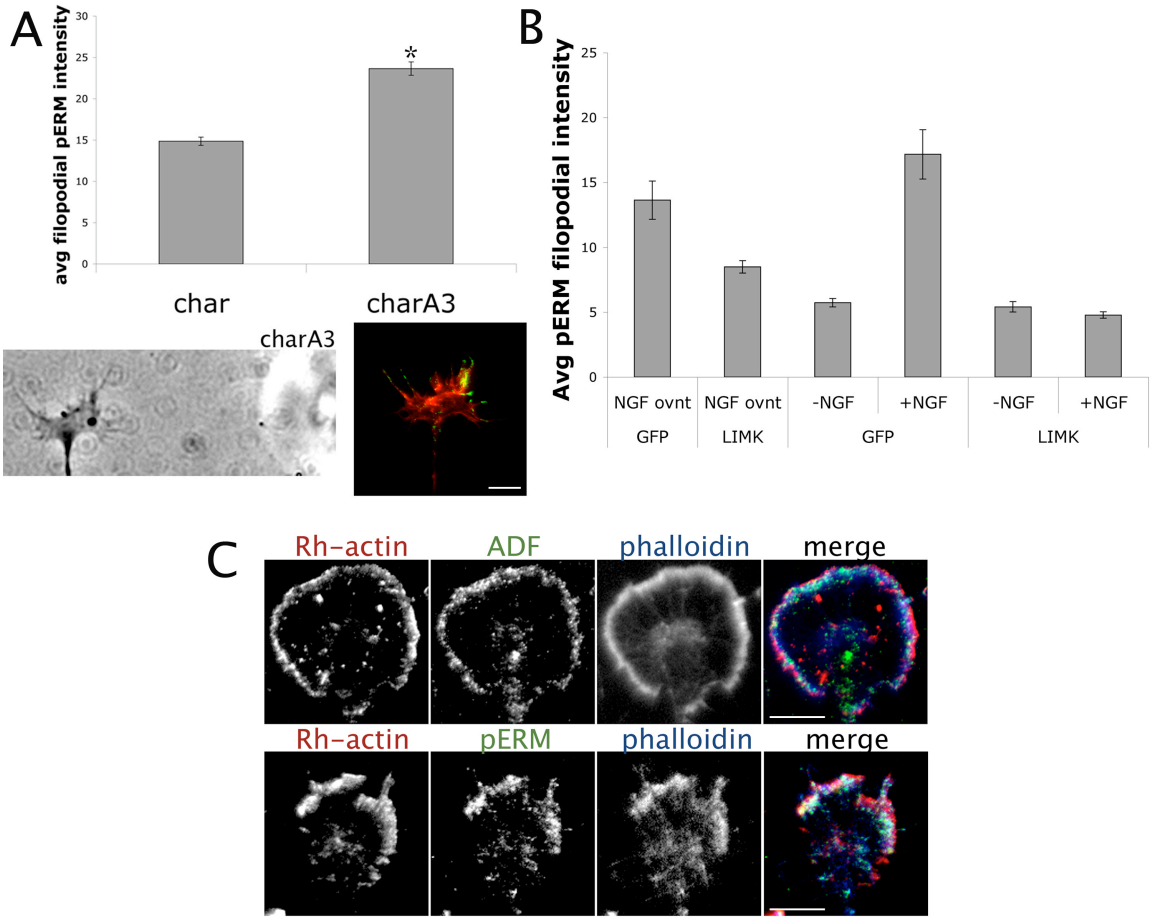

Figure 6. ADF/cofilin activity influences ERM activity. (A) DRG explants were cultured overnight on laminin without NGF, then treated 1 hr with chariot alone or chariot + A3, or a micropipette coated with chariot + A3 was brought to one side of a growth cone for 1 min. Cells were then fixed, stained with Alexa Fluor 568-phalloidin (red) and phospho-ERM (green), and filopodial phospho-ERM intensities were measured. (B) DRGs were transfected with GFP control or constitutively-active LIMK, cultured overnight, treated with NGF as indicated, fixed, and stained for phospho-ERM. Average phospho-ERM filopodial intensities were measured. (C) DRG explants were cultured overnight, treated 15min with 40ng/ml NGF. For ADF condition, cells were permeabilized 1 min with Alexa Fluor 350-phalloidin (blue), Rh-actin labeling was performed 4 min (red), cells were fixed and stained for total ADF (green). For phospho-ERM condition, cells were permeabilized 1 min with

buffer containing Alexa Fluor 350-phalloidin (blue) and 0.1% glutaraldehyde and 0.1% paraformaldehyde, Rh-actin labeling was performed 4 min (red), cells were further fixed 30 min and stained for phospho-ERM (green). Statistical significance using Student's *t* test. Data are means ± SEM; *P<.05. Scale bars 10 microns.

Figure 7.

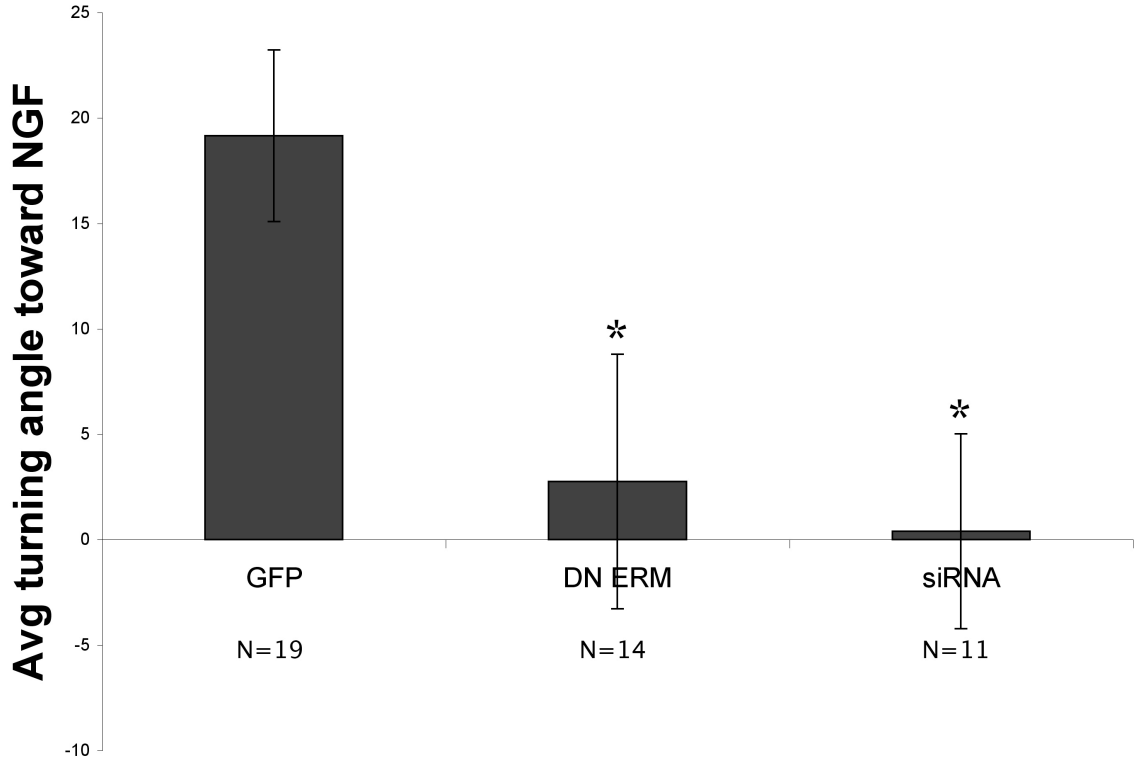

Figure 7. ERMs are involved in proper attractive growth cone guidance to NGF. DRGs were transfected with GFP control, DNERM, or a mixture of GFP and siRNA against radixin and moesin, and cultured overnight without NGF. Transfected growth cones were imaged 15 min then subjected to NGF diffusing from a micropipette to one side and imaged for an additional 45 min, and mean turning angles were measured. Statistical significance using Student's *t* test. Data are means ± SEM; *P<.05.

Supplementary Figure S1.

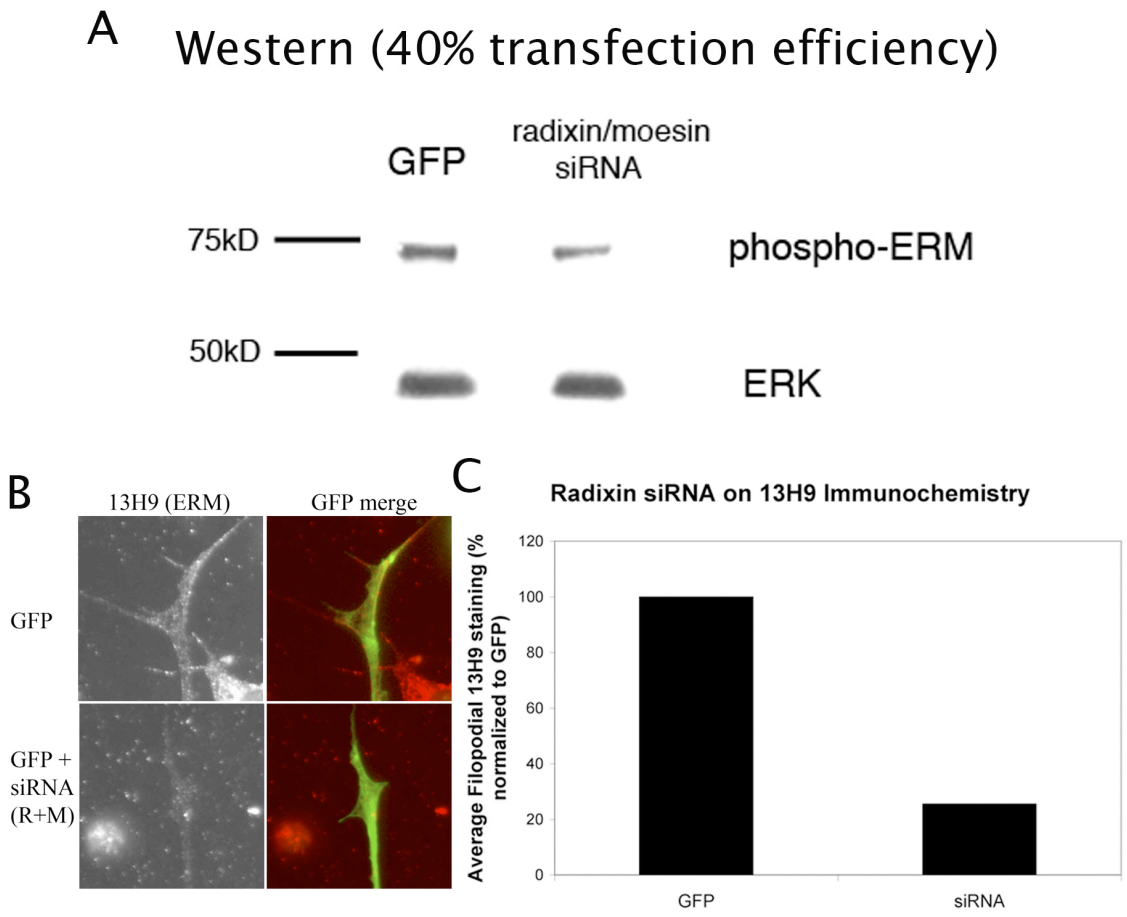

Figure S1. Combined siRNA against radixin and moesin reduces ERM levels. (A) Western blot of DRGs transfected with GFP or GFP + radixin + moesin siRNA. (B) Immunochemistry using 13H9 in growth cones transfected with GFP control or GFP + radixin + moesin siRNA. (C) Filopodial 13H9 intensity in GFP control or siRNA-transfected growth cones.

Discussion

Here we have shown that NGF rapidly increases active phospho-ERM proteins in sensory neuron growth cone filopodia, in both a global and local manner. Disrupting ERM function results in shorter axons, and less motile growth cones with disorganized actin filaments. The increase in F-actin associated with NGF addition is blocked in DNERM-expressing growth cones, which also have higher rates of retrograde actin flow. Although growth cones with disrupted ERM function still exhibit NGF-dependent activation of ADF/cofilin, active AC and barbed ends are displaced from the growth cone periphery. Furthermore, we found the activity of AC influences ERM activity, where increasing active AC with a constitutively-active peptide increases phospho-ERM levels, and reducing AC activity with constitutively-active LIMK reduces phospho-ERM levels. Stimulating DRGs with NGF also results in the similar localization of free F-actin barbed ends, active AC and phospho-ERM proteins at the growth cone leading edge. Lastly, we found impairing ERM function disrupts attractive axon guidance to NGF. Collectively, these data support a mechanism by which ADF/cofilin and ERM activity together mediate NGF-induced F-actin elevation and subsequent growth cone guidance.

In this study we found NGF addition increases active phospho-ERM levels, which agrees with previous studies (Jeon et al., 2010; Amieva and Furthmayr, 1995; Gonzalez-Agosti and Solomon, 1996). The possible signaling cascades involved in NGF-induced ERM activation were not investigated here. NGF binding to its receptors TrkA and p75 activates numerous signaling cascades, and the regulation of ERM activity is complex, with numerous kinases implicated, including Akt, PKC and

PI3K, as well as the activity of Rho GTPases Rho, Rac, and Cdc42 (Jeon et al., 2010; Matsui et al., 1998; Simons et al., 1998; Matsui et al., 1999; Nakamura et al., 2000; Yonemura et al., 2002; Shiue et al., 2005; Baumgartner et al., 2006). All of these signaling molecules are regulated downstream of NGF, and it is likely that multiple signaling molecules regulate ERM activity in neurons. Future studies are needed to focus on factors crucial for growth cone guidance to NGF, such as PLC, PI3K, and the RhoGTPases (Gallo et al., 1997; Ming et al., 1999; Song and Poo, 1999; Sakumura et al., 2005).

We found disrupting ERM function produces abnormal growth cone morphology and motility, which agrees with previous work as well (Paglini et al., 1998; Castelo and Jay, 1999; Parisiadou et al., 2009). In addition, confocal imaging revealed disorganized actin filaments at the center of DNERM growth cones. Thus, ERM proteins appear to either establish or maintain organization of growth cone actin filaments. To this end, ERMs bound to membranous receptors could properly orient actin filaments with their fast-growing barbed ends toward the leading edge. Because ERM proteins bind numerous membrane proteins, identifying the specific ERM binding partners involved in developing growth cones is essential to understanding how, and under what circumstances, ERMs regulate actin organization. The L1 cell-adhesion molecule (L1CAM) has been shown to interact with ERM proteins in neurons and is highly expressed in the developing nervous system (Dickson et al., 2002; Mintz et al., 2003; Haas et al., 2004; Cheng et al., 2005; Sakurai et al., 2008). Other membranous ERM binding partners are also expressed in neurons, including the sodium-hydrogen exchanger NHE1, telencephalin (Denker et al., 2000; Bretscher

et al., 2002; Furutani et al., 2007), and extracellular matrix receptor CD44 (Ikeda et al., 1996).

Here we show that active AC and free F-actin barbed ends are displaced in DNERM growth cones. It is unclear if ERM proteins play a direct role in targeting AC to the leading edge, or indirectly via their affect on actin filament organization. It remains unclear if acute disruption of ERM function would have a similar impact on AC and barbed end localization, a question that could be addressed using Micro-CALI to locally disrupt radixin in growth cones responding to an NGF gradient (Castelo and Jay, 1999). Moreover, it is possible ERM proteins also affect the localization of other important actin-binding proteins and membrane receptors, a topic for future studies.

This study found elevating AC activity also elevated phospho-ERM levels. Active AC increases free F-actin barbed ends, onto which active radixin may preferentially bind (Tsukita et al., 1989). In support of this, we found that active AC and phospho-ERMs both co-localize with free F-actin barbed ends at the growth cone periphery after NGF addition. Phospho-cycling of ERM proteins may permit binding to these barbed ends, stabilizing active ERMs and their association with actin and the membrane.

Our previous study showing local AC activation toward an NGF gradient (Marsick et al., 2010), with the present results showing similar local ERM activation, suggest a model in which a gradient of NGF stimulates an asymmetric increase in F-actin and attractive growth cone turning. AC activation increases free F-actin barbed ends, which phospho-ERMs bind to and tether filaments to the membrane, stabilizing

these filaments toward the cue to support and maintain an increase in F-actin. In addition, ERM proteins may tether crucial proteins to the proximal growth cone region, such as active AC, adhesion receptors like L1CAM, or signaling molecules that perpetuate asymmetric polymerization. ERMs may also function as a localized signaling molecule, by increasing RhoGTPase activity (Takahashi et al., 1997; Hamada et al., 2001). These remaining questions should be addressed in future studies, where the localization and activity of membrane receptors and signaling molecules are examined in growth cones responding to NGF.

In summary, our data demonstrate that NGF rapidly and locally activates growth cone ERM proteins, and the activities of ADF/cofilin and ERMs are integral in mediating growth cone guidance to NGF. Further studies are needed to clarify how AC affects ERM function, as well as the short- and long-term effects of ERM function on F-actin organization and membrane proteins. In addition, these data highlight the importance of investigating how multiple actin-binding proteins impact each another's activity to mediate axon guidance during development, which will inform future efforts to repair damages neural circuits.

Chapter IV: Protein synthesis in distal axons is not required for growth cone responses to guidance cues

This chapter was modified from the original work published as:

Florence K. Roche, Bonnie M. Marsick, and Paul C. Letourneau

Protein synthesis in distal axons is not required for growth cone responses to guidance cues.

J Neurosci 2009 29(3):638-652.

*Bonnie M Marsick contributed directly to the following figures: Figure 3(C-F), Figure 6(E-F), and Figure 8.

Introduction

Neurons are highly polarized with elaborate shapes and highly localized activities. Protein synthesis is not confined to the perikaryon; rather, proteins made in dendrites and axons have important functions (Steward and Schuman, 2003). Defective dendritic protein translation underlies some behavioral deficits and mental retardation (Bramham and Wells, 2007; Dahm and Macchi, 2007; Wang et al., 2007). Axonal protein synthesis is critical in functions of terminals, as well as in development and regeneration (Campenot and Eng, 2000; Hengtst and Jarffrey, 2007; Koenig and Giuditta, 1999; Piper and Holt, 2004; Twiss and van Minnen, 2006; Verma et al., 2005; Zhang and Poo, 2002).

Is local protein synthesis important in axonal growth and guidance? *In vitro* experiments with compartmented chambers indicate that axonal protein synthesis is not required for axonal growth (Blackmore and Letourneau, 2007; Eng et al., 1999). Yet, there are reports that responses to guidance cues require axonal protein synthesis (Brunet et al., 2005; Campbell and Holt, 2001; Farrar and Spencer, 2008; Guirland et al., 2003; Leung et al., 2006; Lin and Holt, 2007; Piper et al., 2006; Wu et al., 2005; Yao et al., 2006). When growth cones enter new environments, local synthesis of receptors could sensitize growth cones to new guidance cues (Brittis and Flanagan, 2002). In addition, growth cone adaptations to changed balances of cues may involve local synthesis of receptors or signaling components (Ming et al., 2002).

Thus, local synthesis of receptors or signaling components may be necessary for growth cone navigation. Is it also necessary to locally make proteins

with general roles in growth cone motility? Recent papers report that RhoA GTPase and ß-actin must be rapidly and locally synthesized for growth cones to respond to several cues (Leung et al., 2006; Wu et al. 2005, Yao et al., 2006). In light of the diverse mechanisms that rapidly regulate RhoA and ß-actin activity, it is unexpected that these components must be locally synthesized to enable responses to guidance cues.

Because previous studies involved few neuronal types, we investigated whether protein synthesis is required for growth cones of other neurons to respond to guidance cues. First, we found that globally inhibiting protein synthesis leads to slowing and arrest of axonal growth over several hours. When protein synthesis inhibitors were added before several positive and negative cues, we found normal growth cone responses. Repulsive cues, ephrin-A2, slit-3, Semaphorin3A (Sema3A) and Semaphorin6A (Sema6A), induced growth cone collapse in the presence of protein synthesis inhibitors. F-actin polymer was lost after adding repulsive cues. Furthermore, attractive cues, nerve growth factor (NGF) and neurotrophin-3 (NT-3), induced growth cone protrusion and increased F-actin despite inhibiting protein synthesis. In addition, growth cones turned toward an NGF source in the presence of protein synthesis inhibitors. In compartmented cultures where axonal protein synthesis was inhibited for many hrs, growth cones still responded to guidance cues. Our data indicate that protein synthesis in distal axons of chick retinal, sympathetic, and DRG neurons and mouse DRG neurons is not required for responses to several guidance cues.

Materials and Methods

Materials F12 medium, DMEM medium, B27 additives, laminin, poly-D-lysine, Alexa Fluor 488 phalloidin, Alexa Flour 568 secondary antibodies, Click-iT AHA (cat. no. C10102) and Click-iT Tetramethylrhodamine Protein Analysis Detection Kit (cat. no. C33370) reagents were purchased from Invitrogen (Carlsbad CA). NGF, NT-3, L1-Fc, slit-3, ephrin-A2-Fc, Sema3A-Fc and Sema6A-Fc were purchased from R & D Systems (Minneapolis MN). Anti-RhoA monoclonal antibodies were purchased from Santa Cruz Biotechnology (Santa Cruz CA), and anti-eIF-4EBP-P rabbit antibodies were purchased from Cell Signaling Technology (Danvers MA). Rabbit anti-ß-actin was a gift from Dr. James Ervasti (University of Minnesota; Prins et al., 2008). Collagen was purchased from Inamed (Fremont CA). Cycloheximide and anisomycin were purchased from Calbiochem (San Diego CA), and MG-132 was from Tocris Bioscience (Ellisville MD).

Neuronal culture Culture dishes, glass coverslips, or 24- or 96-well dishes were coated overnight with 20 µg/ml laminin or 4 µg/ml recombinant L1-Fc mixed with 8 µg/ml Fc in PBS. Explants of E7 and E13 DRGs, E7 temporal retina, and E7 sympathetic ganglia were dissected from chick embryos, and DRGs were removed from E15 mouse embryos, according to procedures approved by the University of Minnesota Institutional Animal Care and Use Committee. Neural tissues were cultured on experimental substrates in F-12 with B27 additives and buffered to pH

7.4 with 10 mM HEPES. Neurotrophins, NGF or NT-3, were added to cultures, as noted. Neural tissues were cultured overnight in a humidified incubator at 37° C.

Axon elongation assay The effect of protein synthesis inhibitors on axon elongation was determined by time-lapse microscopy of axon elongation by DRG or retinal explants cultured in F12 with B27 (and 10 ng/ml NGF for DRGs) on laminin- or L1-coated 96-well dishes. A dish was placed on the warmed stage of a Nikon inverted microscope, and a microscope field of axons was chosen. CHI or anisomycin (or PBS for control) was added at 20 μM, and time-lapse images were collected at 2-5 minute intervals for 2-5 hr. Axon elongation rates of sample populations were determined, using Metamorph software (Molecular Devices) to measure the distance a growth cone migrated in 5-10 minute intervals over a 3-5 hr period.

Growth cone collapse assay Collapse assays were conducted in 24- or 96-well dishes. Explants were cultured overnight. Ten ng/ml NGF was added to cultures of DRGs or sympathetic ganglia. CHI or anisomycin were added in PBS at 20 μM for 15 min. Control dishes received PBS. After 15 min guidance molecules, Sema3A (0.5 μg/ml), ephrin-A2 (1 μm/ml), or slit-3 (1 μg/ml) were added for 30 min in continued presence of protein synthesis inhibitors. Control dishes received PBS. After 30 min, explants were fixed with 0.5% glutaraldehyde in PBS for 20 min at 37° C. After rinsing in PBS, the wells were visualized with a 20X phase contrast

objective, and growth cones were counted as collapsed if they had one or no filopodia.

Growth cone spreading assay DRG explants were cultured overnight in 96-well dishes. A dish was placed on a warmed stage of an inverted microscope, a field of axons was chosen and images were collected once per min for 15 min. Then, 40 ng/ml NGF or NT-3 was added, and images of the same field were collected every minute for 30 min. Growth cone spreading was measured using Metamorph software to outline the borders of growth cones and determine the enclosed areas.

Growth cone turning assay DRG explants were cultured overnight in F12 with B27 on laminin-coated coverslips glued over a hole in the bottom of a culture dish. Micropipette tips were dipped in a 1% nitrocellulose solution and dried. After drying, a tip was dipped several times in a solution of one µg/ml NGF or BSA in PBS. The micropipette was mounted on a micromanipulator. A culture dish was placed on the warmed microscope stage, and the micropipette tip was positioned 50 µm from a growth cone at a 45° angle to the direction of axon elongation. Images were acquired at 30 sec intervals for 15 min before and 45 min after introducing the micropipette tip. CHI was added to some dishes at the beginning of image acquisition. Growth cone turning angles were determined as the change in direction of growth cone migration between the beginning and end of the image acquisition period (Ming et al., 1997).

Compartmented cultures Compartmented cultures were made by putting an E7 DRG explant with attached peripheral root on a substrate, and adhering a 5 mm glass cloning cylinder to the substrate with silicone grease, so the DRG was within the lumen and the peripheral root extended under the 1 mm cylinder wall with its terminus outside the wall. This created two compartments and allowed us to expose the DRG and the peripheral root to different media. For chemotaxis experiments, a 3 mg/ml collagen gel was created in the outside compartment, following the manufacturer's instructions (PurCol, Inamed). Affi-Gel BlueGel chromatography beads were soaked in one µg/ml NGF or BSA in PBS for one hour, rinsed in PBS, and then placed in the collagen gel near the peripheral nerve root with an NGF-bead on one side and a BSA-bead on the other side of the root.

Immunocytochemistry For immunocytochemistry explants cultured on laminin- or L1-coated coverslips were fixed with warmed 4% paraformaldehyde in PBS with 5% sucrose at ph 7.4 for 30 min. After rinsing, explants were treated 15 min with 0.1 M glycine in PBS, and extracted with 0.1% TX-100 in PBS with 2% goat serum and 1% BSA for one hr. Coverslips were incubated with the primary antibodies diluted in PBS containing 1% BSA for one hr. Primary antibody dilutions were 1/100 for anti-RhoA and anti- eIF-4EBP-P, and anti-ß-actin was used, per instructions from Dr. Ervasti (Prins et al., 2008). For labeling F-actin, Alexa Fluor 488-phalloidin was applied at 2.5 µl/100 µl mixed with the primary antibodies. The coverslips were rinsed and then incubated in 0.1% TX-100 in PBS with 2% goat serum and 1% BSA for one hr. Then, Alexa Fluor 568 goat anti-

rabbit or anti-mouse antibodies at 1/1000 dilution were applied in PBS with 1% BSA for one hr. After rinsing, the coverslips were incubated in 0.1% TX-100 in PBS with 2% goat serum and 1% BSA for 30 min, then rinsed, and mounted in anti-fading medium.

Nascent protein synthesis To measure effects of protein synthesis inhibitors CHI and anisomycin on cultured DRG neurons, we used Click-iT reagents from Invitrogen. E7 DRGs were dissociated with 0.2% bacto-trypsin in CMF-PBS for 15 min, then rinsed and plated on poly-D-lysine and laminin-coated glass coverslips in DMEM with B27 additives and 10 ng/ml NGF. After overnight culture, the dishes were rinsed twice with warmed PBS and incubated in methionine-free DMEM for 45 min. During the last 15 min of this period 20 μM CHI or anisomycin or control buffer were added to experimental dishes. Then, the medium was replaced with methionine-free DMEM to which 50 μM of the methionine analog L-azidohomoalanine (AHA; Invitrogen C10102) was added. AHA was omitted from some dishes as a negative control. The dishes were returned to the incubator for 60 min for incorporation of the AHA into nascent proteins with or without protein synthesis inhibitors. After 60 min the dishes were rinsed twice and incubated 30 min in methionine-free DMEM with or without protein synthesis inhibitors. The cultures were fixed with 2% paraformaldehyde and 5% sucrose in PBS for 30 min and then rinsed and incubated in PBS with 0.1 M glycine for 15 min. The coverslips were then drained and placed on parafilm in a humidified 150 mm Petri dish. Using the nomenclature of the Click-iT reagent

kit (Invitrogen C3337, the carboxytetramethylrhodamine alkyne (TAMRA) reagent was prepared by rapidly mixing 150 µl of the Step 1 solution with 120 µl distilled water, then 15 µl of Component C was added with 5 sec vortexing, followed by 15 µl of Step III solution with 5 sec vortexing. Fifty µl of this solution was applied to each coverslip, followed by 5 µl of the Step 2 solution, which was rapidly mixed with the solution on each coverslip. The coverslips were then incubated 30 min in the dark. Then, the coverslips were drained, rinsed twice with distilled water, then twice with methanol for 15 min, before being returned to distilled water and finally mounted on glass slides in anti-fading medium.

To measure the effects of NGF and Sema3A on protein synthesis in DRG neurons, we used the Click-iT reagents as described above. Dissociated DRG neurons were cultured overnight on poly-D-lysine and laminin-coated coverslips in DMEM and B27 additives with 0.1 ng/ml NGF. After rinsing and 45 minute incubation in methionine-free DMEM, the medium was replaced with methionine-free DMEM containing 50 µM AHA and either 40 ng/ml NGF, 1 µg/ml Sema3A or PBS as a control for addition of a guidance cue. Other samples were incubated in methionine-free DMEM without AHA, as a control for the TAMRA reagent procedure. After one hour incubation with AHA and the guidance cues, the dishes were rinsed twice and incubated in methionine-free DMEM for 30 min, followed by fixation and incubation with the TAMRA reagents, as described above.

Quantitative fluorescence determinations

A Spot camera mounted on an Olympus XC-70 inverted microscope was used to acquire images for quantitative fluorescence measurements. For each experiment the camera exposure time and gain setting was set to avoid saturation of intensity values, and all images from an experiment were acquired in a single session with the same exposure for all images. Metamorph software was used for quantitative measurements.

Effects of NGF and Sema3A on phospho-eIF-4EBP content of distal axons E7 DRG explants were cultured overnight on laminin-coated coverslips. Forty ng/ml NGF, one µg/ml Sema3A or PBS were added for 15 min, and then the cultures were fixed and processed for immunofluorescence staining, as described above. For measuring anti-eIF-4EBP-P staining, images of imunofluorescence staining of a sample population of distal axons and growth cones were acquired using a 60X oil immersion objective. The linescan tool was used to determine mean fluorescence intensity of a line 2 pixels wide extending proximally 15 µm from the C-domain of a growth cone into the axon.

Effects of NGF and Sema3A on ß-actin and RhoA content, respectively, of DRG growth cones E7 DRG explants were cultured overnight on laminin-coated coverslips. Twenty µM CHI or PBS was added to cultures for 15 min, and then forty ng/ml NGF, one µg/ml Sema3A or PBS were added to a culture dish for 15 min in the continued presence of CHI or PBS. The cultures were fixed and

processed for immunofluorescence staining with anti-RhoA (Sema3A-treated and controls) or anti-ß-actin (NGF-treated and controls). Images of immunofluorescence staining of a sample population of growth cones were acquired using a 60X oil immersion objective. To measure growth cone content of RhoA or ß-actin, the boundary of the distal 30 m of each growth cone and distal axon was outlined with an outline tool, and the mean integrated pixel intensity of anti-RhoA or anti-ß-actin staining was determined.

Effects of Sema3A and ephrin-A2 on F-actin distribution in DRG and retinal growth cones For measuring effects of ephrin-A2 and Sema3A on F-actin content of growth cones, E7 DRGs and temporal retina explants were cultured overnight on L1-coated coverslips. Twenty µM CHI or PBS was added \for 15 min, and then 40 ng/ml NGF (DRGs) or 2 µg/ml ephrin-A2 (temporal retina) was added for 15 min in the continued presence of CHI or PBS. The cultures were fixed with 4% paraformaldehyde and 5% sucrose for 30 min and then extracted with 0.1% TX-100 in PBS for 15min. F-actin was stained by incubation with 2.5 µl/0.1 ml Alexo Fluor 568 phalloidin in PBS for 60 min. After rinsing, the coverslips were mounted in anti-fading medium. Images of sample populations of growth cones were acquired with a 63X oil immersion objective. Using the linescan tool of Metamorph, phalloidin fluorescence was determined along a two pixel wide by 6 µm line backward from the center of the growth cone leading margin.

Effects of NGF on F-actin content of DRG growth cones E7 DRG explants were cultured overnight on L1-coated coverslips. Twenty μM CHI or PBS was added to cultures for 15 min, and then 40 ng/ml NGF was added for 15 min in the continued presence of CHI or PBS. The cultures were fixed with 4% paraformaldehyde and 5% sucrose for 30 min and then extracted with 0.1% TX-100 in PBS for 15min. F-actin was stained by incubation with 2.5 μl/0.1 ml Alexo Fluor 568 phalloidin in PBS for 60 min. After rinsing, the coverslips were mounted in anti-fading medium. Images of growth cones were acquired with a 60X oil immersion objective. To measure F-actin content, the boundary of each growth cone was outlined with the outline tool, and the mean pixel intensity and integrated pixel intensities of F-actin staining were determined for each growth cone.

Statistical analysis Parameters of population values are reported as mean ± S.E.M. All statistical analysis was by unpaired Student's t-test or Mann-Whitney U test.

Results

NGF and Sema3A activate protein synthesis in DRG neurons

It is reported that guidance cues trigger inactivation of the translation repressor elF-4EBP1 in distal axons (Campbell and Holt, 2001; Cox et al., 2008; Li et al., 2004). Inactivation of e1F-4EBP1 by phosphorylation releases elongation factor elF-4E to initiate mRNA translation. We used phospho-specific antibodies to ask whether the guidance cues NGF and Sema3A induce elF-4EBP1 phosphorylation (elF-BP1-P) in axons extended from E7 chick dorsal root ganglia (DRG). DRG explants were cultured overnight and exposed to NGF or Sema3A for 15 min before fixation and staining with anti- elF-4EBP1-P (Figure 1a-c). Panel 1d shows analysis of mean anti-elF-4EBP-P staining of a line scanned from the center of each growth cone proximally for 15 μm in the axon. The mean staining intensity for elF-4EBP1-P was significantly greater in distal axons of both NGF- and Sema3A-treated DRG cultures than in axons of untreated DRGs. Thus, like previous reports, signaling triggered by NGF and Sema3A inhibits a repressor of mRNA translation in distal axons of DRG neurons.

The inactivation of elF-4EBP1 and activation of elongation initiation factor 4E are associated with increased protein synthesis in response to growth factors and guidance cues (Campbell and Holt, 2001; Li et al., 2004; Takei et al., 2001). We investigated whether protein synthesis in DRG neurons is altered by NGF and Sema3A. To detect nascent proteins we used a non-radioactive reagent, L-azidohomoalanine (AHA), a methionine analog, which is incorporated into

proteins instead of methionine and is detected by reaction of the azido-modified protein with a fluorescent alkyne (see Materials and Methods for detailed procedure). Overnight cultures of dissociated E7 DRGs were exposed to NGF or Sema3A in AHA-containing media for 60 min before fixation, and reaction with the fluorescent alkyne. To control for the labeling procedures, some samples were not given AHA, and to control for the addition of guidance cues, other samples were given AHA but neither NGF or Sema3A. As shown in Figure 2a-e, the mean staining intensity for nascent proteins in both cell bodies and distal axons was increased 60% by NGF addition, compared to cultures not treated NGF. After addition of Sema3A the nascent protein amounts were also elevated from the levels in untreated control neurons. Because this experiment involved one time point, we make no conclusion about effects of NGF or Sema3A on rates of nascent protein synthesis or degradation. Because of the global presentation of ligands and the duration of treatment, we infer nothing about the location of nascent protein synthesis. However, our results indicate that NGF and Sema3A stimulate increased amounts of nascent proteins in cell bodies and axons of DRG neurons. Thus, like previous reports we found that guidance cues increase nascent proteins in neurons (Campbell and Holt, 2001; Zhang et al., 1999; 2001).

DRG axonal elongation is inhibited by global treatment with protein synthesis inhibitors, but not by inhibiting protein synthesis in distal axons only

Before assessing the effects of inhibiting protein synthesis on responses to guidance cues, we showed that cycloheximide (CHI), which inhibits peptide chain

elongation, and anisomycin, which inhibits peptide bond formation, are effective inhibitors of chick neuronal protein synthesis. These drugs were previously used to inhibit protein synthesis in chick neurons (Blackmore and Letourneau, 2007; Luduena, 1973; Oppenheim et al., 1990). To measure the effects of CHI and anisomycin, we used the same Click-iT reagents that we used to determine the effects of NGF and Sema3A on nascent protein synthesis. After washing out methionine-containing DMEM medium, DRG cells were incubated one hr with 50 mM AHA with or without 20 μM CHI or anisomycin. As shown in Figure 2 f-i and quantitated in panel j, CHI- and anisomycin-treated neurons were as weakly labeled as control neurons that were not incubated with the methionine analog, AHA, but only with the fluorescent alkyne reagents. Thus, we could not detect protein synthesis in DRG neurons treated with CHI or anisomycin.

Because it was previously reported that global application of protein synthesis inhibitors did not inhibit axonal extension during a one hr period (Campbell and Holt, 2001), we investigated axonal elongation by DRG and retinal neurons in the global presence of protein synthesis inhibitors. Explants of E7 DRGs and temporal retina were grown in dishes coated with laminin or the cell adhesion molecule L1. CHI, anisomycin or the drug vehicle was added, and rates of axonal elongation were calculated after time-lapse imaging. The mean elongation rate for untreated DRG or retinal axons did not change over four hr of recording, though the elongation rate for DRG axons was significantly faster on laminin than on L1 (130±16 vs 41±6 μm/hr, respectively). During the first hr of treatment with 20 μM CHI or anisomycin, the axonal elongation rate of treated

DRG or retinal neurons was nearly equal to that of control, untreated neurons (Table 1; Figure 3a). During the second hr, axonal growth rates began to slow in the presence of protein synthesis inhibitors (Table 1; Figure 3a). Some growth cones became smaller and less motile, and on laminin some axons retracted. On L1 axonal retraction during the second hr of treatment was less frequent than on laminin, but the rate of axon elongation still slowed (Table 1). Continuing after 2 hr of protein synthesis inhibition, nearly all axons retracted or became quiescent (Figure 3b; Supplemental Figure S1).

We asked whether concurrent inhibition of proteolysis might extend the time that axons elongate in the presence of protein synthesis inhibitors. We added MG-132, an inhibitor of proteosome activity previously used with neurons (Lee and Goldberg 1996; Tursun et al., 2005), to some wells that received CHI. MG-132 alone did not reduce axon elongation over 4 hr (Figure 3b). When CHI was combined with MG-132, fewer axons retracted during hr 2-5 in CHI + MG-132 than in wells treated with CHI alone, but axonal growth had still stopped in CHI + MG-132 by 4-5 hr (Figure 3b). Thus, global inhibition of protein synthesis does not significantly inhibit axonal elongation during the first hr of treatment, but during the second hr axonal growth slowed, and axons began to retract or lose growth cone activity. Concurrent inhibition of protein degradation prolonged the period during which axons could elongate in the absence of protein synthesis.

Previously, compartmented chambers were used to show that protein synthesis in distal axons is not required for axonal elongation (Blackmore and Letourneau, 2007; Eng et al., 1999). We devised a compartmented dish to

investigate whether distal protein synthesis is required for DRG axon elongation. An E7 DRG with the attached peripheral root was placed in the lumen of a 5 mm diameter glass cloning cylinder, which was stuck to the substrate with silicon grease. The distal portion of the peripheral root was extended under the cylinder wall, so the end of the root was outside the cylinder. We determined that the inside of the cloning cylinder and the dish outside the cylinder were separate compartments by showing that blue dye placed in one compartment did not diffuse into the other compartment over 24 hr. In addition, different heights of the liquid medium could be maintained in the two compartments. When control medium was in the distal compartment, Schwann cells migrated with axons that extended from the end of the peripheral nerve (Figure 3c). After 24 hr axons and Schwann cells had extended hundreds of μm from the nerve root. If 20 μM CHI was in the distal axon compartment, axons still elongated for many hr (Figure 3d), but Schwann cells did not leave the nerve roots (compare Figure 3c and d). Because of the separation of the compartments, axons and Schwann cells migrated from the explants in the perikaryon compartment of dishes with CHI in the distal axon compartment (Figure 3e and f are similar, despite CHI in the axon compartment). Axonal growth rates were comparable in untreated (144±13 μm/hr) or CHI-treated (140±14 μm/hr) distal axonal compartments. Thus, although axonal growth from DRG explants stops after one hr of global inhibition of protein synthesis, protein synthesis is not required in distal axons for DRG axonal growth for >24 hr.

Induction of growth cone collapse by repulsive cues does not require protein synthesis

Growth cone collapse assays were conducted with E7 and E13 DRG explants that were exposed to Sema3A, E8 sympathetic chain ganglia exposed to Sema6A, and E7 temporal retinal explants exposed to negative cues, ephrin-A2 and slit-3 (Table 2; Figure 4). Explants were cultured 24 hr in laminin-coated wells, and then 20 μM CHI or anisomycin or control vehicle were added for 15 min before adding Sema3A to DRG cultures, or ephrin-A2 or slit-3 to temporal retinal cultures for 30 min. As illustrated in Figure 4 and presented in Table 2, the low collapse rates of untreated growth cones and the high growth cone collapse induced by these repulsive guidance cues were not different in the presence of CHI than results from explants treated with the drug vehicle (Mann-Whitney U test). Without repulsive cues, the growth cone collapse frequency did not exceed 16%, despite the presence of protein synthesis inhibitors for 45 min. After adding repulsive cues, the collapse frequency was >80% for Sema3A, Sema6A and ephrin-A2 and >60% for slit-3 with or without protein synthesis inhibitors. In addition to studies with chick DRGs, we investigated whether protein synthesis was required for growth cones of embryonic mouse DRG neurons to respond to Sema3A. DRGs were explanted from E15 mice and cultured 24 hr on laminin. Cultures were treated 15 min with CHI or the vehicle for 15 min, before adding Sema3A. As shown in Figure 4m-p and Table 2, CHI treatment did not inhibit the collapse response of mouse DRG growth cones to Sema3A. Some E7 DRG explants were cultured 8 days before treatment. Many growing axons with active

growth cones were present with a mean growth rate of 64 ±5 μm/hr (n=22), and the growth rate did not change, when 20 μM CHI was added for 30 min (69±4 μm/hr, n=22). When 1 μg/ml Sema3A was added to the CHI-treated dishes, 95% growth cones rapidly collapsed. Thus, protein synthesis is not required for growth cone collapse by several neuronal types in response to several negative cues.

We tested the effects of inhibiting protein synthesis on retinal growth cone responses to surface-bound ephrin-A2. Contact with 6 μm ephrin-A2-coated beads induced 90% of temporal retinal growth cones to collapse or turn away from the beads (n=20; Weinl et al. 2004), while contacts with BSA-coated beads induced no turning or collapse (n=8). In the presence of CHI added simultaneously with beads to E7 temporal retinal explants, growth cones did not collapse after contact with BSA-coated beads (n=9), while 95% of CHI-treated growth cones (n=23) collapsed or turned away after contacting ephrin-A2 beads (Figure 4q-v). These results, consistent with responses to soluble repulsive cues, indicate that protein synthesis is not required for responses to repulsive guidance cues.

The loss of F-actin induced by repulsive cues does not require protein synthesis

Downstream signaling from guidance cue receptors regulates actin filament dynamics via Rho GTPases (Guan and Rao, 2003; Hu et al., 2001; Wahl et al, 2000). Because it was reported that local RhoA synthesis is required for Sema3A-induced growth cone collapse (Wu et al., 2005), we investigated the effects of ephrin-A2 and Sema3A on actin filament organization in control and CHI-treated retinal and DRG growth cones. E7 retinal and DRG explants were cultured on L1,

because axonal retraction induced by repulsive cues is diminished on L1, while growth cone collapse still occurs. After 15 min pretreatment with CHI or the control vehicle, explants were exposed to repulsive cues for 15 min, fixed and stained with rhodamine-phalloidin to label F-actin. Figure 5 shows images and line scans of the distribution of F-actin at the leading margins of control, ephrin-A2 or Sema3A-treated retinal and DRG growth cones, respectively, without and with CHI. Control growth cones had a peak of actin filament density at the leading margin, followed by a flat level of filament density further back in the growth cone (Figure 5a, e, f, j). Actin filament distribution and density in growth cones treated 30 min with CHI was identical to controls (Figure 5b, g). In growth cones treated 15 min with ephrin-A2 (temporal retina) or Sema3A (DRG), the peak in actin filament density at the leading edge was absent, and as previously seen (Fan et al., 1993), actin filament density was significantly lower throughout the leading margin (Figure 5 c, e, h, j). Growth cones of neurons treated 15 min with CHI, and then 15 min with ephrin-A2 or Sema3A and CHI were not different from growth cones treated with repulsive cues alone (Figure 5 d, i). Thus, protein synthesis is not required for signaling downstream from repulsive cues that reduces actin filament content.

It is reported that Sema3A stimulates RhoA mRNA translation, and Sema3A increased RhoA density in rat DRG growth cones (Wu et al., 2005). We conducted similar determination of RhoA staining intensity in growth cones of DRG neurons treated with Sema3A with or without inhibiting protein synthesis. As shown in Figure 5k-o, we found no significant changes in mean RhoA staining

intensity in DRG growth cones after Sema3A treatment in control or CHI-treated dishes. Thus, treatment of chick DRG neurons with Sema3A did not significantly change the RhoA content of growth cones.

The induction of growth cone spreading, increased F-actin and growth cone turning by NGF does not require protein synthesis

We examined the effects of CHI on responses of E7 DRG growth cones to attractive cues NGF and NT-3. E7 DRG explants were cultured overnight in L1-coated wells in F12 and B27 without neurotrophins. Growth cone behaviors were recorded before and after adding 40 ng/ml NGF (Figure 6a; Supplemental videos S1 and S2) or NT-3 (Figure 6b). Growth cones rapidly expanded in response to either neurotrophin. As measured in Figure 6c and d (also supplemental videos S3 and S4), this expansion response was not inhibited by 15 min pretreatment with CHI, which remained in the media with the neurotrophins. In another experiment we extended the CHI pretreatment period to two hr before adding NGF. We observed that after two hr in CHI the spreading response of growth cones to NGF addition was absent (Supplemental Figure S2). Thus, chick embryo growth cones normally contain sufficient components to spread in response to neurotrophins without need for protein synthesis.

We next determined the turning response of E7 DRG growth cones toward a soluble NGF gradient. When an NGF-coated micropipette was placed near growth cones, growth cones turned toward the micropipette with a mean turning angle of 12±2.5 ° (n=17; Figure 6e). Using criteria of Ming et al., (1997; >5° is a

positive turn, -5° to +5° is no turn, <-5° is a negative turn), 65% of turns were positive, 35% did not turn, and 0% were negative turns. Turning response to a BSA-coated pipette was –0.6±2.4°(n=9), significantly different from the NGF response ($p < 0.005$; 11% of turns were positive, 11% negative, and 88% did not turn). We then conducted assays in the presence of CHI, which was added 15 min before placing the micropipette. Growth cone turning toward the pipette occurred with a mean turning angle of 5.4±2.1° (n=19; Figure 6f; 42% positive turns, 53% no turns, 5% negative turns). This was statistically different from the turning angle of non-CHI treated growth cones toward NGF ($p < 0.05$, t test). However, the turning response of CHI-treated growth cones toward a BSA-coated pipette was –1.7±2.2° (n=11; 0% positive turns, 91% no turns, 9% negative turns), which was statistically different from the 5.4±2.1° turning response to an NGF micropipette ($p < 0.05$). Thus, global inhibition of protein synthesis did reduce growth cone turning toward NGF, although the attractive turning response was still present.

Growth cone spreading is correlated with increased F-actin content in NGF-treated growth cones. To examine changes in actin filament content in DRG growth cones after adding NGF, E7 DRG explants were exposed to global NGF for 15 min, then fixed and stained with rhodamine-phalloidin to quantify F-actin. As shown in Figure 7, the total integrated staining for F-actin in DRG growth cones was increased 250% at 15 min after adding NGF (Figure 7 a, b, f). This increase in F-actin was unaffected by 15 min pretreatment with CHI before and during NGF treatment (Figure 7 c, d, f). Thus, protein synthesis is not required for the rapid increase in F-actin and growth cone spreading that is induced by NGF.

It is reported that 5 min treatment with netrin or BDNF increased the ß-actin content of *Xenopus* growth cones (Leung et al., 2006; Yao et al, 2006). We treated DRG explants with NGF for 15 min with or without 15 minute CHI pretreatment, and then fixed and stained the cultures with ß actin antibodies (Figure 7g-j). By quantitative immunofluorescence, we found that NGF treatment did not increase the total integrated staining for ß-actin in DRG growth cones and distal axons (Figure 7k). As noted above, NGF treatment did result in increased F-actin content (Figure 7f), and ß-actin distribution was altered in spread NGF-treated growth cones, being concentrated at the leading edge. CHI treatment did not alter total integrated anti–ß-actin staining of growth cones, whether exposed or not exposed to NGF (Figure 7 I, j, k). Thus, NGF treatment did not change the ß-actin content of DRG growth cones and distal axons.

Growth cone responses to guidance cues in compartmented dishes

We used compartmented cultures to ask whether 24 hr inhibition of distal protein synthesis affects growth cone collapse in response to Sema3A. When 1 µg/ml Sema3A was added to axonal compartments treated 24 hr with CHI, 73% of growth cones of E7 DRG neurons collapsed within 10 min (n=24; Figure 8a, b).

We found that the spreading response of E7 DRG growth cones to global NGF addition also occurred after inhibiting axonal protein synthesis for 24 hr (Figure 8c-f). To investigate whether protein synthesis in axons is required for a long term turning response to NGF, we used the compartmented culture and placed agarose beads soaked in either NGF or BSA into a collagen matrix that was

formed in the axonal compartment (Figure 8g and h). The collagen matrix included either 20 μM CHI or the control vehicle. After 24 hr, we analyzed axon orientation with respect to the NGF or BSA beads. We drew a line halfway between the beads and measured the orientation angle of the terminal 200 μm of each axon with respect to the closer bead (Figure 8g and h). In gels with control vehicle the orientation angle to a BSA bead was 14±7°, while orientation to the NGF bead was 46±4°. These values were statistically different ($p < 0.0005$). In gels containing 20 μM CHI, axon orientation toward a BSA bead was 11±8°, while orientation angle toward an NGF bead was 65±7°($p < 0.0001$). Thus, DRG axons elongating from a nerve root into collagen could orient toward an NGF-bead despite continuous presence of CHI. These results show that axonal protein synthesis is not required for DRG growth cones to be guided by an NGF gradient.

Table 1: Effects of Protein Synthesis Inhibitors on Rate of Axonal Elongation

Neuron	Inhibitor	Substrate	0-1 hr (% Control Rate)	1-2hr (% Control Rate)
DRG	cycloheximide	laminin	98±9	54±12
	anisomycin	laminin	88±14	39±11
	puromycin	laminin	75±10	26±14
DRG	cycloheximide	L1	76±15	34±12
	anisomycin	L1	96±13	25±9
Retina	cycloheximide	L1	83±11	59±9
	anisomycin	L1	84±8	67±9

Table 1: E7 DRG or temporal retina explants were cultured in laminin- or L1-coated wells in F12, B27 with 10 ng/ml added to DRG cultures. After 24 hr 20 µM CHI, anisomycin or puromycin or the drug vehicle was added to a well of a dish on a warm microscope stage, and video images were collected at 2-5 min intervals for 2 hr or more. Axon elongation rates were determined using Metamorph software to measure axon elongation at 5-10 min intervals. Average axon elongation ± S.E.M. in drug-treated cultures is expressed as percentage of the elongation rate in vehicle-treated control cultures.

Table 2: Effects of Protein Synthesis Inhibitors on Growth Cone Collapse

Neuron Type	Inhibitor	Guidance Cue	% Collapsed	# GC Counted
E7 Retina	control	control	7%	237
	control	ephrin-A2	81%	194
	CHI	control	9%	206
	CHI	ephrin-A2	90%	126
E7 Retina	control	control	9%	232
	control	ephrin-A2	83%	142
	anisomycin	control	16%	210
	anisomycin	ephrin-A2	88%	184
E7 Retina	control	control	9%	267
	control	ephrin-A2	92%	167
	puromycin	control	7%	215
	puromycin	ephrin-A2	93%	162
E7 Retina	control	control	4%	154
	control	slit-3	66%	128
	CHI	control	5%	209
	CHI	slit-3	66%	106
E7 Retina	control	control	9%	253
	control	slit-3	57%	165
	anisomycin	control	6%	219
	anisomycin	slit-3	64%	148
E7 DRG	control	control	8%	183
	control	Sema3A	91%	228
	CHI	control	7%	210
	CHI	Sema3A	93%	150
E7 DRG	control	control	6%	177
	control	Sema3A	97%	107
	anisomycin	control	8%	106
	anisomycin	Sema3A	92%	78
E13 DRG	control	control	5%	184
	control	Sema3A	93%	168
	CHI	control	5%	214
	CHI	Sema3A	95%	140
E13 DRG	control	control	9%	161
	control	Sema3A	95%	199
	anisomycin	control	9%	143

	anisomycin	Sema3A	93%	149
E7 Symp gang	control	control	9%	200
	control	Sema6A	86%	160
	CHI	control	15%	193
	CHI	Sema6A	94%	188
E7 Symp gang	control	control	13%	233
	control	Sema6A	82%	156
	anisomycin	control	10%	188
	anisomycin	Sema6A	95%	212
E15 mouse DRG	control	control	7%	294
	control	Sema3A	94%	188
	CHI	control	12%	251
	CHI	Sema3A	97%	218

Table 2. Explants of E7 chick DRG, temporal retina, sympathetic ganglia or E15 mouse DRG ganglia were cultured on laminin in F12 with B27. Ten ng/ml NGF was added to DRG and sympathetic cultures. After 24 hr, explants were treated 15 min with vehicle or 20 μM CHI or anisomycin, followed by 30 min incubation with guidance cues in continued presence of vehicle or protein synthesis inhibitor. Explants were fixed, and growth cones were scored as collapsed, if they had one filopodium or less. The Mann-Whitney U test was used to assess whether protein synthesis inhibitors significantly altered the collapse data of either vehicle-treated or guidance cue-treated cultures. The test indicated that protein synthesis inhibitors had no effect on intrinsic growth cone collapse and or on responses to repulsive guidance cues.

Figure 1.

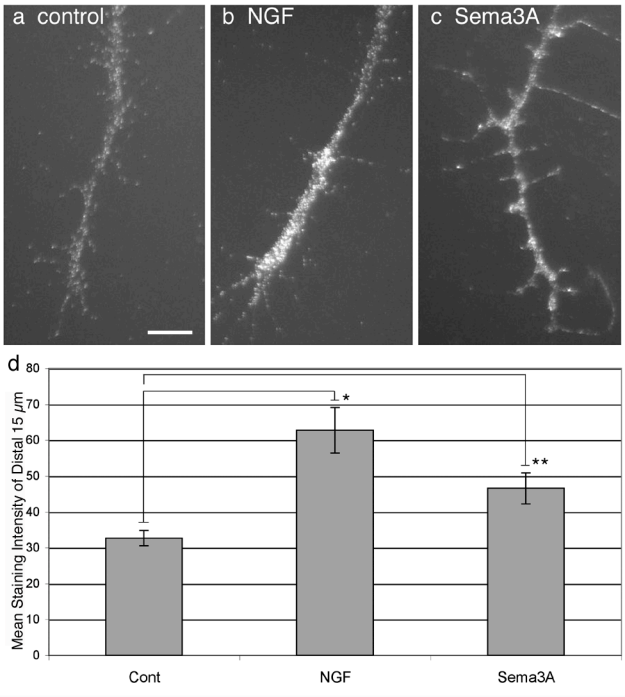

Figure 1. NGF and Sema3A increase phosphorylation of elF-4EBP1. Distal axons of chick E7 DRG neurons stained with anti-phospho-elF-4EBP1 in control medium (a) or after 15 min stimulation with 40 ng/ml NGF (b) or 0.5 µg/ml Sema3A (c). Panel d shows mean staining intensity along a 2 pixel wide line and 15 µm long starting at the growth cone C-domain and into the distal axon. * $p < 0.005$, ** $p < 0.01$. Scale bar = 10 µm.

Figure 2.

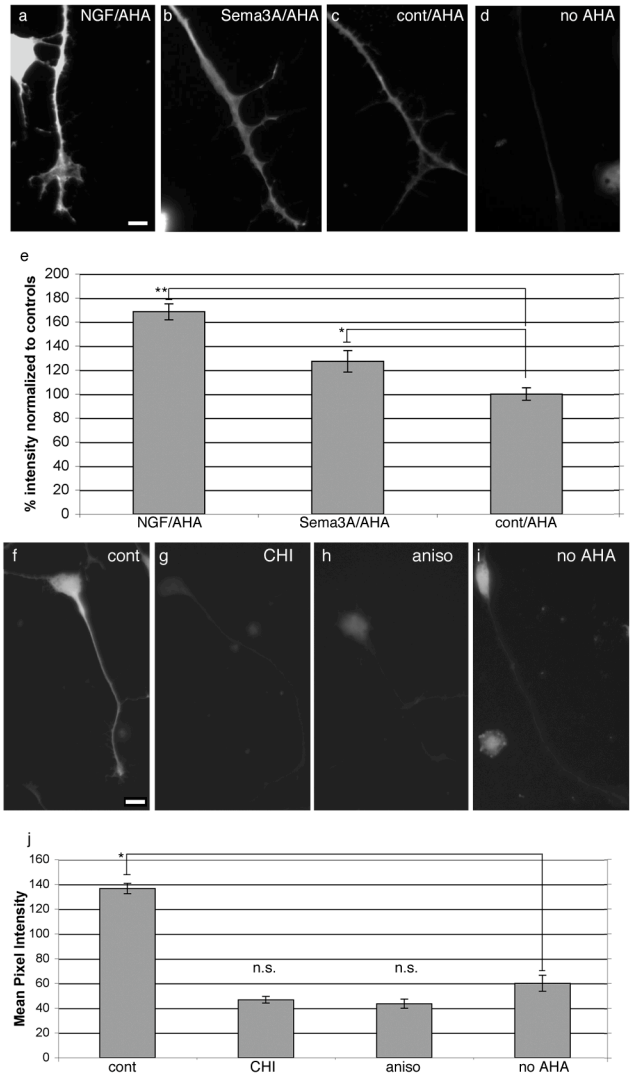

Figure 2. Nascent protein synthesis in E7 DRG neurons. The methionine analog, L-azidohomoalanine (AHA), in methionine-free DMEM was added to dissociated cells treated with 40 ng/ml NGF (a), 0.5 µg/ml Sema3A (b), or control medium (c) for 60 min. Cells in panel d received no AHA. Cells were fixed and incubated with fluorescent alkyne to label the AHA incorporated into nascent proteins. Panel e shows the mean staining intensity of NGF- and Sema3A-treated distal axons segments relative to unstimulated neurons. Mean ± SEM. * $p < 0.05$, ** $p < 0.001$. Panels f-i show that the protein synthesis inhibitors, CHI and anisomycin, inhibit protein synthesis. Dissociated DRG cells cultured overnight in medium with 10 ng/ml NGF were incubated 60 min in methionine-free DMEM with AHA (f) or

with addition of 20 μM CHI (g) or 20 μM anisomycin (h). Cells in panel i received no AHA. Fluorescent alkyne labeling of the CHI- and anisomycin-treated neurons and axons (f, g) was as weak as labeling of cells that were not incubated with AHA (h). Scale bar = 10 μm, panels a-d; 15 μm panels f-i. Panel j shows the mean staining intensity of distal axons. Mean ± SEM. * $p < 0.00001$.

Figure 3.

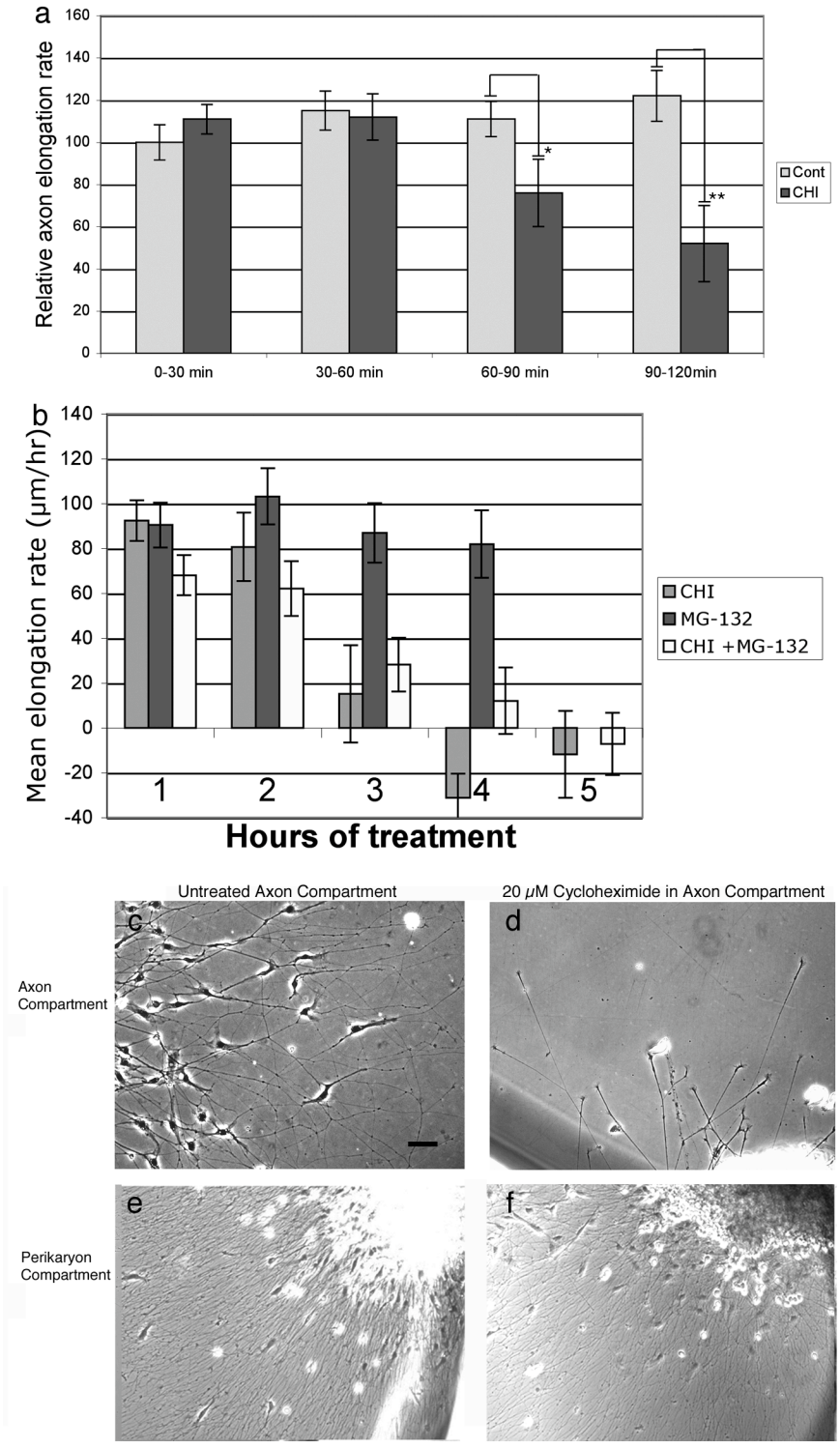

Figure 3. Effects of cycloheximide on axonal growth by E7 DRG neurons. E7 DRG explants were cultured overnight on laminin. Panel a shows the effects of 20

μM CHI on axon elongation rate, compared to vehicle-treated controls, over 120 min. The inhibitory effects of CHI are significant after 90 min. Mean ± SEM. * $p < 0.15$, ** $p < 0.001$. Panel b shows that the proteosome inhibitor MG-132 delays the time when axon elongation stops after inhibiting protein synthesis. Mean ± SEM. Panels c-f show DRG axon elongation in compartmented dishes. In a control axon compartment (c) axons elongate and Schwann cells migrate from the peripheral nerve root, but in a 24 hr CHI-treated axon compartment (d) only axons elongate from the peripheral root. In the untreated cell body compartments of both control (e) and CHI-treated (f) cultures axons and Schwann cells migrate from the explants. Scale bar = 50 μm.

Figure 4.

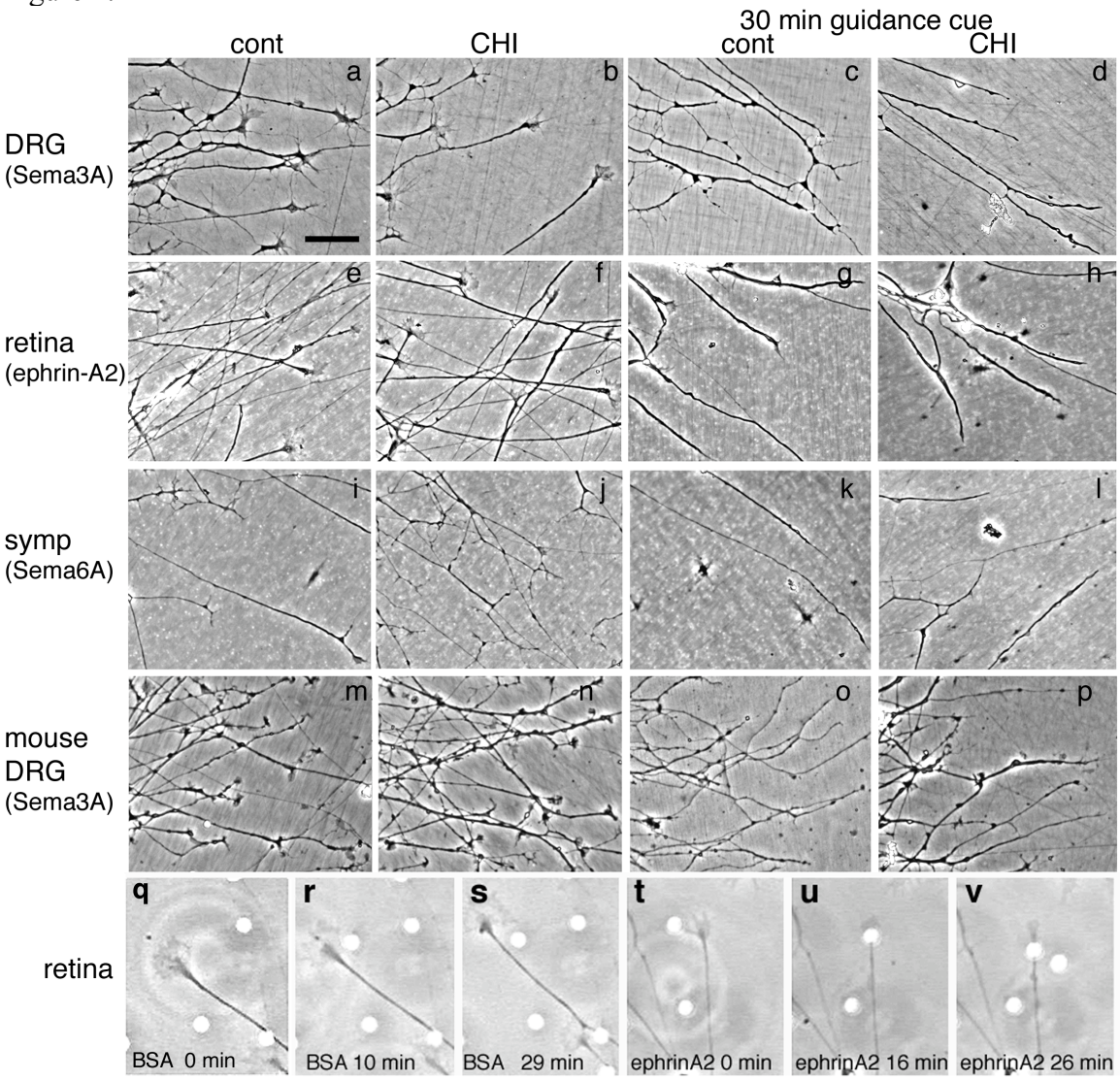

Figure 4. Protein synthesis inhibition does not block responses to repulsive guidance cues. Explants of E7 chick DRGs, temporal retina, sympathetic ganglia and E15 mouse DRGs were cultured overnight in F12 with B27. Ten ng/ml NGF was added to DRG and sympathetic explants. Chick and mouse DRGs were exposed to Sema3A (c, d, o, p), temporal retinal explants to ephrin-A2 (f, h) and sympathetic explants to Sema6A (j, l) for 30 min. Some explants were pretreated with CHI for 15 min before and during exposure to Sema3A (d, p), ephrin-A2 (h) or Sema6A (l). Control explants were exposed to vehicle (a, e ,l, m) or CHI (b, f, j, n) alone for 45 min. Panels q-s show two CHI-treated retinal axons (lower right and upper left) touching and

migrating past BSA-coated beads, while a CHI-treated retinal axon (t-v) stops and collapses after contacting an ephrin-A2-coated bead. Scale bar = 50 μm.

Figure 5.

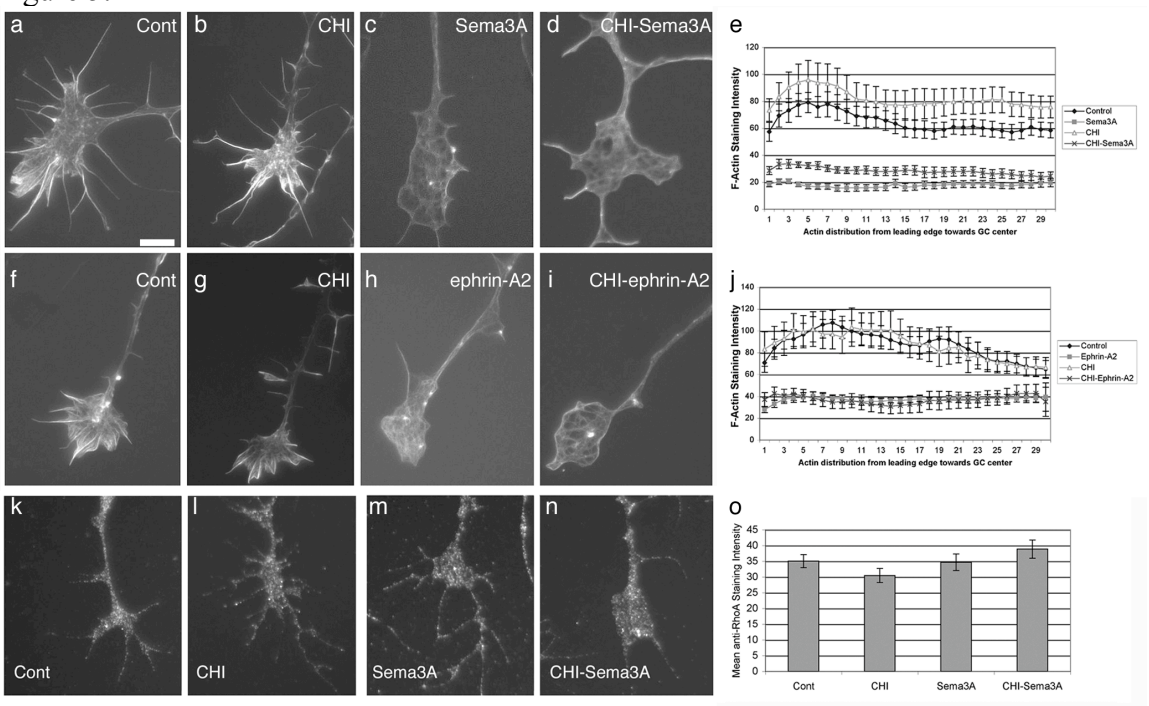

Figure 5. CHI treatment does not affect Sema3A- and ephrin-A2-induced loss of F-actin, and Sema3A does not increase RhoA content of DRG growth cones. E7 DRG explants were cultured overnight in F12, B27, NGF (a-d; k-n) and retinal explants were cultured in F12, B27 (f-i). Sema3A was added to DRG explants for 15 min with (d, n) or without (c, m) 15 min CHI pretreatment. Ephrin-A2 was added to retinal explants for 15 min with (i) or without (h) 15 min CHI pretreatment. Vehicle- (a, f, k) and CHI-treated (b, g, l) control explants were treated 30 min without repulsive cues. Panels e and j shows mean F-actin staining intensities along lines scanned for 6 μm backward from the growth cone leading edges. Mean ± SEM. Panel o shows mean pixel intensity of anti-RhoA staining within traced growth cone borders. Scale bar = 10 μm. Mean ± SEM. no significant differences.

Figure 6.

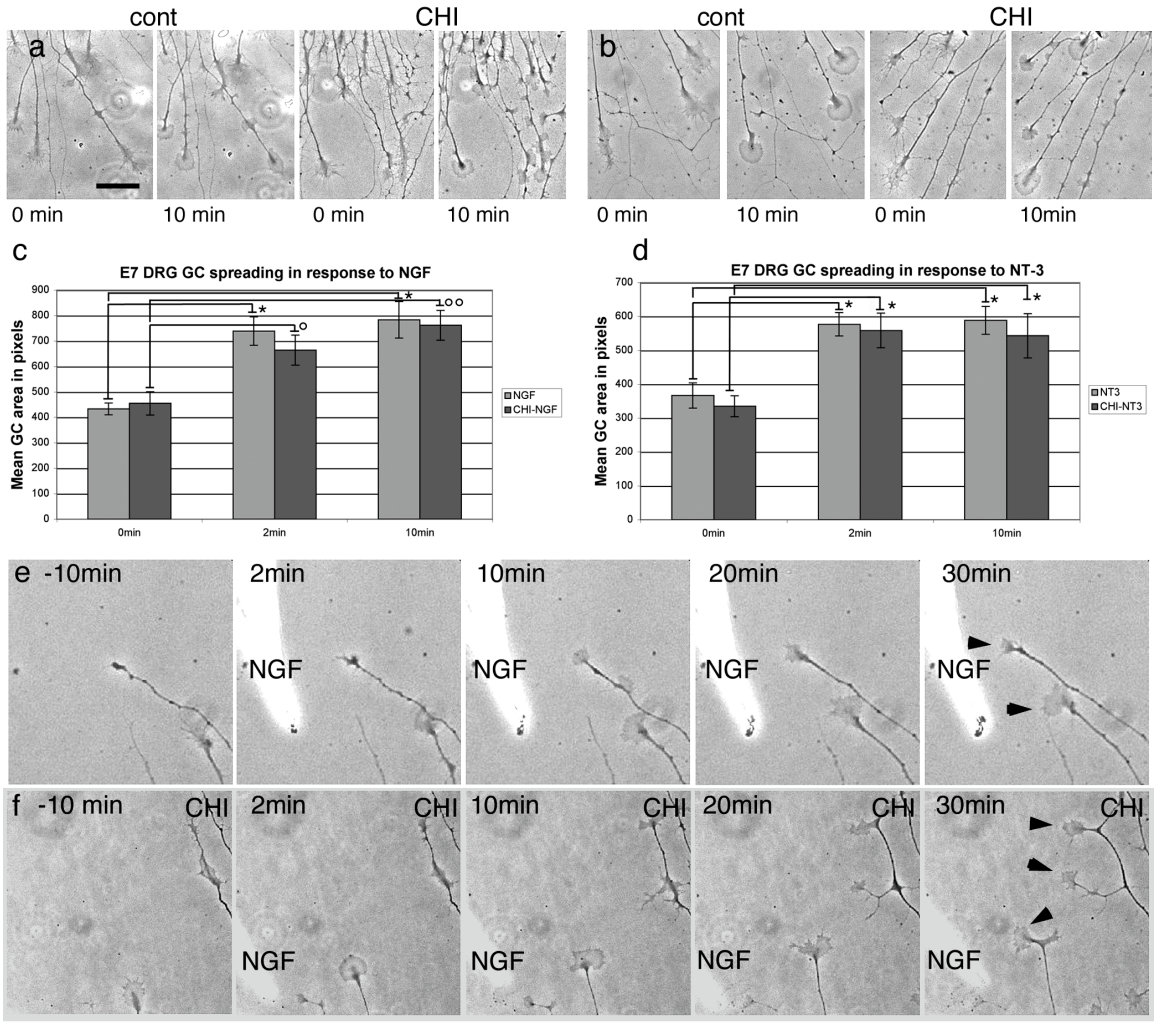

Figure 6. Effects of CHI on growth cone spreading and turning in response to NGF and NT-3. E7 DRG explants were cultured overnight in F12, B27 on L1. Images were acquired immediately before and 10 min after adding 40 ng/ml NGF (a) or NT-3 (b). CHI was added for 15 min before and during treatment with NGF (a) or NT-3 (b). Panels c and d show mean growth cone area in pixels at 0, 2, and 10 min treatment with NGF, * $p < 0.0001$, ° $p < 0.05$, °° $p < 0.001$ (panel c) or NT-3, * $p < 0.002$ (panel d). Mean ± SEM. Panel e shows time-lapse images of growth cones (arrowheads) turning towards an NGF micropipette. The first image was 10 min before introducing the pipette, and following images were 2, 10, 20 and 30 min later. Panel f shows time-lapse images of the attractive turning (arrowhead) of a

growth cone that was treated with CHI 15 min before and during exposure to an NGF gradient from a micropipette. Scale bar = 50 μm in panels a, b, e, f.

Figure 7.

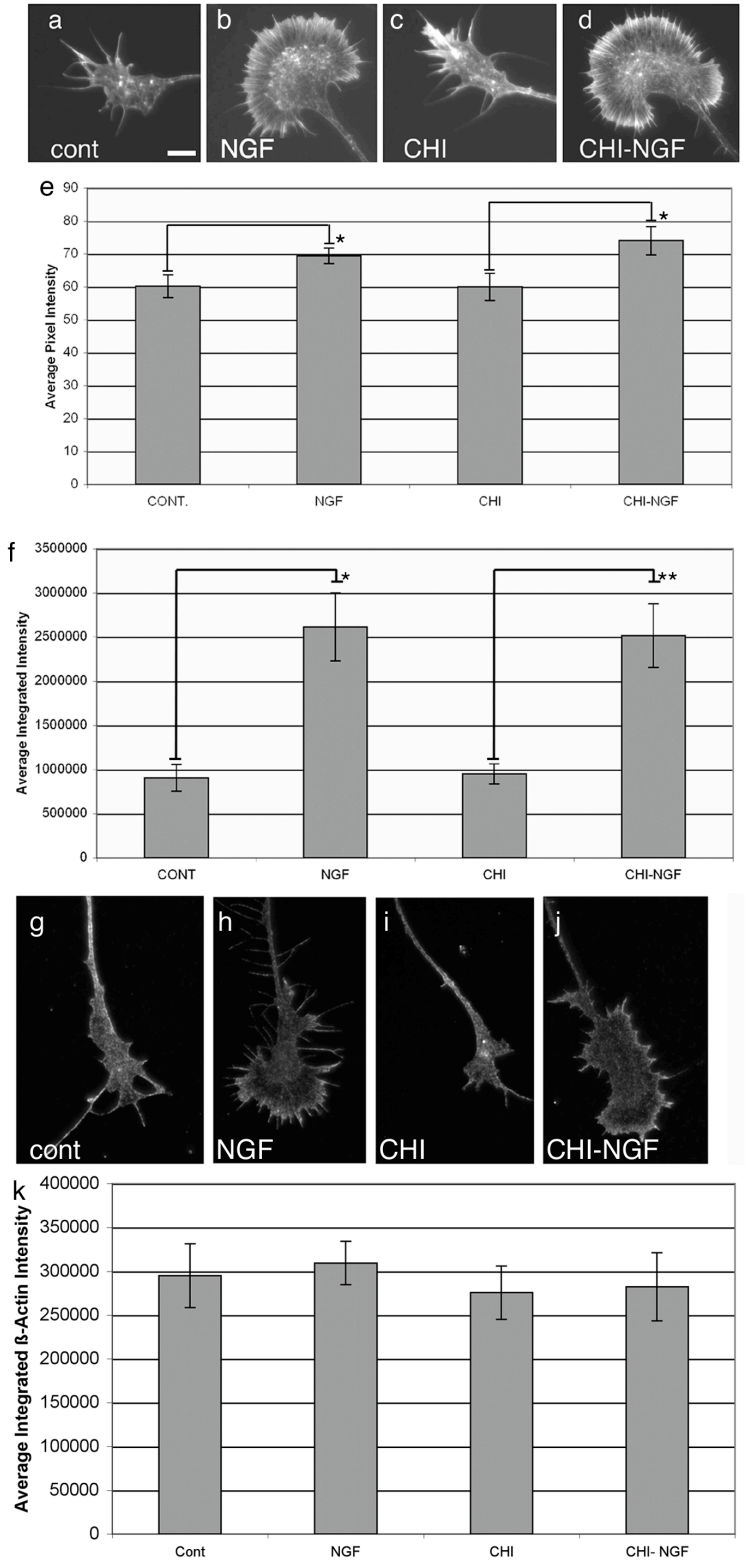
a
cont
b
NGF
c
CHI
d
CHI-NGF
e
Average Pixel Intensity
90
80
70
60
50
40
30
20
10
0
CONT.
NGF
CHI
CHI-NGF
*
*
f
Average Integrated Intensity
3500000
3000000
2500000
2000000
1500000
1000000
500000
0
CONT
NGF
CHI
CHI-NGF
*
**
g
cont
h
NGF
i
CHI
j
CHI-NGF
k
Average Integrated ß-Actin Intensity
400000
350000
300000
250000
200000
150000
100000
50000
0
Cont
NGF
CHI
CHI- NGF

Figure 7. CHI treatment does not affect NGF-induced increase in F-actin, and NGF does not increase ß-actin content of DRG growth cones. E7 DRG explants were cultured overnight in F12, B27. NGF was added for 15 min with (d, j) or without (b, h) 15 min pretreatment with CHI. Vehicle- (a, g) and CHI- (c, i) treated control explants were treated 30 min without NGF. Panel e shows average F-actin staining intensity per pixel. Mean ± SEM. * $p < 0.05$. Panel f shows average integrated pixel intensity within traced growth cone borders. Mean ± SEM, * $p < 0.005$, * $p < 0.001$. Panel k shows mean integrated anti-ß-actin staining within the distal 30 µm of the distal axons and growth cone borders. Mean ± SEM. Scale bar = 10 µm.

Figure 8.

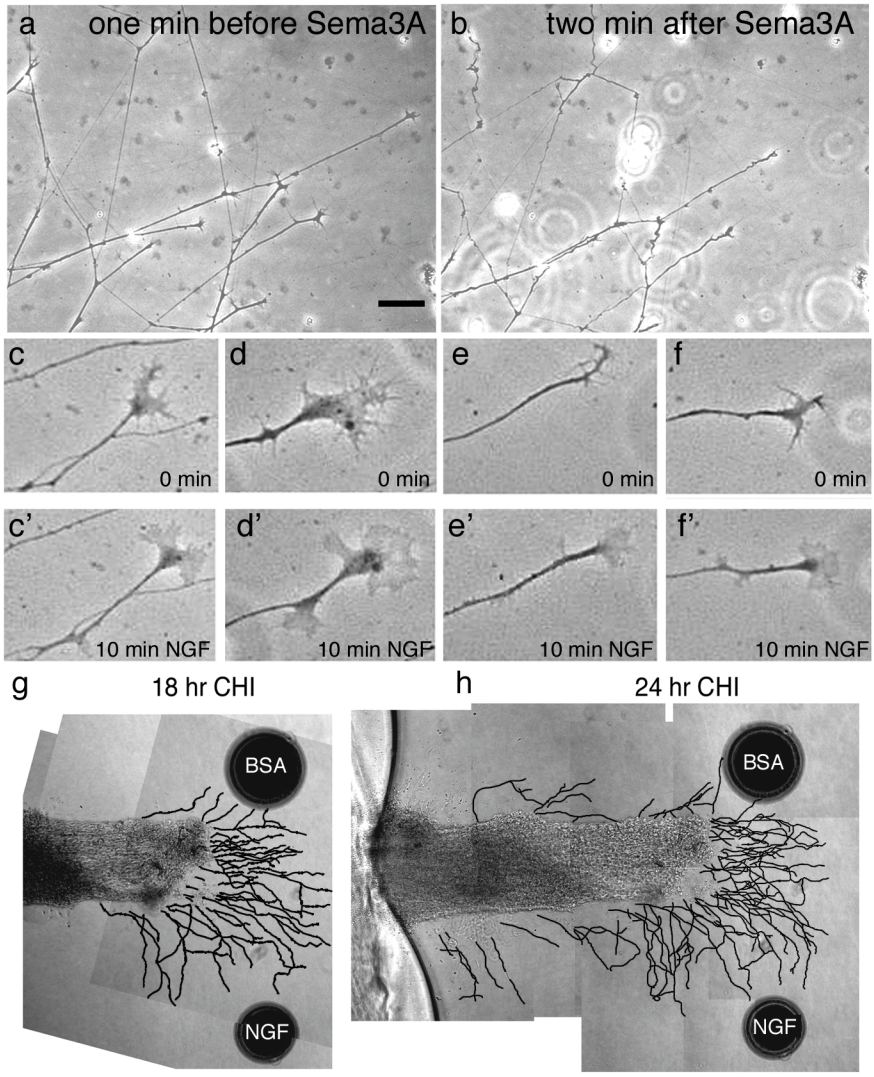

Figure 8. Growth cone responses to Sema3A and NGF are not inhibited by 24 hr CHI treatment in axon compartment. E7 DRG explants were cultured overnight in F12, B27 in compartmented chambers with 20 μM CHI in the axon compartment. Panels a and b show growth cones one min before (a) and two min after (b) adding 1 μg/ml Sema3A. Growth cones collapsed. Panels c-f show growth cones 5 min before (c-f) and 5 min after (c'-f') adding 40 ng/ml NGF. Increased growth cone spreading is seen. Panels g and h show montages of axon growth from the end of a CHI-treated peripheral root in a collagen matrix containing an NGF- and a BSA-soaked bead. Axons are traced in red. Axon orientation toward the NGF bead, but

not the BSA bead is seen. Scale bar = 50 µm in panels a, b; 20 µm in panels c-f; 150 µm in panels g, h.

Discussion

Axonal protein synthesis supports multiple functions in adult terminals, including neurotransmission, plasticity and regeneration (Jimenez-Diaz et al., 2008; Klann and Dever, 2004; Piper and Holt, 2004; Twiss and van Minnen, 2006; Verma et al., 2005). Protein synthesis in developing axons totals approximately 5% of neuronal protein (Eng et al., 1999; Lee and Hollenbeck, 2003). However, studies with compartmented cultures indicate that axonal growth does not require axonal protein synthesis (Blackmore and Letourneau, 2007; Eng et al., 1999). Recent papers report that local protein synthesis is required for responses to guidance cues (Lin and Holt, 2007). We investigated this requirement for chick retinal, DRG and sympathetic neurons and mouse DRG neurons. Unlike other reports, we found that protein synthesis is not required for chick and mouse DRG and chick retinal and sympathetic growth cones to respond to ephrin-A2, slit-3, semaphorins, NGF and NT-3. Our assays included cues presented globally to growth cones and cues locally presented on beads or in a gradient. Furthermore, in studies not previously done, in a compartmented dish where distal axons were in the continuous presence of CHI, but neuronal perikarya were not, axons elongated for hours and growth cones responded to guidance cues in the absence of local protein synthesis.

Like previous reports, NGF and Sema3A stimulated phosphorylation of the translation repressor, elF-4EBP1. Likewise, nascent protein synthesis in DRG neurons was increased by global addition of NGF or Sema3A. Thus, our findings, like previous findings (Campbell and Holt, 2001; Cox et al., 2008; Takei et al.,

2001), suggest that common axonal mechanisms regulate protein synthesis in response to extrinsic factors.

When protein synthesis inhibitors were globally applied to DRG or retinal explants, the axonal growth rate remained normal for one hour, but eventually elongation slowed, growth cone motility diminished, and many axons retracted. Axonal growth may stop because axonal assembly eventually uses all available components. It may also be that proteins with critical roles in growth cone motility are degraded or not recycled. We noted that growth cones began to detach and retract during prolonged protein synthesis inhibition. Adhesion receptors that mediate growth cone traction are reutilized via endocytotic/exocytotic recycling (Caswell and Norman, 2006; Dequidt et al., 2007; Tojima et al., 2006). Perhaps, when protein synthesis is blocked, degradative events during recycling exhaust adhesive receptors and arrest growth cones. In support of this, growth cone detachment and axonal retraction that occurred after one hr CHI treatment was delayed, when we inhibited protein synthesis and protein degradation.

When protein synthesis inhibitors were present in the axonal compartment of a compartmented chamber, axonal elongation was undiminished for 24 hr or more. This indicates that all proteins necessary for axonal growth are made in perikarya and transported distally. As in prior studies (Blackmore and Letourneau, 2007; Eng et al., 1999), axons in our cultures grew several millimeters without distal protein synthesis. Axons in developing embryos reach their targets after similarly growing several millimeters or less. However, adult projection axons can be 10-100 times longer than when they initially connected to their targets. Even at these lengths fast axonal

transport can deliver vesicle-bound proteins to terminals in a few hr, but proteins that travel via slow transport, including cytoskeletal components, would take days or weeks to reach ends of long axons. Thus, protein synthesis in adult axons is critical to replace degraded proteins, maintain cytoskeletal integrity, mediate plasticity, and support regeneration (Campenot and Eng, 2000; Hengtst and Jarffrey, 2007; Koenig and Giuditta, 1999; Piper and Holt, 2004; Twiss and van Minnen, 2006; Verma et al., 2005; Zhang and Poo, 2002).

Why are our results different from reports that local protein synthesis is required for growth cone responses to guidance cues? One possibility involves the neurons and animal species involved. We used DRG neurons, sympathetic neurons and retinal neurons from embryonic chicks and mice. Other labs used embryonic *Xenopus* retinal (Campbell and Holt, 2001; Leung et al., 2006; Piper et al., 2006) or spinal cord neurons (Guirland et al., 2003; Yao et al., 2006), and one study used fetal rat DRGs (Wu et al., 2005). Retinal and DRG neurons are common between these studies, so it is unclear that these different results are due to different neuronal phenotypes. The differentiation state of *Xenopus* spinal cord neurons is uncertain, as the spinal cords were from young embryos, and the neurons were uncharacterized.

Another source of differences may lie in different levels of metabolism in these *in vitro* studies. Perhaps, our neurons had high metabolic rates that generated sufficient proteins in the perikarya to supply all growth cone functions. In support of this, after 24 hr culture E7 DRG axons had extended >2000 μm, E7 retinal axons had extended >1000 μm, and E7 DRG explants maintained axonal growth

rates of >1 mm/day for at least 8 days. These lengths exceed axon lengths in published figures of *Xenopus* retinal and spinal neurons or rat DRG neurons. *Xenopus* spinal cord neuronal axons were only 100-200 μm long and were cultured on poly-lysine (Guirland et al., 2003; Yao et al., 2006), unlike the natural substrates we used. Axonal growth by *Xenopus* spinal neurons is most vigorous in the first 12 hours, most growth occurs in the first 24 hr, and few neurons survive 4 days (Tabi and Poo, 1991). Another indication of high activity in our neurons was the rapidity of growth cone responses to guidance cues. Upon adding NGF, increased growth cone spreading and F-actin was evident by 2 min. Retinal and DRG growth cones began to collapse within 2 min of adding ephrin-A2 or Sema3A. This rapid response is consistent with mechanisms that activate signaling pathways rather than protein synthesis. *Xenopus* retinal growth cone turning toward netrin was not seen until ten min after netrin-induced ß-actin synthesis was detected (Leung et al., 2006).

Perhaps, growth cones in our cultures were rich in proteins that function in growth cone motility, while levels of these proteins were low in other studies. We found that 45 min CHI treatment produced no significant decreases in growth cone content of RhoA or of ß-actin, as expected if protein levels are high. Neither did 15-30 min treatment of DRG explants with Sema3A or NGF induce detectable increases in RhoA or ß-actin content of growth cones, respectively. Leung et al. (2006) reported that in *Xenopus* retinal growth cones ß-actin staining intensity was 30% higher after five min netrin treatment. Assuming a retinal growth cone contains 500-1000 ribosomes (Campbell and Holt, 2001), and it takes about one

min to synthesize an actin molecule (Trachsel, 1991), these growth cones would have to initially contain about 17,000 actin monomers for the addition of 5,000 monomers (1,000 molecules/min for 5 min) to constitute a 30% increase. Actin and tubulin are the most abundant proteins in chick brain growth cones (Cypher and Letourneau, 1991), and based on cytoplasmic G-actin pools in chick brain neurons (30-37 μM; Devineni et al., 1999), we estimate a 10 μm x 20 μm x 1 μm DRG growth cone contains about 4 X 10^6 ß-actin monomers, 100X more than *Xenopus* retinal growth cones. In the studies of Wu et al. (2005) rat DRG explants were cultured three days before use. As seen in Figure 3 of Wu et al. (2005), RhoA was barely detectable in embryonic rat DRG growth cones. On the other hand, our DRG growth cones stained robustly for RhoA with or without Sema3A treatment, and we found that growth cones in 8 day old DRG cultures collapsed rapidly in response to Sema3A, even with CHI treatment. Our results are consistent with the hypothesis that growth cones of actively growing axons contain sufficient RhoA and ß-actin to respond to guidance cues without protein synthesis. Though our data show that guidance cues stimulate protein synthesis in axons of E7 DRG neurons, our data also show that these events do not detectably increase growth cone levels of RhoA or ß-actin and are not required for responding to guidance cues.

Global treatment with CHI did affect DRG growth cones. After two hr inhibition of protein synthesis, DRG growth cones did not spread in response to NGF. Globally applied CHI reduced the attractive turning of DRG growth cones to an NGF pipette. Turning is more complex than growth cone spreading, and may involve exocytosis of vesicle-associated proteins (Tojima et al., 2006) that are

transported at fast axonal transport rates of 50-400 mm/day (Squire et al., 2008). Such proteins could be moved from the perikaryon to the tip of a 1000 μm axon in just 4-30 min (or 30 sec-3 min in a 100 μm *Xenopus* spinal neuron axon), which is within the duration of a turning response. Thus, because vesicle transport is so rapid, global application of protein synthesis inhibitors cannot distinguish a growth cone location from a cell body location for protein synthesis that is necessary for growth cone turning.

Therefore, unlike previous reports, we used compartmented dishes to examine whether distal axonal protein synthesis is required for responses to guidance cues. Because DRG growth cones responded to globally applied Sema3A or NGF and could turn towards an NGF source when distal protein synthesis was inhibited for 24 hr, our results clearly showed that proteins made in the perikaryon and transported to growth cones of DRG neurons are sufficient for axonal elongation and growth cone guidance.

In summary, we confirmed reports that guidance cues stimulate protein synthesis in distal axons. Protein synthesis may occur in developing axons from the earliest times of neuronal polarization and axonal differentiation, via targeted mRNA transport into axons and via signaling by extrinsic cues that regulates mRNA translation (Kiebler and Bassell, 2006). Axonally synthesized proteins constitute a small fraction of the total protein in developing neurons (Eng et al., 1999; Lee and Hollenbeck, 2003), although axonally translated mRNAs are enriched for proteins with roles in axonal growth and growth cone motility (Lee and Hollenbeck, 2003; Piper and Holt, 2004; Zhang et al., 2001). As neurons develop, axon terminals

reach their targets, elongate by intercalary growth (Pfister et al., 2004), and form mature endings. During this maturation, distal protein synthesis gains in significance, allowing axon terminals to respond to local stimuli.

Our results indicate that proteins made in distal axons and growth cones of E7 chick neurons are not necessary for axonal elongation and growth cone responses to guidance cues. Other reports indicate that distally synthesized proteins are required for responses to guidance cues. As indicated by the substantially greater axonal growth we observed, the difference between our results and others concerning the need for distal protein synthesis may occur because different neurons operate at different levels of metabolism, at least under *in vitro* conditions, so that axonal protein synthesis in some neurons becomes functionally important at an earlier developmental stage than in other neurons. Studies to probe the roles of distal protein synthesis in growth cone navigation *in vivo* could help resolve these differences.

Chapter V: Final Discussion

Nervous system development involves spatial and temporal patterns of molecular cues that direct growth cones along specific trajectories to reach target tissues. Growth cones detect cues via membrane receptors that transduce extracellular signals intracellularly, triggering signaling that culminates in cytoskeletal modifications through actin-binding proteins. Currently, our understanding of which actin-binding proteins are activated downstream of specific guidance cues and how these remodel actin filaments remains incomplete. This dissertation work has identified two actin-binding proteins that mediate growth cone guidance to NGF, and addressed their mechanisms for altering actin filament dynamics to produce appropriate growth cone turning.

The first chapter characterized the role of ADF/cofilin in attractive growth cone guidance. Two guidance cues, NGF and netrin-1, induce a rapid increase in growth cone membrane protrusion and F-actin in sensory and retinal neurons, respectively. This increase involves ADF/cofilin protein activation, which increases free F-actin barbed ends and polymerization. Locally elevating AC activity is sufficient to induce attractive growth cone turning, and reducing AC activity blunts attractive growth cone turning to NGF and netrin-1. These data support a model by which NGF and netrin locally increase AC activity to induce local actin polymerization and attractive turning.

The next chapter examined the role of the ERM membrane-cytoskeleton linker proteins in attractive guidance to NGF. Acute NGF increases active phospho-ERM levels in growth cones, and disrupting ERM function results in smaller growth cones with disorganized actin filaments. Although disrupting ERM function does not

affect activation of AC by NGF, DNERM expression does block the associated increase in F-actin, and results in the displacement of active AC and barbed ends from the growth cone periphery. Moreover, elevating active AC levels increases phospho-ERM levels and reducing AC activity blocks the NGF-induced phospho-ERM increase. Lastly, disrupting ERM function or protein levels reduces attractive guidance to NGF.

The final chapter addressed the role of local protein synthesis in axon guidance. Although guidance cues stimulate local protein synthesis in growth cones, protein synthesis inhibitors in distal axon segments do not block attractive guidance to NGF. These data suggest cue-induced changes in the activities of existing proteins such as AC and ERMs, and transport of newly synthesized proteins from the cell body, are sufficient to mediate growth cone guidance under some cellular and context-dependent circumstances.

The data presented in this thesis culminate in a model for attractive growth cone guidance to NGF. The binding of NGF to its receptor TrkA initiates intracellular signaling cascades, possibly including PI3K and the RhoGTPases (Figure 1A). This signaling then increases the levels of active (dephosphorylated) ADF/cofilin and (phosphorylated) ERM proteins. Active ADF/cofilin severs actin filaments at the leading edge, increasing F-actin free barbed ends and stimulating polymerization. Meanwhile, active ERMs are recruited to the membrane, where they anchor and stabilize new and existing actin filaments. The simultaneous activation of ADF/cofilin and ERM proteins thus act to increase in F-actin levels (Figure 1A).

When a growth cone encounters a gradient of NGF, this increase in ADF/cofilin and ERM activity occurs locally, increasing membrane protrusion and F-actin toward the NGF source (Figure 1B). Active ERM proteins may also locally recruit membrane adhesion molecules or provide scaffolding to localize additional signaling molecules. Thus, local activation of ADF/cofilin and ERM proteins produce an asymmetric increase in F-actin, which results in the growth cone turning toward the NGF source (Figure 1B).

Actin filament dynamics in filopodia and lamellipodia enable the growth cone to continually sample its extracellular environment. In vivo, growth cones pause at choice points and become enlarged, increasing their surface area and imparting greater discernment of spatial cues. The remodeling of actin filaments also mediates growth cone steering in response to cues. Therefore, actin filaments, and the actin-binding proteins that regulate their dynamics, are crucial to the growth cone's ability to both sense and respond to guidance cues.

Numerous actin-binding proteins have been identified and characterized using cell-free systems or in cell migration assays, but few have been described in the context of growth cone guidance. Furthermore, how actin-binding proteins interact directly and indirectly is also poorly understood, yet important to consider in the growth cone's constantly changing intra- and extracellular environment. While it is accepted that attractive cues increase F-actin in the proximal growth cone region, few links have been made between guidance cues, actin-binding proteins, and the mechanisms underlying this increase. For example, an increase in actin filaments can be achieved by increasing polymerization, decreasing depolymerization, reducing

retrograde actin flow, or a combination of these. The work presented here demonstrates that a local increase in free F-actin barbed ends and polymerization are sufficient to induce asymmetric F-actin levels and attractive growth cone turning. This initial increase in F-actin in the growth cone side toward the cue may also amplify the relative concentration gradient of NGF across the growth cone width, and reinforce regional activation of other signaling molecules and actin-binding proteins involved in continuing the new direction of growth. In support of this, we found AC activity increased local active ERM levels, further stabilizing the actin cytoskeleton toward the NGF source. Future studies are needed to better understand regional changes in protein localization in turning growth cones.

Although the work here demonstrates the importance of ERM proteins in attractive growth cone guidance to NGF, their precise function remains unclear. Active ERMs may simply provide a physical link between actin filaments and the membrane, thereby stabilizing the cytoskeleton toward the cue to support further polymerization and turning. In addition, ERM proteins may influence the localization of membrane receptors. Active ERMs interact with L1CAM, which is expressed in the developing nervous system (Dickson et al., 2002; Mintz et al., 2003; Cheng et al., 2005; Sakurai et al., 2008), and a study in immune cells also found radixin binds to the cytoplasmic tail of integrins and affects cell adhesion (Tang et al., 2007). This is especially interesting given that NGF stimulation increases integrin clustering in filopodial tips (Grabham and Goldberg, 1997; Grabham et al., 2000). Future studies examining the localization of membrane proteins in DNERM growth cones are needed evaluate this possibility. Lastly, ERM proteins may influence signaling by

locally increasing the activity of RhoGTPases, which have well-established roles in regulating actin-binding proteins in growth cones. The diversity of functions implicated for ERM proteins suggests they influence growth cone guidance in multiple ways.

Data presented in this thesis highlight the importance of using caution if broadly generalizing data to other organisms or contexts. Numerous studies investigating axon guidance *in vitro* utilize similar organisms and cell types, which helps compare results across studies. However, a host of studies in *Xenopus* found local protein synthesis necessary for axon guidance, yet we found local protein synthesis is not necessary for axon guidance in our chick and mouse neurons under our conditions (Roche et al., 2009). We also found growth cone actin levels differ between chick and *Xenopus*, and our chick DRG growth cones turn toward the region of higher AC activity, whereas a study in *Xenopus* found growth cones turn away from the region of higher AC activity (Marsick et al., 2010; Wen et al., 2007). Therefore, the results in this work underscore the need for a more comprehensive understanding of the factors and contexts that impact growth cone guidance *in vitro*, in addition to more a better understanding of growth cone guidance *in vivo*.

Lastly, the effect of NGF on the actin cytoskeleton and the role of protein synthesis both have implications for the treatment spinal cord injuries. For functional regeneration to be successful, we must determine how to re-establish the correct connections, under conditions where many guidance cues may no longer be present. Understanding how specific guidance cues direct growth cones will be integral to successfully repairing damaged circuits.

Figure 1.

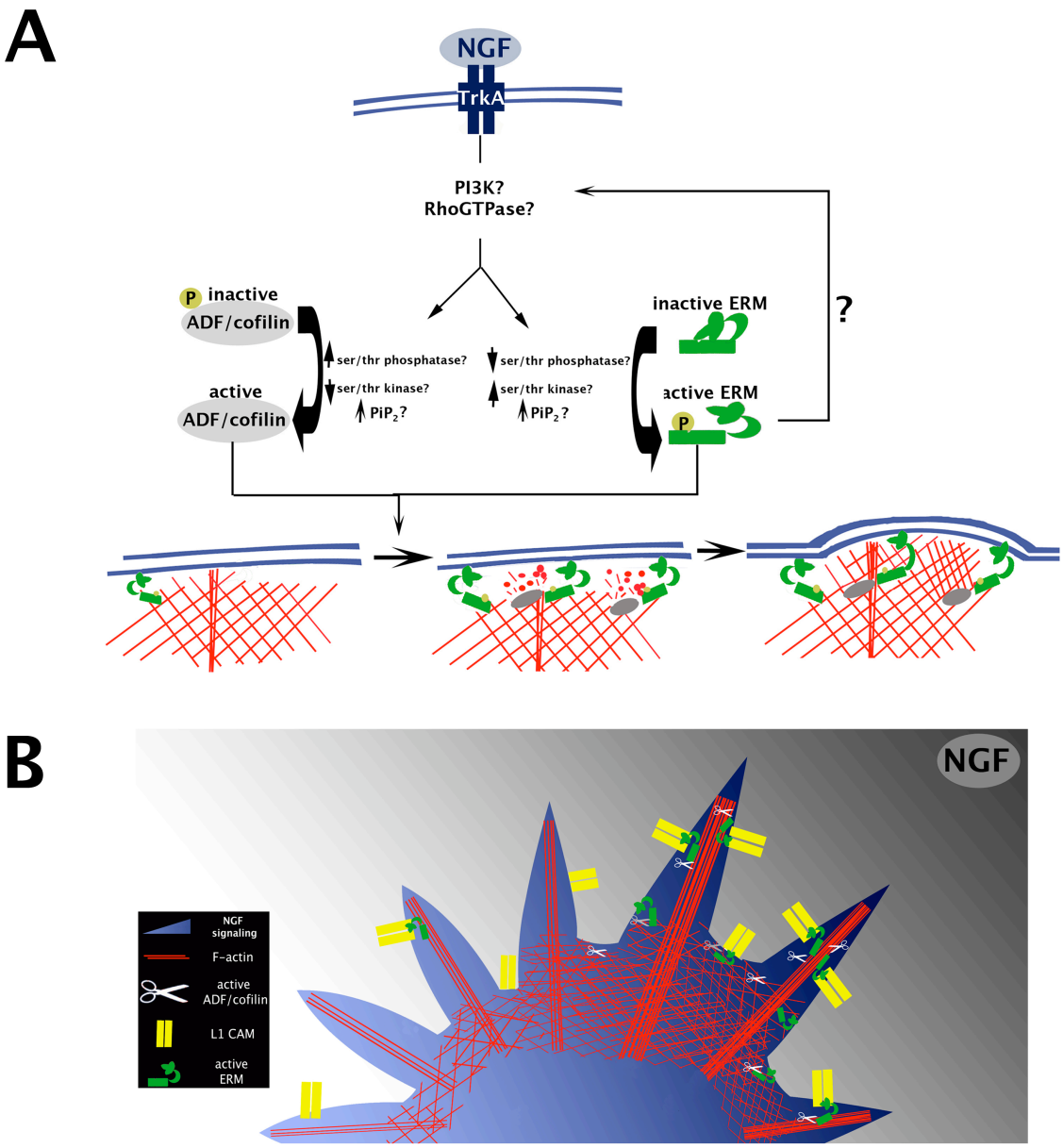

Figure 1. Model for attractive growth cone guidance to NGF. A) NGF binds to its receptor TrkA, triggering intracellular signaling cascades that activate ADF/cofilin and Ezrin/Radixin/Moesin (ERM) proteins. Active ADF/cofilin severs actin filaments near the membrane of the leading edge, increasing free F-actin barbed ends and stimulating polymerization. Active ERM proteins anchor new and existing filaments to the membrane, stabilizing and supporting an increase in F-actin. Active ERMs may

also feed back to regulate the activity of RhoGTPases. B) A localized source of NGF activates ADF/cofilin and ERM proteins locally to increase F-actin toward the NGF source. Active ERM proteins may also asymmetrically localize adhesion molecules, such as L1CAM, to the growth cone membrane. Thus, the local activities of ADF/cofilin and ERM proteins culminate in increased F-actin and subsequent growth cone turning toward NGF.

References

Aberle H, Schwartz H, Kemler R (1996) Cadherin-catenin complex: protein interactions and their implications for cadherin function. J Cell Biochem 61:514-523.

Aizawa H, Wakatsuki S, Ishii A, Moriyama K, Sasaki Y, Ohashi K, Sekine-Aizawa Y, Sehara-Fujisawa A, Mizuno K, Goshima Y, Yahara I (2001) Phosphorylation of cofilin by LIM-kinase is necessary for semaphorin 3A-induced growth cone collapse. Nat Neurosci 4:367-373.

Alvarez J, Giuditta A, Koenig E (2000) Protein synthesis in axons and terminals: significance for maintenance, plasticity and regulation of phenotype. With a critique of slow transport theory. Prog Neurobiol 62:1-62.

Amieva MR, Furthmayr H (1995) Subcellular localization of moesin in dynamic filopodia, retraction fibers, and other structures involved in substrate exploration, attachment, and cell-cell contacts. Exp Cell Res 219:180-196.

Andrianantoandro E, Pollard TD (2006) Mechanism of actin filament turnover by severing and nucleation at different concentrations of ADF/cofilin. Mol Cell 24:13-23.

Arber S, Barbayannis FA, Hanser H, Schneider C, Stanyon CA, Bernard O, Caroni P (1998) Regulation of actin dynamics through phosphorylation of cofilin by LIM-kinase. Nature 393:805-809.

Bamburg JR (1999) Proteins of the ADF/cofilin family: essential regulators of actin dynamics. Annu Rev Cell Dev Biol 15:185-230.

Bamburg JR, Bray D (1987) Distribution and cellular localization of actin depolymerizing factor. J Cell Biol 105:2817-2825.

Barak LS, Nothnagel EA, DeMarco EF, Webb WW (1981) Differential staining of actin in metaphase spindles with 7-nitrobenz-2-oxa-1,3-diazole-phallacidin and fluorescent DNase: is actin involved in chromosomal movement? Proc Natl Acad Sci U S A 78:3034-3038.

Bassell GJ, Zhang H, Byrd AL, Femino AM, Singer RH, Taneja KL, Lifshitz LM, Herman IM, Kosik KS (1998) Sorting of beta-actin mRNA and protein to neurites and growth cones in culture. J Neurosci 18:251-265.

Baumgartner M, Sillman AL, Blackwood EM, Srivastava J, Madson N, Schilling JW, Wright JH, Barber DL (2006) The Nck-interacting kinase phosphorylates ERM proteins for formation of lamellipodium by growth factors. Proc Natl Acad Sci U S A 103:13391-13396.

Bentley D, Toroian-Raymond A (1986) Disoriented pathfinding by pioneer neurone growth cones deprived of filopodia by cytochalasin treatment. Nature 323:712-715.

Bentley D, O'Connor TP (1994) Cytoskeletal events in growth cone steering. Curr Opin Neurobiol 4:43-48.

Bernard O (2007) Lim kinases, regulators of actin dynamics. Int J Biochem Cell Biol 39:1071-1076.

Bernstein BW, Bamburg JR ADF/Cofilin: a functional node in cell biology. Trends Cell Biol.

Birkenfeld J, Betz H, Roth D (2001) Inhibition of neurite extension by overexpression of individual domains of LIM kinase 1. J Neurochem 78:924-927.

Blackmore M, Letourneau PC (2007) Protein synthesis in distal axons is not required for axon growth in the embryonic spinal cord. Dev Neurobiol 67:976-986.

Blanchoin L, Pollard TD (1999) Mechanism of interaction of Acanthamoeba actophorin (ADF/Cofilin) with actin filaments. J Biol Chem 274:15538-15546.

Blanchoin L, Pollard TD, Mullins RD (2000) Interactions of ADF/cofilin, Arp2/3 complex, capping protein and profilin in remodeling of branched actin filament networks. Curr Biol 10:1273-1282.

Bramham CR, Wells DG (2007) Dendritic mRNA: transport, translation and function. Nature Rev 8: 776-789.

Bretscher A, Edwards K, Fehon RG (2002) ERM proteins and merlin: integrators at the cell cortex. Nat Rev Mol Cell Biol 3:586-599.

Brittis PA, Lu Q, Flanagan JG (2002) Axonal protein synthesis provides a mechanism for localized regulation at an intermediate target. Cell 110: 223-235.

Brown JA, Bridgman PC (2009) Disruption of the cytoskeleton during Semaphorin 3A induced growth cone collapse correlates with differences in actin organization and associated binding proteins. Dev Neurobiol 69:633-646.

Brown JA, Wysolmerski RB, Bridgman PC (2009) Dorsal root ganglion neurons react to semaphorin 3A application through a biphasic response that requires multiple myosin II isoforms. Mol Biol Cell 20:1167-1179.

Brummelkamp TR, Bernards R, Agami R (2002) A system for stable expression of short interfering RNAs in mammalian cells. Science 296:550-553.

Brunet I, Weinl C, Piper M, Trembeau A, Volovitch A, Harris W, Prochiantz A, Holt C (2005) The transcription factor Engrailed-2 guides retinal axons. Nature 438: 94-98.

Buck KB, Zheng JQ (2002) Growth cone turning induced by direct local modification of microtubule dynamics. J Neurosci 22:9358-9367.

Burkel BM, von Dassow G, Bement WM (2007) Versatile fluorescent probes for actin filaments based on the actin-binding domain of utrophin. Cell Motil Cytoskeleton 64:822-832.

Campbell DS, Holt CE (2001) Chemotropic responses of retinal growth cones mediated by rapid local protein synthesis and degradation. Neuron 32:1013-1026.

Campenot RB (1977) Local control of neurite development by nerve growth factor. Proc Natl Acad Sci U S A 74:4516-4519.

Campenot RB (1994) NGF and the local control of nerve terminal growth. J Neurobiol 25:599-611.

Campenot RB, Eng H (2000) Protein synthesis in axons and its possible functions. J Neurocytol 29: 793-798.

Carlier MF, Ressad F, Pantaloni D (1999) Control of actin dynamics in cell motility. Role of ADF/cofilin. J Biol Chem 274:33827-33830.

Carlier MF, Laurent V, Santolini J, Melki R, Didry D, Xia GX, Hong Y, Chua NH, Pantaloni D (1997) Actin depolymerizing factor (ADF/cofilin) enhances the rate of filament turnover: implication in actin-based motility. J Cell Biol 136:1307-1322.

Casaccia-Bonnefil P, Gu C, Chao MV (1999) Neurotrophins in cell survival/death decisions. Adv Exp Med Biol 468:275-282.

Castelo L, Jay DG (1999) Radixin is involved in lamellipodial stability during nerve growth cone motility. Mol Biol Cell 10:1511-1520.

Caswell PT, Norman JC (2006) Integrin trafficking and the control of cell migration. Traffic 7: 14-21.

Challacombe JF, Snow DM, Letourneau PC (1996) Actin filament bundles are required for microtubule reorientation during growth cone turning to avoid an inhibitory guidance cue. J Cell Sci 109 (Pt 8):2031-2040.

Challacombe JF, Snow DM, Letourneau PC (1997) Dynamic microtubule ends are required for growth cone turning to avoid an inhibitory guidance cue. J Neurosci 17:3085-3095.

Chan C, Beltzner CC, Pollard TD (2009) Cofilin dissociates Arp2/3 complex and branches from actin filaments. Curr Biol 19:537-545.

Chan CE, Odde DJ (2008) Traction dynamics of filopodia on compliant substrates. Science 322:1687-1691.

Chao MV, Hempstead BL (1995) p75 and Trk: a two-receptor system. Trends Neurosci 18:321-326.

Charest PG, Firtel RA (2007) Big roles for small GTPases in the control of directed cell movement. Biochem J 401:377-390.

Chen H, Bernstein BW, Sneider JM, Boyle JA, Minamide LS, Bamburg JR (2004) In vitro activity differences between proteins of the ADF/cofilin family define two distinct subgroups. Biochemistry 43:7127-7142.

Chen TJ, Gehler S, Shaw AE, Bamburg JR, Letourneau PC (2006) Cdc42 participates in the regulation of ADF/cofilin and retinal growth cone filopodia by brain derived neurotrophic factor. J Neurobiol 66:103-114.

Chen WP, Chang YC, Hsieh ST (1999) Trophic interactions between sensory nerves and their targets. J Biomed Sci 6:79-85.

Cheng L, Itoh K, Lemmon V (2005) L1-mediated branching is regulated by two ezrin-radixin-moesin (ERM)-binding sites, the RSLE region and a novel juxtamembrane ERM-binding region. J Neurosci 25:395-403.

Chien CB, Rosenthal DE, Harris WA, Holt CE (1993) Navigational errors made by growth cones without filopodia in the embryonic Xenopus brain. Neuron 11:237-251.

Cook G, Tannahill D, Keynes R (1998) Axon guidance to and from choice points. Curr Opin Neurobiol 8:64-72.

Cox LJ, Hengst U, Gurskaya NG, Lukyanov KA, Jaffrey SR (2008) Intra-axonal translation and retrograde trafficking of CREB promotes neuronal survival. Nature Cell Biol 10: 149-159.

Cramer LP (1999) Role of actin-filament disassembly in lamellipodium protrusion in motile cells revealed using the drug jasplakinolide. Curr Biol 9:1095-1105.

Cypher C, Letourneau PC (1991) Identification of cytoskeletal, focal adhesion, and cell adhesion proteins in growth cone particles isolated from developing chick brain. J Neurosci Res 30:259-265.
Dahm R, Macchi P (2007) Human pathologies associated with defective RNA transport and localization in the nervous system. Biol Cell 99: 649-661.
Davies AM (2000) Neurotrophins: more to NGF than just survival. Curr Biol 10:R374-376.
Davis JQ, Bennett V (1994) Ankyrin binding activity shared by the neurofascin/L1/NrCAM family of nervous system cell adhesion molecules. J Biol Chem 269:27163-27166.
Deiner MS, Kennedy TE, Fazeli A, Serafini T, Tessier-Lavigne M, Sretavan DW (1997) Netrin-1 and DCC mediate axon guidance locally at the optic disc: loss of function leads to optic nerve hypoplasia. Neuron 19:575-589.
Denker SP, Huang DC, Orlowski J, Furthmayr H, Barber DL (2000) Direct binding of the Na--H exchanger NHE1 to ERM proteins regulates the cortical cytoskeleton and cell shape independently of H(+) translocation. Mol Cell 6:1425-1436.
Dent EW, Gertler FB (2003) Cytoskeletal dynamics and transport in growth cone motility and axon guidance. Neuron 40:209-227.
Dent EW, Barnes AM, Tang F, Kalil K (2004) Netrin-1 and semaphorin 3A promote or inhibit cortical axon branching, respectively, by reorganization of the cytoskeleton. J Neurosci 24:3002-3012.
Dent EW, Callaway JL, Szebenyi G, Baas PW, Kalil K (1999) Reorganization and movement of microtubules in axonal growth cones and developing interstitial branches. J Neurosci 19:8894-8908.
Dequidt C, Dnaglot L, Alberts P, Galli T, Choquet D, Thoumine O (2007) Fast turnover of L1 adhesion in neuronal growth cones involving both surface diffusion and exo/endocytosis of L1 molecules. Mol. Biol. Cell 18: 3131-3143.
Devineni N, Minamide LS, Niu M, Safer D, Verma R, Bamburg JR, Nachmias VT (1999) A quantitative analysis of G-actin binding proteins and the G-actin pool in developing chick brain. Brain Res 823:129-140.
Dickson TC, Mintz CD, Benson DL, Salton SR (2002) Functional binding interaction identified between the axonal CAM L1 and members of the ERM family. J Cell Biol 157:1105-1112.
Doi Y, Itoh M, Yonemura S, Ishihara S, Takano H, Noda T, Tsukita S (1999) Normal development of mice and unimpaired cell adhesion/cell motility/actin-based cytoskeleton without compensatory up-regulation of ezrin or radixin in moesin gene knockout. J Biol Chem 274:2315-2321.
Drescher U, Bonhoeffer F, Muller BK (1997) The Eph family in retinal axon guidance. Curr Opin Neurobiol 7:75-80.
Du J, Frieden C (1998) Kinetic studies on the effect of yeast cofilin on yeast actin polymerization. Biochemistry 37:13276-13284.

Eiseler T, Doppler H, Yan IK, Kitatani K, Mizuno K, Storz P (2009) Protein kinase D1 regulates cofilin-mediated F-actin reorganization and cell motility through slingshot. Nat Cell Biol 11:545-556.

Endo M, Ohashi K, Sasaki Y, Goshima Y, Niwa R, Uemura T, Mizuno K (2003) Control of growth cone motility and morphology by LIM kinase and Slingshot via phosphorylation and dephosphorylation of cofilin. J Neurosci 23:2527-2537.

Eng H, Lund K, Campenot RB (1999) Synthesis of ß-tubulin, actin, and other proteins in axons of sympathetic neurons in compartmented cultures. J Neurosci *19*: 1-9.

Esposito D, Patel P, Stephens RM, Perez P, Chao MV, Kaplan DR, Hempstead BL (2001) The cytoplasmic and transmembrane domains of the p75 and Trk A receptors regulate high affinity binding to nerve growth factor. J Biol Chem 276:32687-32695.

Fan J, Mansfield SG, Redmond T, Gordon-Weeks PR, Raper JA (1993) The organization of F-actin and microtubules in growth cones exposed to a brain-derived collapsing factor. J Cell Biol 121:867-878.

Farrar NR, Spencer GE (2008) Pursuing a 'turning point' in growth cone research. Devel Biol 318 : 102-111.

Forscher P, Smith SJ (1988) Actions of cytochalasins on the organization of actin filaments and microtubules in a neuronal growth cone. J Cell Biol 107:1505-1516.

Frantz C, Barreiro G, Dominguez L, Chen X, Eddy R, Condeelis J, Kelly MJ, Jacobson MP, Barber DL (2008) Cofilin is a pH sensor for actin free barbed end formation: role of phosphoinositide binding. J Cell Biol 183:865-879.

Furutani Y, Matsuno H, Kawasaki M, Sasaki T, Mori K, Yoshihara Y (2007) Interaction between telencephalin and ERM family proteins mediates dendritic filopodia formation. J Neurosci 27:8866-8876.

Gallo G (2008) Semaphorin 3A inhibits ERM protein phosphorylation in growth cone filopodia through inactivation of PI3K. Dev Neurobiol 68:926-933.

Gallo G, Letourneau PC (1998a) Axon guidance: GTPases help axons reach their targets. Curr Biol 8:R80-82.

Gallo G, Letourneau PC (1998b) Localized sources of neurotrophins initiate axon collateral sprouting. J Neurosci 18:5403-5414.

Gallo G, Letourneau PC (2000) Neurotrophins and the dynamic regulation of the neuronal cytoskeleton. J Neurobiol 44:159-173.

Gallo G, Letourneau PC (2004) Regulation of growth cone actin filaments by guidance cues. J Neurobiol 58:92-102.

Gallo G, Lefcort FB, Letourneau PC (1997) The trkA receptor mediates growth cone turning toward a localized source of nerve growth factor. J Neurosci 17:5445-5454.

Garvalov BK, Flynn KC, Neukirchen D, Meyn L, Teusch N, Wu X, Brakebusch C, Bamburg JR, Bradke F (2007) Cdc42 regulates cofilin during the establishment of neuronal polarity. J Neurosci 27:13117-13129.

Gautreau A, Poullet P, Louvard D, Arpin M (1999) Ezrin, a plasma membrane-microfilament linker, signals cell survival through the phosphatidylinositol 3-kinase/Akt pathway. Proc Natl Acad Sci U S A 96:7300-7305.
Gehler S, Shaw AE, Sarmiere PD, Bamburg JR, Letourneau PC (2004b) Brain-derived neurotrophic factor regulation of retinal growth cone filopodial dynamics is mediated through actin depolymerizing factor/cofilin. J Neurosci 24:10741-10749.
Ghosh M, Song X, Mouneimne G, Sidani M, Lawrence DS, Condeelis JS (2004) Cofilin promotes actin polymerization and defines the direction of cell motility. Science 304:743-746.
Giniger E (2002) How do Rho family GTPases direct axon growth and guidance? A proposal relating signaling pathways to growth cone mechanics. Differentiation 70:385-396.
Gitai Z, Yu TW, Lundquist EA, Tessier-Lavigne M, Bargmann CI (2003) The netrin receptor UNC-40/DCC stimulates axon attraction and outgrowth through enabled and, in parallel, Rac and UNC-115/AbLIM. Neuron 37:53-65.
Glebova NO, Ginty DD (2004) Heterogeneous requirement of NGF for sympathetic target innervation in vivo. J Neurosci 24:743-751.
Gohla A, Bokoch GM (2002) 14-3-3 regulates actin dynamics by stabilizing phosphorylated cofilin. Curr Biol 12:1704-1710.
Gohla A, Birkenfeld J, Bokoch GM (2005) Chronophin, a novel HAD-type serine protein phosphatase, regulates cofilin-dependent actin dynamics. Nat Cell Biol 7:21-29.
Goldberg DJ, Foley MS, Tang D, Grabham PW (2000) Recruitment of the Arp2/3 complex and mena for the stimulation of actin polymerization in growth cones by nerve growth factor. J Neurosci Res 60:458-467.
Gomez TM, Robles E (2004) The great escape; phosphorylation of Ena/VASP by PKA promotes filopodial formation. Neuron 42:1-3.
Gomez TM, Zheng JQ (2006) The molecular basis for calcium-dependent axon pathfinding. Nat Rev Neurosci 7:115-125.
Gomez TM, Roche FK, Letourneau PC (1996) Chick sensory neuronal growth cones distinguish fibronectin from laminin by making substratum contacts that resemble focal contacts. J Neurobiol 29:18-34.
Gomez TM, Harrigan D, Henley J, Robles E (2003) Working with Xenopus spinal neurons in live cell culture. Methods Cell Biol 71:129-156.
Gonzalez-Agosti C, Solomon F (1996) Response of radixin to perturbations of growth cone morphology and motility in chick sympathetic neurons in vitro. Cell Motil Cytoskeleton 34:122-136.
Goode BL, Drubin DG, Barnes G (2000) Functional cooperation between the microtubule and actin cytoskeletons. Curr Opin Cell Biol 12:63-71.
Gordon-Weeks PR (2004) Microtubules and growth cone function. J Neurobiol 58:70-83.
Grabham PW, Goldberg DJ (1997) Nerve growth factor stimulates the accumulation of beta1 integrin at the tips of filopodia in the growth cones of sympathetic neurons. J Neurosci 17:5455-5465.

Grabham PW, Foley M, Umeojiako A, Goldberg DJ (2000) Nerve growth factor stimulates coupling of beta1 integrin to distinct transport mechanisms in the filopodia of growth cones. J Cell Sci 113 (Pt 17):3003-3012.
Guan KL, Rao Y (2003) Signalling mechanisms mediating neuronal responses to guidance cues. Nat Rev Neurosci 4:941-956.
Guirland C, Buck KB, Gibney JA, DiCicco-Bloom E, Zheng JQ (2003) Direct cAMP signaling through G-protein-coupled receptors mediates growth cone attraction induced by pituitary adenlyate cyclase-activating peptide. J Neurosci 23: 2274-2283.
Gundersen RW (1985) Sensory neurite growth cone guidance by substrate adsorbed nerve growth factor. J Neurosci Res 13:199-212.
Gundersen RW, Barrett JN (1979) Neuronal chemotaxis: chick dorsal-root axons turn toward high concentrations of nerve growth factor. Science 206:1079-1080.
Gungabissoon RA, Bamburg JR (2003) Regulation of growth cone actin dynamics by ADF/cofilin. J Histochem Cytochem 51:411-420.
Haas MA, Vickers JC, Dickson TC (2004) Binding partners L1 cell adhesion molecule and the ezrin-radixin-moesin (ERM) proteins are involved in development and the regenerative response to injury of hippocampal and cortical neurons. Eur J Neurosci 20:1436-1444.
Hall A, Nobes CD (2000) Rho GTPases: molecular switches that control the organization and dynamics of the actin cytoskeleton. Philos Trans R Soc Lond B Biol Sci 355:965-970.
Hamada K, Seto A, Shimizu T, Matsui T, Takai Y, Tsukita S, Tsukita S, Hakoshima T (2001) Crystallization and preliminary crystallographic studies of RhoGDI in complex with the radixin FERM domain. Acta Crystallogr D Biol Crystallogr 57:889-890.
Hanft LM, Rybakova IN, Patel JR, Rafael-Fortney JA, Ervasti JM (2006) Cytoplasmic gamma-actin contributes to a compensatory remodeling response in dystrophin-deficient muscle. Proc Natl Acad Sci U S A 103:5385-5390.
Hassankhani A, Steinhelper ME, Soonpaa MH, Katz EB, Taylor DA, Andrade-Rozental A, Factor SM, Steinberg JJ, Field LJ, Federoff HJ (1995) Overexpression of NGF within the heart of transgenic mice causes hyperinnervation, cardiac enlargement, and hyperplasia of ectopic cells. Dev Biol 169:309-321.
Hayashi K, Yonemura S, Matsui T, Tsukita S (1999) Immunofluorescence detection of ezrin/radixin/moesin (ERM) proteins with their carboxyl-terminal threonine phosphorylated in cultured cells and tissues. J Cell Sci 112 (Pt 8):1149-1158.
Henderson CE (1996) Role of neurotrophic factors in neuronal development. Curr Opin Neurobiol 6:64-70.
Hengst U, Jaffrey SR (2007) Function and translational regulation of mRNA in developing axons. Sem in Cell and Dev Biol 18: 209-215.
Henry MD, Gonzalez Agosti C, Solomon F (1995) Molecular dissection of radixin: distinct and interdependent functions of the amino- and carboxy-terminal domains. J Cell Biol 129:1007-1022.

Hong K, Nishiyama M, Henley J, Tessier-Lavigne M, Poo M (2000) Calcium signalling in the guidance of nerve growth by netrin-1. Nature 403:93-98.
Hopker VH, Shewan D, Tessier-Lavigne M, Poo M, Holt C (1999) Growth-cone attraction to netrin-1 is converted to repulsion by laminin-1. Nature 401:69-73.
Hotulainen P, Paunola E, Vartiainen MK, Lappalainen P (2005) Actin-depolymerizing factor and cofilin-1 play overlapping roles in promoting rapid F-actin depolymerization in mammalian nonmuscle cells. Mol Biol Cell 16:649-664.
Hu H, Marton TF, Goodman, CS (2001) Plexin B mediates axon guidance in *Drosophila* by simultaneously inhibiting active Rac and enhancing RhoA signaling. Neuron 32: 39-51.
Huang TY, DerMardirossian C, Bokoch GM (2006) Cofilin phosphatases and regulation of actin dynamics. Curr Opin Cell Biol 18:26-31.
Huang TY, Minamide LS, Bamburg JR, Bokoch GM (2008) Chronophin mediates an ATP-sensing mechanism for cofilin dephosphorylation and neuronal cofilin-actin rod formation. Dev Cell 15:691-703.
Huber AB, Kolodkin AL, Ginty DD, Cloutier JF (2003) Signaling at the growth cone: ligand-receptor complexes and the control of axon growth and guidance. Annu Rev Neurosci 26:509-563.
Ichetovkin I, Grant W, Condeelis J (2002) Cofilin produces newly polymerized actin filaments that are preferred for dendritic nucleation by the Arp2/3 complex. Curr Biol 12:79-84.
Ikeda K, Nakao J, Asou H, Toya S, Shinoda J, Uyemura K (1996) Expression of CD44H in the cells of neural crest origin in peripheral nervous system. Neuroreport 7:1713-1716.
Jeon S, Park JK, Bae CD, Park J NGF-induced moesin phosphorylation is mediated by the PI3K, Rac1 and Akt and required for neurite formation in PC12 cells. Neurochem Int.
Jin M, Guan CB, Jiang YA, Chen G, Zhao CT, Cui K, Song YQ, Wu CP, Poo MM, Yuan XB (2005) Ca2+-dependent regulation of rho GTPases triggers turning of nerve growth cones. J Neurosci 25:2338-2347.
Jimenez-Diaz L, Geranton SM, Passmore GM, Leith JL, Fisher AS, Berliocchi L, Sivasubramaniam AK, Sheasby A, Lumb BM, Hunt SP (2008) Local translation in primary afferent fibers regulates nociception. PloS ONE 3: e1961.
Kalil K, Dent EW (2005) Touch and go: guidance cues signal to the growth cone cytoskeleton. Curr Opin Neurobiol 15:521-526.
Kaplan DR, Miller FD (2000) Neurotrophin signal transduction in the nervous system. Curr Opin Neurobiol 10:381-391.
Kelly RB, Grote E (1993) Protein targeting in the neuron. Annu Rev Neurosci 16:95-127.
Kennedy TE, Serafini T, de la Torre JR, Tessier-Lavigne M (1994) Netrins are diffusible chemotropic factors for commissural axons in the embryonic spinal cord. Cell 78:425-435.

Khan MA, Okumura N, Okada M, Kobayashi S, Nakagawa H (1995) Nerve growth factor stimulates tyrosine phosphorylation of paxillin in PC12h cells. FEBS Lett 362:201-204.
Kiebler MA, Bassell GJ (2006) Neuronal RNA granules: movers and makers. Neuron 51: 685-690.
Kiryushko D, Berezin V, Bock E (2004) Regulators of neurite outgrowth: role of cell adhesion molecules. Ann N Y Acad Sci 1014:140-154.
Klann E, Dever TE (2004) Biochemical mechanisms for translational regulation in synaptic plasticity. Nature Rev Neurosci 5: 931-942.
Koenig E, Giuditta A (1999) Protein-synthesizing machinery in the axon compartment. Neuroscience 89:5-15.
Kohno K, Kawakami T, Hiruma H (2005) Effects of soluble laminin on organelle transport and neurite growth in cultured mouse dorsal root ganglion neurons: difference between primary neurites and branches. J Cell Physiol 205:253-261.
Korobova F, Svitkina T (2008) Arp2/3 complex is important for filopodia formation, growth cone motility, and neuritogenesis in neuronal cells. Mol Biol Cell 19:1561-1574.
Kozma R, Sarner S, Ahmed S, Lim L (1997) Rho family GTPases and neuronal growth cone remodelling: relationship between increased complexity induced by Cdc42Hs, Rac1, and acetylcholine and collapse induced by RhoA and lysophosphatidic acid. Mol Cell Biol 17:1201-1211.
Kuhn TB, Meberg PJ, Brown MD, Bernstein BW, Minamide LS, Jensen JR, Okada K, Soda EA, Bamburg JR (2000) Regulating actin dynamics in neuronal growth cones by ADF/cofilin and rho family GTPases. J Neurobiol 44:126-144.
Kurita S, Watanabe Y, Gunji E, Ohashi K, Mizuno K (2008) Molecular dissection of the mechanisms of substrate recognition and F-actin-mediated activation of cofilin-phosphatase Slingshot-1. J Biol Chem 283:32542-32552.
Lebrand C, Dent EW, Strasser GA, Lanier LM, Krause M, Svitkina TM, Borisy GG, Gertler FB (2004) Critical role of Ena/VASP proteins for filopodia formation in neurons and in function downstream of netrin-1. Neuron 42:37-49.
Lee DH, Goldberg, AL (1996) Selective inhibitors of the proteosome-dependent and vacuolar pathways of protein degradation in Saccharomyces cerevisae. J Biol Chem 272: 27280-27284.
Lee SK, Hollenbeck PJ (2003) Organization and translation of mRNA in sympathetic axons. J Cell Sci 116: 4467-4478.
Letourneau PC (1978) Chemotactic response of nerve fiber elongation to nerve growth factor. Dev Biol 66:183-196.
Letourneau PC (1996) The cytoskeleton in nerve growth cone motility and axonal pathfinding. Perspect Dev Neurobiol 4:111-123.
Letourneau PC, Ressler AH (1984) Inhibition of neurite initiation and growth by taxol. J Cell Biol 98:1355-1362.
Letourneau PC, Cypher C (1991) Regulation of growth cone motility. Cell Motil Cytoskeleton 20:267-271.

Letourneau PC, Shattuck TA, Ressler AH (1987) "Pull" and "push" in neurite elongation: observations on the effects of different concentrations of cytochalasin B and taxol. Cell Motil Cytoskeleton 8:193-209.

Leung KM, van Horck FP, Lin AC, Allison R, Standart N, Holt CE (2006) Asymmetrical beta-actin mRNA translation in growth cones mediates attractive turning to netrin-1. Nat Neurosci 9:1247-1256.

Li C, Sasaki Y, Takei K, Yamomoto H, Shouji M, Sugiyama Y, Kawakami T, Nakamura F, Yagi T, Oshima T, Goshima Y (2004) Correlation between semaphorin3A-induced facilitation of axonal transport and local activation of a translation initiation factor eukaryotic translation initiation factor 4E. J Neurosci 24: 6161-6170.

Li X, Meriane M, Triki I, Shekarabi M, Kennedy TE, Larose L, Lamarche-Vane N (2002b) The adaptor protein Nck-1 couples the netrin-1 receptor DCC (deleted in colorectal cancer) to the activation of the small GTPase Rac1 through an atypical mechanism. J Biol Chem 277:37788-37797.

Li Z, Aizenman CD, Cline HT (2002c) Regulation of rho GTPases by crosstalk and neuronal activity in vivo. Neuron 33:741-750.

Lin AC, Holt CE (2007) Local translation and directional steering in axons. Embo J 26:3729-3736.

Lin AC, Holt CE (2008) Function and regulation of local axonal translation. Curr Opin Neurobiol 18:60-68.

Lin CH, Forscher P (1993) Cytoskeletal remodeling during growth cone-target interactions. J Cell Biol 121:1369-1383.

Lin CH, Thompson CA, Forscher P (1994) Cytoskeletal reorganization underlying growth cone motility. Curr Opin Neurobiol 4:640-647.

Liu RY, Schmid RS, Snider WD, Maness PF (2002) NGF enhances sensory axon growth induced by laminin but not by the L1 cell adhesion molecule. Mol Cell Neurosci 20:2-12.

Loudon RP, Silver LD, Yee HF, Jr., Gallo G (2006) RhoA-kinase and myosin II are required for the maintenance of growth cone polarity and guidance by nerve growth factor. J Neurobiol 66:847-867.

Lowery LA, Van Vactor D (2009) The trip of the tip: understanding the growth cone machinery. Nat Rev Mol Cell Biol 10:332-343.

Luduena MA (1973) Nerve cell differentiation in vitro. Dev Biol 33:268-284.

Machesky LM, Mullins RD, Higgs HN, Kaiser DA, Blanchoin L, May RC, Hall ME, Pollard TD (1999) Scar, a WASp-related protein, activates nucleation of actin filaments by the Arp2/3 complex. Proc Natl Acad Sci U S A 96:3739-3744.

Maciver SK (1998) How ADF/cofilin depolymerizes actin filaments. Curr Opin Cell Biol 10:140-144.

Maciver SK, Pope BJ, Whytock S, Weeds AG (1998) The effect of two actin depolymerizing factors (ADF/cofilins) on actin filament turnover: pH sensitivity of F-actin binding by human ADF, but not of Acanthamoeba actophorin. Eur J Biochem 256:388-397.

Mackay DJ, Nobes CD, Hall A (1995) The Rho's progress: a potential role during neuritogenesis for the Rho family of GTPases. Trends Neurosci 18:496-501.
Maekawa M, Ishizaki T, Boku S, Watanabe N, Fujita A, Iwamatsu A, Obinata T, Ohashi K, Mizuno K, Narumiya S (1999) Signaling from Rho to the actin cytoskeleton through protein kinases ROCK and LIM-kinase. Science 285:895-898.
Marsh L, Letourneau PC (1984) Growth of neurites without filopodial or lamellipodial activity in the presence of cytochalasin B. J Cell Biol 99:2041-2047.
Marsick B M, Flynn K C, Santiago-Medina M, Bamburg J R, Letourneau PC (2010) Activation of ADF/cofilin mediates attractive growth cone turning toward nerve growth factor and netrin-1. Dev Neurobiol, in press
Mason C, Erskine L (2000) Growth cone form, behavior, and interactions in vivo: retinal axon pathfinding as a model. J Neurobiol 44:260-270.
Matsui T, Yonemura S, Tsukita S, Tsukita S (1999) Activation of ERM proteins in vivo by Rho involves phosphatidyl-inositol 4-phosphate 5-kinase and not ROCK kinases. Curr Biol 9:1259-1262.
Matsui T, Maeda M, Doi Y, Yonemura S, Amano M, Kaibuchi K, Tsukita S, Tsukita S (1998) Rho-kinase phosphorylates COOH-terminal threonines of ezrin/radixin/moesin (ERM) proteins and regulates their head-to-tail association. J Cell Biol 140:647-657.
McClatchey AI, Fehon RG (2009) Merlin and the ERM proteins--regulators of receptor distribution and signaling at the cell cortex. Trends Cell Biol 19:198-206.
McGough A, Pope B, Chiu W, Weeds A (1997) Cofilin changes the twist of F-actin: implications for actin filament dynamics and cellular function. J Cell Biol 138:771-781.
McKerracher L, Chamoux M, Arregui CO (1996) Role of laminin and integrin interactions in growth cone guidance. Mol Neurobiol 12:95-116.
Meberg PJ, Bamburg JR (2000) Increase in neurite outgrowth mediated by overexpression of actin depolymerizing factor. J Neurosci 20:2459-2469.
Meberg PJ, Ono S, Minamide LS, Takahashi M, Bamburg JR (1998) Actin depolymerizing factor and cofilin phosphorylation dynamics: response to signals that regulate neurite extension. Cell Motil Cytoskeleton 39:172-190.
Menesini Chen MG, Chen JS, Levi-Montalcini R (1978) Sympathetic nerve fibers ingrowth in the central nervous system of neonatal rodent upon intracerebral NGF injections. Arch Ital Biol 116:53-84.
Miki H, Yamaguchi H, Suetsugu S, Takenawa T (2000) IRSp53 is an essential intermediate between Rac and WAVE in the regulation of membrane ruffling. Nature 408:732-735.
Ming G, Song H, Berninger B, Inagaki N, Tessier-Lavigne M, Poo M (1999) Phospholipase C-gamma and phosphoinositide 3-kinase mediate cytoplasmic signaling in nerve growth cone guidance. Neuron 23:139-148.
Ming GL, Song HJ, Berninger B, Holt CE, Tessier-Lavigne M, Poo MM (1997) cAMP-dependent growth cone guidance by netrin-1. Neuron 19:1225-1235.

Ming GL, Wong ST, Henley J, Yuan XB, Song HJ, Spitzer NC, Poo MM (2002) Adaptation in the chemotactic guidance of nerve growth cones. Nature 417:411-418.
Mintz CD, Dickson TC, Gripp ML, Salton SR, Benson DL (2003) ERMs colocalize transiently with L1 during neocortical axon outgrowth. J Comp Neurol 464:438-448.
Mitchison T, Kirschner M (1988) Cytoskeletal dynamics and nerve growth. Neuron 1:761-772.
Mitra SK, Hanson DA, Schlaepfer DD (2005) Focal adhesion kinase: in command and control of cell motility. Nat Rev Mol Cell Biol 6:56-68.
Moore SW, Kennedy TE (2006) Protein kinase A regulates the sensitivity of spinal commissural axon turning to netrin-1 but does not switch between chemoattraction and chemorepulsion. J Neurosci 26:2419-2423.
Moore SW, Tessier-Lavigne M, Kennedy TE (2007) Netrins and their receptors. Adv Exp Med Biol 621:17-31.
Moore SW, Lai Wing Sun K, Xie F, Barker PA, Conti M, Kennedy TE (2008a) Soluble adenylyl cyclase is not required for axon guidance to netrin-1. J Neurosci 28:3920-3924.
Moore SW, Correia JP, Lai Wing Sun K, Pool M, Fournier AE, Kennedy TE (2008b) Rho inhibition recruits DCC to the neuronal plasma membrane and enhances axon chemoattraction to netrin 1. Development 135:2855-2864.
Morris MC, Depollier J, Mery J, Heitz F, Divita G (2001) A peptide carrier for the delivery of biologically active proteins into mammalian cells. Nat Biotechnol 19:1173-1176.
Mouneimne G, DesMarais V, Sidani M, Scemes E, Wang W, Song X, Eddy R, Condeelis J (2006) Spatial and temporal control of cofilin activity is required for directional sensing during chemotaxis. Curr Biol 16:2193-2205.
Mouneimne G, Soon L, DesMarais V, Sidani M, Song X, Yip SC, Ghosh M, Eddy R, Backer JM, Condeelis J (2004) Phospholipase C and cofilin are required for carcinoma cell directionality in response to EGF stimulation. J Cell Biol 166:697-708.
Mullins RD, Heuser JA, Pollard TD (1998) The interaction of Arp2/3 complex with actin: nucleation, high affinity pointed end capping, and formation of branching networks of filaments. Proc Natl Acad Sci U S A 95:6181-6186.
Nagata-Ohashi K, Ohta Y, Goto K, Chiba S, Mori R, Nishita M, Ohashi K, Kousaka K, Iwamatsu A, Niwa R, Uemura T, Mizuno K (2004) A pathway of neuregulin-induced activation of cofilin-phosphatase Slingshot and cofilin in lamellipodia. J Cell Biol 165:465-471.
Nakamura N, Oshiro N, Fukata Y, Amano M, Fukata M, Kuroda S, Matsuura Y, Leung T, Lim L, Kaibuchi K (2000) Phosphorylation of ERM proteins at filopodia induced by Cdc42. Genes Cells 5:571-581.
Ng T, Shima D, Squire A, Bastiaens PI, Gschmeissner S, Humphries MJ, Parker PJ (1999) PKCalpha regulates beta1 integrin-dependent cell motility through association and control of integrin traffic. Embo J 18:3909-3923.

Niggli V, Rossy J (2008) Ezrin/radixin/moesin: versatile controllers of signaling molecules and of the cortical cytoskeleton. Int J Biochem Cell Biol 40:344-349.
Nishiyama M, Hoshino A, Tsai L, Henley JR, Goshima Y, Tessier-Lavigne M, Poo MM, Hong K (2003) Cyclic AMP/GMP-dependent modulation of Ca2+ channels sets the polarity of nerve growth-cone turning. Nature 423:990-995.
Niwa R, Nagata-Ohashi K, Takeichi M, Mizuno K, Uemura T (2002) Control of actin reorganization by Slingshot, a family of phosphatases that dephosphorylate ADF/cofilin. Cell 108:233-246.
Nobes CD, Hall A (1995a) Rho, rac and cdc42 GTPases: regulators of actin structures, cell adhesion and motility. Biochem Soc Trans 23:456-459.
O'Connor TP, Bentley D (1993) Accumulation of actin in subsets of pioneer growth cone filopodia in response to neural and epithelial guidance cues in situ. J Cell Biol 123:935-948.
Ohta Y, Kousaka K, Nagata-Ohashi K, Ohashi K, Muramoto A, Shima Y, Niwa R, Uemura T, Mizuno K (2003) Differential activities, subcellular distribution and tissue expression patterns of three members of Slingshot family phosphatases that dephosphorylate cofilin. Genes Cells 8:811-824.
Ooashi N, Kamiguchi H (2009) The cell adhesion molecule L1 controls growth cone navigation via ankyrin(B)-dependent modulation of cyclic AMP. Neurosci Res 63:224-226.
Oppenheim RW, Prevette D, Tytell M, Homma S (1990) Naturally occurring and induced neuronal death in the chick embryo in vivo requires protein and RNA synthesis: evidence for the role of cell death genes. Dev Biol 138:104-113.
Orian-Rousseau V, Morrison H, Matzke A, Kastilan T, Pace G, Herrlich P, Ponta H (2007) Hepatocyte growth factor-induced Ras activation requires ERM proteins linked to both CD44v6 and F-actin. Mol Biol Cell 18:76-83.
Paglini G, Kunda P, Quiroga S, Kosik K, Caceres A (1998) Suppression of radixin and moesin alters growth cone morphology, motility, and process formation in primary cultured neurons. J Cell Biol 143:443-455.
Pak CW, Flynn KC, Bamburg JR (2008) Actin-binding proteins take the reins in growth cones. Nat Rev Neurosci 9:136-147.
Parisiadou L, Xie C, Cho HJ, Lin X, Gu XL, Long CX, Lobbestael E, Baekelandt V, Taymans JM, Sun L, Cai H (2009) Phosphorylation of ezrin/radixin/moesin proteins by LRRK2 promotes the rearrangement of actin cytoskeleton in neuronal morphogenesis. J Neurosci 29:13971-13980.
Patel TD, Jackman A, Rice FL, Kucera J, Snider WD (2000) Development of sensory neurons in the absence of NGF/TrkA signaling in vivo. Neuron 25:345-357.
Pavlov D, Muhlrad A, Cooper J, Wear M, Reisler E (2007) Actin filament severing by cofilin. J Mol Biol 365:1350-1358.
Pfister BJ, Iwata A, Meaney DF, Smith DH (2004) Extreme stretch growth of integrated axons. J Neurosci 24:7978-7983.
Piper M, Holt C (2004) RNA translation in axons. Annu Rev Cell Dev Biol 20:505-523.

Piper M, Salih S, Weinl C, Holt CE, Harris WA (2005) Endocytosis-dependent desensitization and protein synthesis-dependent resensitization in retinal growth cone adaptation. Nat Neurosci 8:179-186.
Piper M, Anderson R, Dwivedy A, Weinl C, van Horck F, Leung KM, Cogill E, Holt C (2006) Signaling mechanisms underlying Slit2-induced collapse of Xenopus retinal growth cones. Neuron 49:215-228.
Pollard TD, Borisy GG (2003) Cellular motility driven by assembly and disassembly of actin filaments. Cell 112:453-465.
Prag S, Parsons M, Keppler MD, Ameer-Beg SM, Barber P, Hunt J, Beavil AJ, Calvert R, Arpin M, Vojnovic B, Ng T (2007) Activated ezrin promotes cell migration through recruitment of the GEF Dbl to lipid rafts and preferential downstream activation of Cdc42. Mol Biol Cell 18:2935-2948.
Prins KW, Lowe DA, Ervasti JM (2008) Skeletal muscle-specific ablation of gamma(cyto)-actin does not exacerbate the mdx phenotype. PLoS One 3:e2419.
Quinn CC, Pfeil DS, Wadsworth WG (2008) CED-10/Rac1 mediates axon guidance by regulating the asymmetric distribution of MIG-10/lamellipodin. Curr Biol 18:808-813.
Ren XD, Kiosses WB, Sieg DJ, Otey CA, Schlaepfer DD, Schwartz MA (2000) Focal adhesion kinase suppresses Rho activity to promote focal adhesion turnover. J Cell Sci 113 (Pt 20):3673-3678.
Ressad F, Didry D, Egile C, Pantaloni D, Carlier MF (1999) Control of actin filament length and turnover by actin depolymerizing factor (ADF/cofilin) in the presence of capping proteins and ARP2/3 complex. J Biol Chem 274:20970-20976.
Ridley AJ, Paterson HF, Johnston CL, Diekmann D, Hall A (1992) The small GTP-binding protein rac regulates growth factor-induced membrane ruffling. Cell 70:401-410.
Rivas RJ, Burmeister DW, Goldberg DJ (1992) Rapid effects of laminin on the growth cone. Neuron 8:107-115.
Robles E, Gomez TM (2006) Focal adhesion kinase signaling at sites of integrin-mediated adhesion controls axon pathfinding. Nat Neurosci 9:1274-1283.
Roche FK, Marsick BM, Letourneau PC (2009) Protein synthesis in distal axons is not required for growth cone responses to guidance cues. J Neurosci 29:638-652.
Round J, Stein E (2007) Netrin signaling leading to directed growth cone steering. Curr Opin Neurobiol 17:15-21.
Sabry JH, O'Connor TP, Evans L, Toroian-Raymond A, Kirschner M, Bentley D (1991) Microtubule behavior during guidance of pioneer neuron growth cones in situ. J Cell Biol 115:381-395.
Sakumura Y, Tsukada Y, Yamamoto N, Ishii S (2005) A molecular model for axon guidance based on cross talk between rho GTPases. Biophys J 89:812-822.
Sakurai T, Gil OD, Whittard JD, Gazdoiu M, Joseph T, Wu J, Waksman A, Benson DL, Salton SR, Felsenfeld DP (2008) Interactions between the L1 cell

adhesion molecule and ezrin support traction-force generation and can be regulated by tyrosine phosphorylation. J Neurosci Res 86:2602-2614.
Sarmiere PD, Bamburg JR (2004) Regulation of the neuronal actin cytoskeleton by ADF/cofilin. J Neurobiol 58:103-117.
Schuman EM (1999) Neurotrophin regulation of synaptic transmission. Curr Opin Neurobiol 9:105-109.
Seeley PJ, Greene LA (1983) Short-latency local actions of nerve growth factor at the growth cone. Proc Natl Acad Sci U S A 80:2789-2793.
Shaw AE, Minamide LS, Bill CL, Funk JD, Maiti S, Bamburg JR (2004) Cross-reactivity of antibodies to actin- depolymerizing factor/cofilin family proteins and identification of the major epitope recognized by a mammalian actin-depolymerizing factor/cofilin antibody. Electrophoresis 25:2611-2620.
Shekarabi M, Moore SW, Tritsch NX, Morris SJ, Bouchard JF, Kennedy TE (2005) Deleted in colorectal cancer binding netrin-1 mediates cell substrate adhesion and recruits Cdc42, Rac1, Pak1, and N-WASP into an intracellular signaling complex that promotes growth cone expansion. J Neurosci 25:3132-3141.
Shiue H, Musch MW, Wang Y, Chang EB, Turner JR (2005) Akt2 phosphorylates ezrin to trigger NHE3 translocation and activation. J Biol Chem 280:1688-1695.
Simons PC, Pietromonaco SF, Reczek D, Bretscher A, Elias L (1998) C-terminal threonine phosphorylation activates ERM proteins to link the cell's cortical lipid bilayer to the cytoskeleton. Biochem Biophys Res Commun 253:561-565.
Song HJ, Poo MM (1999) Signal transduction underlying growth cone guidance by diffusible factors. Curr Opin Neurobiol 9:355-363.
Song H, Poo MM (2001) The cell biology of neuronal navigation. Nat Cell Biol 3:E81–E88.
Soosairajah J, Maiti S, Wiggan O, Sarmiere P, Moussi N, Sarcevic B, Sampath R, Bamburg JR, Bernard O (2005) Interplay between components of a novel LIM kinase-slingshot phosphatase complex regulates cofilin. Embo J 24:473-486.
Squire LR, Berg D, Bloom FE, du Lac S, Ghosh A, Spitzer NC,eds (2008) Fundamental Neuroscience, Third Edition, (Burlington MA; Elsevier, Inc.)
Strasser GA, Rahim NA, VanderWaal KE, Gertler FB, Lanier LM (2004) Arp2/3 is a negative regulator of growth cone translocation. Neuron 43:81-94.
Steward O, Schuman EM (2003) Compartmentalized synthesis and degradation of proteins in neurons. Neuron 40: 347-359.
Suter DM, Forscher P (1998) An emerging link between cytoskeletal dynamics and cell adhesion molecules in growth cone guidance. Curr Opin Neurobiol 8:106-116.
Suter DM, Forscher P (2000) Substrate-cytoskeletal coupling as a mechanism for the regulation of growth cone motility and guidance. J Neurobiol 44:97-113.
Svitkina TM, Borisy GG (1999) Arp2/3 complex and actin depolymerizing factor/cofilin in dendritic organization and treadmilling of actin filament array in lamellipodia. J Cell Biol 145:1009-1026.

Sydor AM, Su AL, Wang FS, Xu A, Jay DG (1996) Talin and vinculin play distinct roles in filopodial motility in the neuronal growth cone. J Cell Biol 134:1197-1207.

Tabi N, Poo MM (1991) Culturing spinal neurons and muscle cells from *Xenopus* embryos. In Culturing Nerve Cells, G. Banker and K. Goslin, eds. (Cambridge MA; The MIT Press), pp. 137-154.

Takahashi K, Sasaki T, Mammoto A, Takaishi K, Kameyama T, Tsukita S, Takai Y (1997) Direct interaction of the Rho GDP dissociation inhibitor with ezrin/radixin/moesin initiates the activation of the Rho small G protein. J Biol Chem 272:23371-23375.

Takei N, Kawamura M, Hara K, Yonezawa K, Nawa H (2001) Brain-derived neurotrophic factor enhances neuronal translation by activating multiple initiation processes. J Biol Chem 276: 42818-42825.

Tanaka E, Kirschner MW (1995) The role of microtubules in growth cone turning at substrate boundaries. J Cell Biol 128:127-137.

Tanaka E, Sabry J (1995) Making the connection: cytoskeletal rearrangements during growth cone guidance. Cell 83:171-176.

Tanaka E, Ho T, Kirschner MW (1995) The role of microtubule dynamics in growth cone motility and axonal growth. J Cell Biol 128:139-155.

Tang P, Cao C, Xu M, Zhang L (2007) Cytoskeletal protein radixin activates integrin alpha(M)beta(2) by binding to its cytoplasmic tail. FEBS Lett 581:1103-1108.

Tessier-Lavigne M, Goodman CS (1996) The molecular biology of axon guidance. Science 274:1123-1133.

Theriot JA, Mitchison TJ (1991) Actin microfilament dynamics in locomoting cells. Nature 352:126-131.

Tojima T, Akiyama H, Itofusa R, Li Y, Katayama H, Miyawaki A, Kamiguchi H (2006) Attractive axon guidance involves asymmetric membrane transport and exocytosis in the growth cone. Nature Neurosci 10: 58-66.

Toshima J, Toshima JY, Takeuchi K, Mori R, Mizuno K (2001) Cofilin phosphorylation and actin reorganization activities of testicular protein kinase 2 and its predominant expression in testicular Sertoli cells. J Biol Chem 276:31449-31458.

Trachsel H (1991) Translation in Eukaryotes. CRC Press. Boca Raton FL. 440 pp.

Tsukita S, Hieda Y, Tsukita S (1989) A new 82-kD barbed end-capping protein (radixin) localized in the cell-to-cell adherens junction: purification and characterization. J Cell Biol 108:2369-2382.

Tursun B, Schluter A, Peters MA, Viehweger B, Ostendorff HP, Soosairajah J, Drung A, Bossenz M, Johnsen SA, Schwiezer M, Bernard O, Bach I (2005) The ubiquitin ligase Rnf6 regulates LIM kinase I levels in axonal growth cones. Genes & Dev 19: 2307-2319.

Twiss .L, van Minnen J (2006) New insights into neuronal regeneration : the role of axonal protein synthesis in pathfinding and axonal extension. Neurotrauma 23: 295-308.

Van Troys M, Huyck L, Leyman S, Dhaese S, Vandekerkhove J, Ampe C (2008) Ins and outs of ADF/cofilin activity and regulation. Eur J Cell Biol 87:649-667.

Varnum-Finney B, Reichardt LF (1994) Vinculin-deficient PC12 cell lines extend unstable lamellipodia and filopodia and have a reduced rate of neurite outgrowth. J Cell Biol 127:1071-1084.

Verma P, Chierzl S, Codd AM, Campbell DS, Meyer RL, Holt CE, Fawcett JW (2005) Axonal protein synthesis and degradation are necessary for efficient growth cone regeneration. J Neurosci 25: 331-342.

Wahl S, Barth H, Ciossek T, Aktories K, Mueller BK (2000) Ephrin-A5 induces collapse of growth cones by activating Rho and Rho kinase. J Cell Biol 149: 263-270.

Wang W, van Nierkerk E, Willis DE, Twiss JL (2007) RNA transport and localized protein synthesis in neurological disorders and neural repair. Develop Neurobiol 67: 1166-1182.

Weinl C, Becker N, Loeschinger J (2004) Responses of temporal retinal growth cones to ephrinA5-coated beads. J Neurobiol 62: 219-230.

Weiner OD, Servant G, Welch MD, Mitchison TJ, Sedat JW, Bourne HR (1999) Spatial control of actin polymerization during neutrophil chemotaxis. Nat Cell Biol 1:75-81.

Wen Z, Guirland C, Ming GL, Zheng JQ (2004) A CaMKII/calcineurin switch controls the direction of Ca(2+)-dependent growth cone guidance. Neuron 43:835-846.

Wen Z, Han L, Bamburg JR, Shim S, Ming GL, Zheng JQ (2007) BMP gradients steer nerve growth cones by a balancing act of LIM kinase and Slingshot phosphatase on ADF/cofilin. J Cell Biol 178:107-119.

Woo S, Gomez TM (2006) Rac1 and RhoA promote neurite outgrowth through formation and stabilization of growth cone point contacts. J Neurosci 26:1418-1428.

Woo S, Rowan DJ, Gomez TM (2009) Retinotopic mapping requires focal adhesion kinase-mediated regulation of growth cone adhesion. J Neurosci 29:13981-13991.

Wu KY, Hengst U, Cox LJ, Macosko EZ, Jeromin A, Urquhart ER, Jaffrey SR (2005) Local translation of RhoA regulates growth cone collapse. Nature 436:1020-1024.

Yamashita T, Tucker KL, Barde YA (1999) Neurotrophin binding to the p75 receptor modulates Rho activity and axonal outgrowth. Neuron 24:585-593.

Yang N, Higuchi O, Ohashi K, Nagata K, Wada A, Kangawa K, Nishida E, Mizuno K (1998) Cofilin phosphorylation by LIM-kinase 1 and its role in Rac-mediated actin reorganization. Nature 393:809-812.

Yao J, Sasaki Y, Wen Z, Bassell GJ, Zheng JQ (2006) An essential role for beta-actin mRNA localization and translation in Ca2+-dependent growth cone guidance. Nat Neurosci 9:1265-1273.

Yonemura S, Matsui T, Tsukita S, Tsukita S (2002) Rho-dependent and -independent activation mechanisms of ezrin/radixin/moesin proteins: an essential role for polyphosphoinositides in vivo. J Cell Sci 115:2569-2580.

Yuan XB, Jin M, Xu X, Song YQ, Wu CP, Poo MM, Duan S (2003) Signalling and crosstalk of Rho GTPases in mediating axon guidance. Nat Cell Biol 5:38-45.

Zebda N, Bernard O, Bailly M, Welti S, Lawrence DS, Condeelis JS (2000) Phosphorylation of ADF/cofilin abolishes EGF-induced actin nucleation at the leading edge and subsequent lamellipod extension. J Cell Biol 151:1119-1128.

Zhang HL, Eom T, Oleynikov Y, Shenoy SM, Liebelt DA, Dictenberg JB, Singer RH, Bassell GJ (2001) Neurotrophin-induced transport of a beta-actin mRNP complex increases beta-actin levels and stimulates growth cone motility. Neuron 31: 261-275.

Zhang HL, Singer RH, Bassell GJ (1999) Neurotrophin regulation of beta-actin mRNA and protein localization within growth cones. J Cell Biol 147:59-70.

Zhang X, Poo MM (2002) Localized synaptic potentiation by BDNF requires local protein synthesis in the developing axon. Neuron 36: 675-688.

Zheng JQ, Kelly TK, Chang B, Ryazantsev S, Rajasekaran AK, Martin KC, Twiss JL (2001) A functional role for intra-axonal protein synthesis during axonal regeneration from adult sensory neurons. J Neurosci 21: 9291-9303.

Zheng J, Buxbaum RE, Heidemann SR (1993) Investigation of microtubule assembly and organization accompanying tension-induced neurite initiation. J Cell Sci 104 (Pt 4):1239-1250.

Zhou FQ, Waterman-Storer CM, Cohan CS (2002) Focal loss of actin bundles causes microtubule redistribution and growth cone turning. J Cell Biol 157:839-849.

Zhou FQ, Zhou J, Dedhar S, Wu YH, Snider WD (2004) NGF-induced axon growth is mediated by localized inactivation of GSK-3beta and functions of the microtubule plus end binding protein APC. Neuron 42:897-912.